FINAL REPORT – REVISION 1

BHP Yandi E8 Groundwater Model

Yandi
Western Australia

Prepared for:

BHP

BHP WAIO
Level 37, 125 St Georges Terrace
Perth WA, 6000

Prepared by:

INTERA

INTERA Geosciences Pty Ltd
166/580 Hay St
Perth, WA 6000

FEBRUARY 2024

Executive Summary

BHP's Yandi mine is situated approximately 100 km north-west of Newman in the Pilbara Region of Western Australia. The mine's orebody comprises the Marillana Creek Chanel Iron Deposit (CID), which is also the main aquifer in the region. Groundwater abstraction required for the dewatering and other mine operations started in 1991 and resulted in significant drawdown within the CID.

As part of the final mining stages, BHP WAIO is applying for a mine permit for its easternmost pit, named E8. The Part IV submission process requires the conceptualization of the local groundwater system and an assessment of associated groundwater drawdowns. To that end, BHP WAIO commissioned INTERA Geosciences Pty Ltd (INTERA) with development of a numerical groundwater flow model for Yandi E8 mine and adjacent areas.

The numerical model had to include a large number of hydraulic stressors that occurred within the model domain since the commencement of mining in 1991. These stressors were both naturally occurring (namely changes in rainfall rates and subsequent diffuse recharge and seepage from Marillana Creek) and associated with the mine operations, including dewatering through wells and sumps, excess water discharge and diversion of Marillana Creek.

History matching was undertaken comparing simulated groundwater levels through historical measurements undertaken in hundreds of monitoring boreholes over a period of 30 years. Simulated heads show a very good agreement with historical measurements, with a few exceptions mostly associated with potential errors in historical pumping rates and boundary conditions used to represent the Rio Tinto Pits.

Predictive model runs were undertaken to provide estimates of total drawdown and individual contributions from climate (i.e., rainfall rates), mining operations and the proposed E8 pit. Model results suggest that drawdown contributions from the E8 pit will be restricted to its immediate vicinity. Simulated inflows for E8 pit show peaks of up to 12 ML/day (associated with sharp changes in target groundwater levels prescribed in the pit boundary conditions), stabilizing to 10 ML/day from end of 2028.

The comparison of predictive model results with additional data collected after the history matching (borehole HYM0011M) suggests that predictive drawdowns within the Alluvium Aquifer are being overestimated in the vicinity of E8. It is possible that the vertical connection between Alluvium and CID aquifers are overestimated in the model, given that a single layer was assigned for each aquifer and no representation was given to lower permeability portions of the CID. Other potential factors in the overestimation of Alluvium drawdown include:

- Limited monitoring in the alluvium

- Uncertain geometry of the alluvium, particular at local scales, and

- Uncertainty around the infiltration of Yandi discharge, both in time and duration.

In light of these facts, drawdown predictions within the Alluvium Aquifer should be considered with caution.

Table of Contents

List of Appendices

List of Figures

List of Tables

1. Introduction and background

BHP's Yandi mine is situated approximately 100 km north-west of Newman in the Pilbara Region of Western Australia. The mine's orebody comprises the Marillana Creek Chanel Iron Deposit (CID), which is also the main aquifer in the region. Groundwater abstraction required for the dewatering and other mine operations started in 1991 and resulted in significant drawdown around the area.

As part of the final mining stages, BHP WAIO is applying for a mine permit for its easternmost pit, named E8. The Part IV submission process requires the conceptualization of the local groundwater system and an assessment of associated groundwater drawdowns. To that end, BHP WAIO commissioned INTERA Geosciences Pty Ltd (INTERA) with development of a numerical groundwater flow model for Yandi E8 mine and adjacent areas.

This draft report summarizes the findings of this groundwater modelling study, describing the numerical model and methodologies applied during its development, predictions of interest and recommendations for further work.

2. Modelling objectives and predictions of interest

The overall objective of this study was to develop an up-to-date groundwater model including the latest available information, in order to provide several predictions of interest, and quantify the uncertainty associated with them. Specific objectives for this study were defined by BHP WAIO in the Request for Proposal (RfP) document and include:

- Support BHP with the conceptualization of the entire Yandi hydrogeological system, with focus on the relationships between the Channel Iron Deposit (CID), overlying alluvium and Ministers North aquifers,

- Provide predictive estimates of groundwater drawdown in the alluvium and CID resulting from the mining operations,

- Analysis of potential relationships between CID drawdown caused by Yandi and Yandicoogina mines and groundwater level decline being observed at Ministers North, and

- Identify areas of hydrogeological uncertainty relevant to the predictions of interest and provide strategies to reduce it.

Predictions of interest provided by the numerical model were essentially changes in the groundwater level associated with the various mining activities, as follows:

- Spatial distributions of drawdown within the different aquifers for present-day (2023) and end-of-mine (EOM) snapshots;

- Simulated historical and predictive groundwater level hydrographs in groundwater monitoring borehole locations and additional tracking points in the western portion of the CID aquifer; and

- Time series of simulated water balance components (such as recharge and dewatering) for contextualization purposes.

Associated uncertainties of each prediction of interest have been quantified and reported in this document.

3. Data basis

The development of the numerical groundwater model was based on several data sets provided by BHP WAIO and other publicly available data sets, including:

- Previous reports on local hydrogeology and groundwater modelling;

- Groundwater monitoring data;

- Historical pumping rates from dewatering wells;

- Previous groundwater model files;

- Digital Elevation Models (DEM);

- Weather data; and

- Shapefiles containing the mine structures.

Details on the different data sources utilized in this study are presented in Table 1. In addition, expert opinions and specialized literature were consulted and considered during this study.

Table 1 – Summary of accessed data sources.

Setting	Public data	Site specific data
Topography	SRTM 30m DEM	-
Climate	DES – SILO climate data (daily rainfall and evaporation) at location (lat / long): -22.75 / 119.00	Weather station MCWS001 rainfall data
Hydrology	Secondary drainage retrieved from SRTM	Marillana Creek shapefile and locations of diversions
Geological and hydrogeological setting	-	Extent and depth of the CID, Munjina, Yandicoogina and Ministers North aquifer Extent and depth of Alluvium exported from FEFLOW model (Golder, 2015) Yandi Groundwater Flow Model report (Golder, 2015)
Groundwater levels	-	Yandi and Ministers North well construction and water level data
Surface water	-	Flat Rocks, Iowa Creek, and Landbridge US/DS water levels
Wells, sumps, and discharge	-	Abstraction wells and sump location, pumping data and discharge rates, infill data for 1996-2001 Abstraction rates exported from FEFLOW model (Golder, 2015) for 1991-1996 Assumed dewatering depths for Rio Tinto pits provided by BHP
Mining settings	-	Rio Tinto pits estimated extent
Groundwater model	-	FEFLOW model files (Golder, 2015)

4. Conceptual Model synopsis

The hydrogeological conceptual model for Yandi E8 and surrounding area has been developed by BHPIO and is presented in a separate document. For the purposes of contextualization, a brief synopsis of the conceptual model is presented herein.

In terms of hydrostratigraphy, the study area has been divided into four major units, namely:

- Alluvium Sediments, consisting of recent unconsolidated sediments of low to high permeability occurring along the Marillana Creek and major tributaries.

- Channel Iron Deposits (CID), comprised by Archean rocks of the Marillana Formation. This unit has particularly high permeabilities and is restricted to the paleochannel extending roughly along the Marillana Creek and low topography areas.

- Ministers North aquifer, comprised of mineralized rocks from the Brockman Iron formation. This unit has moderate to high permeability and its groundwater levels show a strong correlation with rainfall rates.

- Undifferentiated basement, consisting of weathered horizons and fracture zones in the basement rocks from the Weeli Wolli Formation over the entire study area, presenting low to moderate permeabilities.

The Marillana Creek runs through the Yandi mine area, generally following the direction of the palaeochannel, but crisscrossing and running parallel to it in several places. Groundwater recharge occurs through seepage from the Marillana Creek during significant rainfall/runoff events, and to a much lesser extent through diffuse recharge over the study area. As a result, groundwater levels present a good correlation with topographical levels and rainfall rates. In the case of the CID, recharge to this unit occurs predominantly in areas when it is overlayed by the alluvium sediments.

With the commencement of mining activities in the area, significant dewatering has taken place since 1991, with an average rate of 22 ML/d and a maximum rate of 50 ML/d achieved in 2012. Dewatering has been undertaken with 145 production wells, all installed in the CID aquifer.

Excess water generated by dewatering was discharged in to three locations of the Marillana Creek, with an average of 20 ML/d between 1997 and 2021. CID groundwater levels in the area have responded to both dewatering and discharge. In all areas of Yandi, CID groundwater levels have fallen by several 10's of metres, while areas near the Eastern discharge area have resulted in localized mounding.

The diversion of Marillana Creek in two locations within the study area is also likely to have promoted local adjustments in groundwater levels.
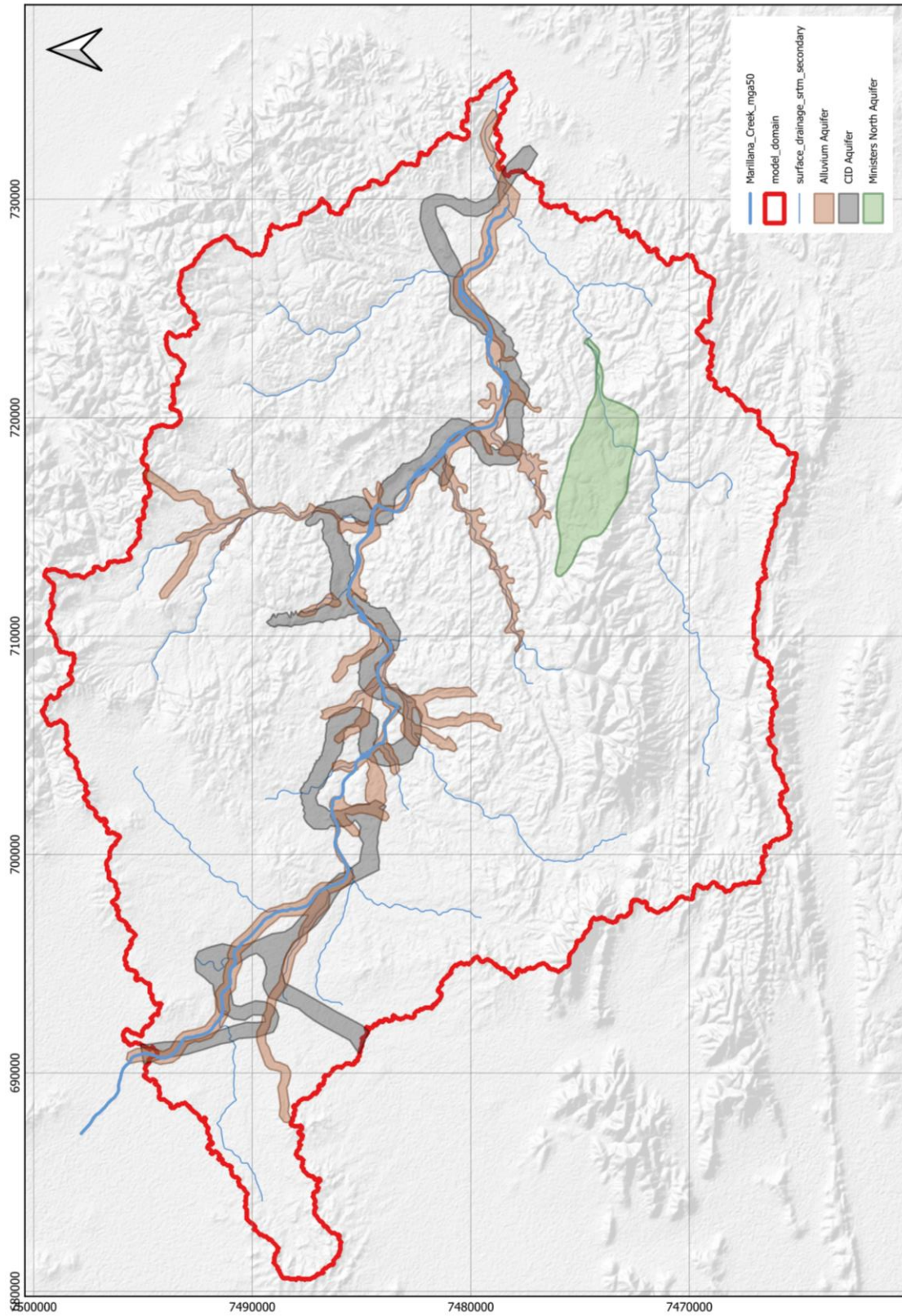
Figure 4-1: Extent of Alluvium Sediments, CID, and Ministers North aquifers.

5. Model setup

5.1 Modelling platform

The numerical model was developed using MODFLOW 6 (Hughes et al., 2017) as the engine, in conjunction with the Flopy libraries (Bakker et al., 2016) and the PEST++ suite (White, 2021). Modflow 6 was the chosen modelling engine due to the following reasons:

- Wide use and acceptance in the modelling community;

- Faster running times when compared to equivalent finite-element codes in most situations;

- Free and open-source software, which facilitates the distribution to BHP WAIO and other stakeholders (if required); and

- Ability of MODFLOW 6 to simulate pit lakes using a specific lake model, which formulation enables the tight coupling between simulated pit lakes and surrounding groundwater environment.

The model setup, history matching and uncertainty analyses was developed using scripted workflows for building the inputs, running the different models, and postprocessing of MODFLOW 6 and PEST++ results. The use of scripted workflows facilitates reproducibility of the various simulations and modelling activities undertaken throughout the study.

5.2 Model domain and spatial discretization

The numerical model domain has been extended beyond previous modelling studies to include the entire watershed within which the Yandi pits are located. An unstructured layered discretization by vertices (DISV) grid was employed, enabling local refinement around features of interest. A base cell size of 500 by 500 m was assigned. Where the grid coincides with the horizontal extent of the Alluvium Sediments, CID and Ministers North units, cell sizes were refined to 125 by 125 m, resulting in a total of 22,760 cells per layer. The model domain and grid discretization are displayed in Figure 5-1.

Vertically, the model domain was divided in three layers, used to delineate the different hydrogeological units as follows:

- Layer 1 – Representing the Alluvium Sediments;

- Layer 2 – Representing the CID; and

- Layer 3 – Representing the Undifferentiated basement and Ministers North aquifer.

The geometry and extent of Alluvium and CID aquifers were extrapolated beyond the areas which BHP had geology data. For these areas, BHP WAIO has provided shapefiles with estimated extent for each aquifer. Thicknesses for these areas were extrapolated based on the geometry of these units (in particular thicknesses) in areas where drilling data was available.

For layers 1 (Alluvium Sediments) and 2 (CID), model cells beyond the extent of these units were assigned a thickness of 0 m and set as "vertical pass through" cells and thus do not exist in the simulation. The extents of each geological units and their thickness were extracted from the previous modelling work and GIS data provided by BHPIO. Topographical elevations used in the model and thicknesses for each model layer are shown in Figure 5-2 and Figure 5-3.
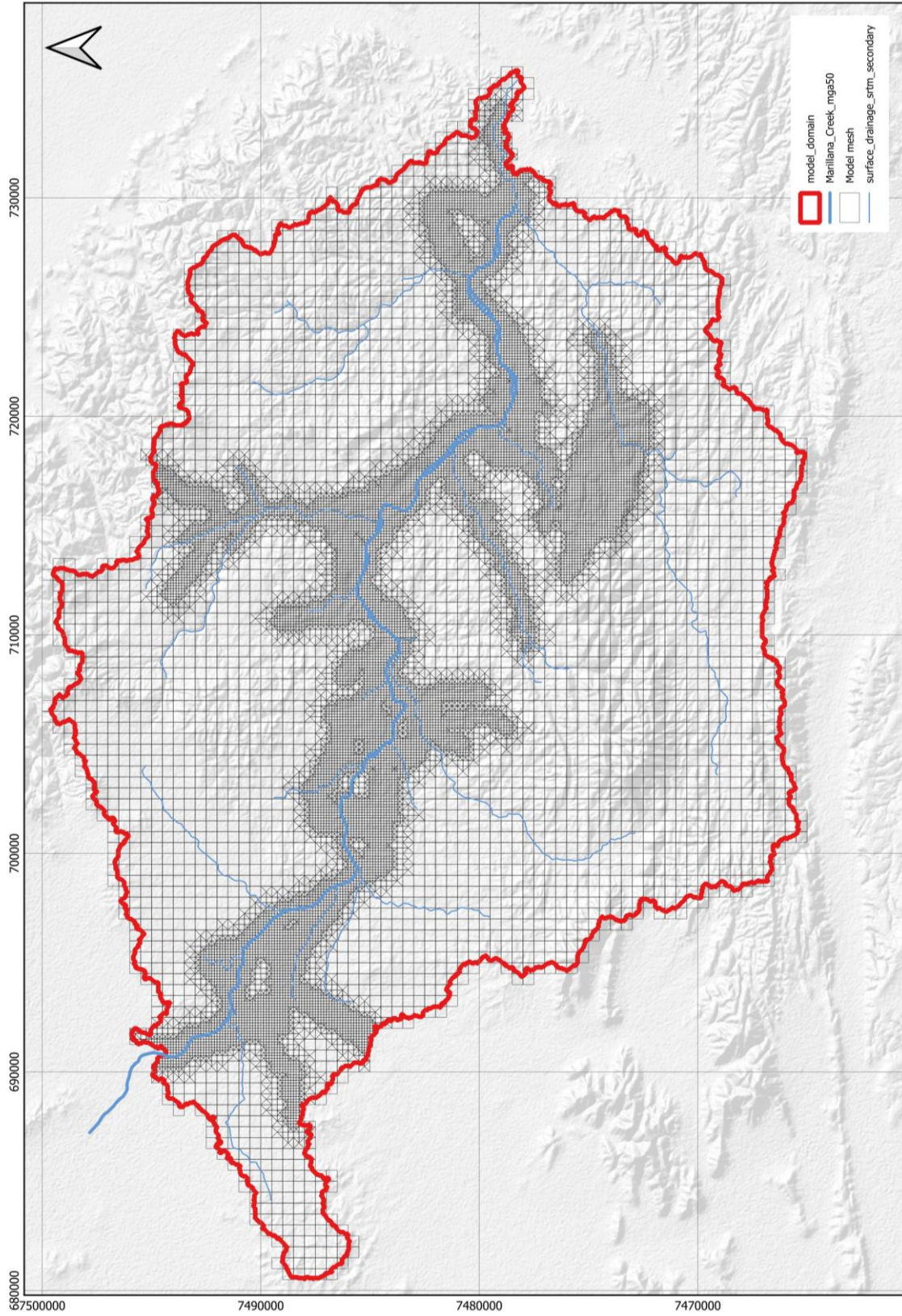
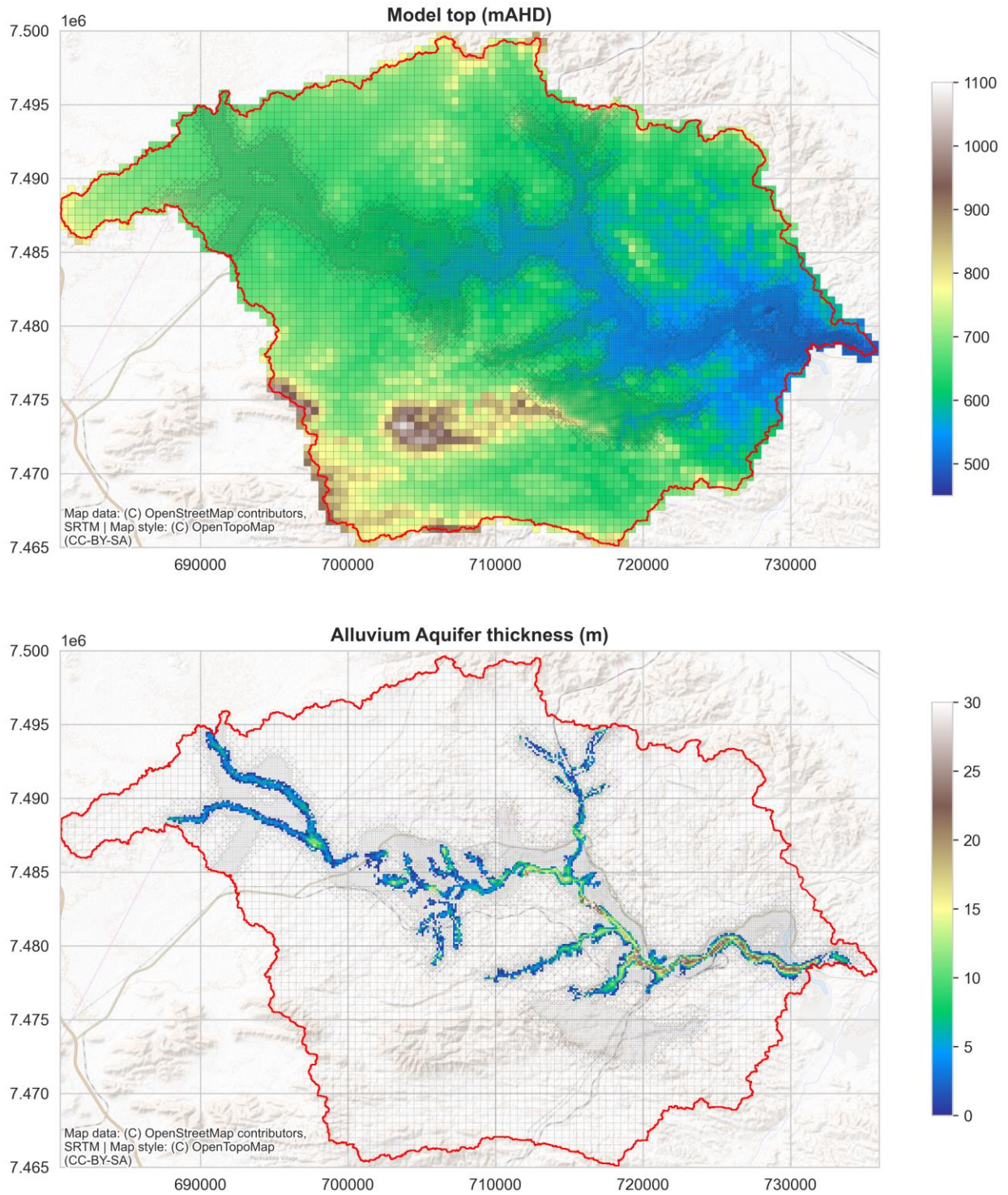Figure 5-1: Model domain and mesh.

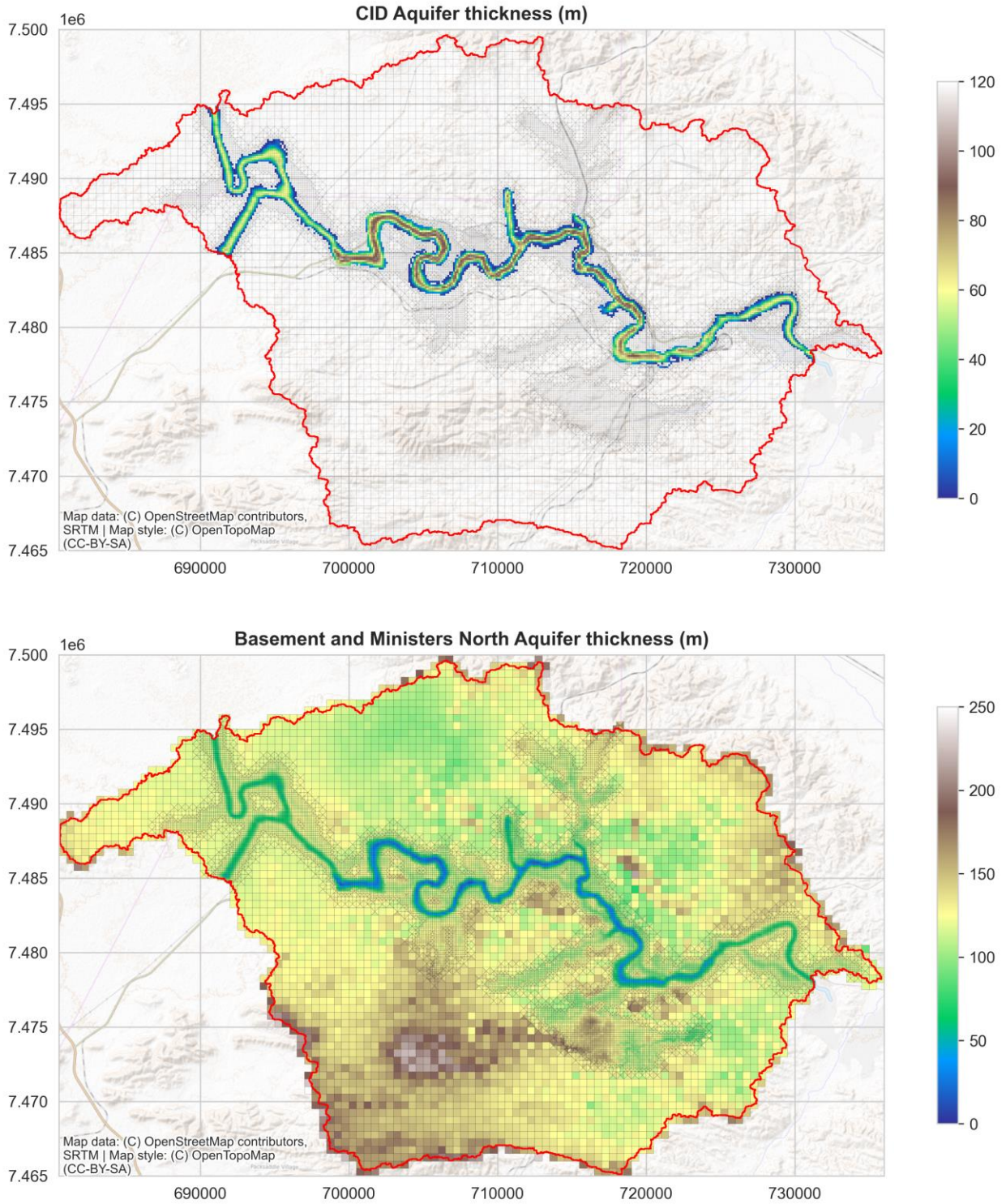Figure 5-2: Top of model elevations (top) and Alluvium Aquifer thickness (bottom).

Figure 5-3: Aquifer thicknesses for CID (top), Basement and Ministers North (bottom) aquifers.

5.3   Temporal discretization

In terms of temporal discretization, the numerical model was divided into three periods, namely:

- Pre-mine, where steady-state conditions were assumed,

- Historical mining, starting from date of the earliest dewatering record (January 1991) up to end of 2023, and

- Predictive life-of-mine, where the simulation was continued for a 7-year period up to end of 2029.

The model was simulated using 1 steady-state stress period (i.e., period where boundary conditions remain constant) for the pre-mine period, followed by monthly transient stress periods for historical and predictive mining periods, with a total of 470 stress periods. Each transient stress period was divided in four time-steps to facilitate model convergence.

5.4   Boundary conditions – Pre mine

Boundary conditions were implemented in the model to simulated exchanges between the model domain and surrounding environments (for example, rainfall recharge, or surface drainage). Pre-mine boundary conditions were implemented in the model to represent the natural groundwater dynamics. These boundaries were implemented using the various boundary packages from MODFLOW 6, as described in the following sections.

5.4.1 Rainfall recharge

The recharge (RCH) package was used to simulate diffuse recharge from rainfall over the entire model domain. As such, recharge was defined as a function of historical rainfall. Rainfall data was sourced from the SILO data set (http://www.longpaddock.qld.gov.au/silo) for the location S22.75, E 119.00.

Prescribed recharge rates were assigned as a function of the historical rainfall rates, and a multiplier to represent the fraction of rainfall water that infiltrates into the aquifers. For the steady-state stress period, the average value for the period of 1991-2022 was used (413 mm/year). Rainfall multipliers were spatially distributed over the model domain and adjusted during the history matching (as discussed in the following section).

Lastly, recharge was assigned to the topmost active cell for each vertical prism of the model mesh. In other words, in areas where flow through cells were assigned (e.g., pinch outs for Alluvium Sediments and CID aquifers), recharge was assigned to underlying active layers.
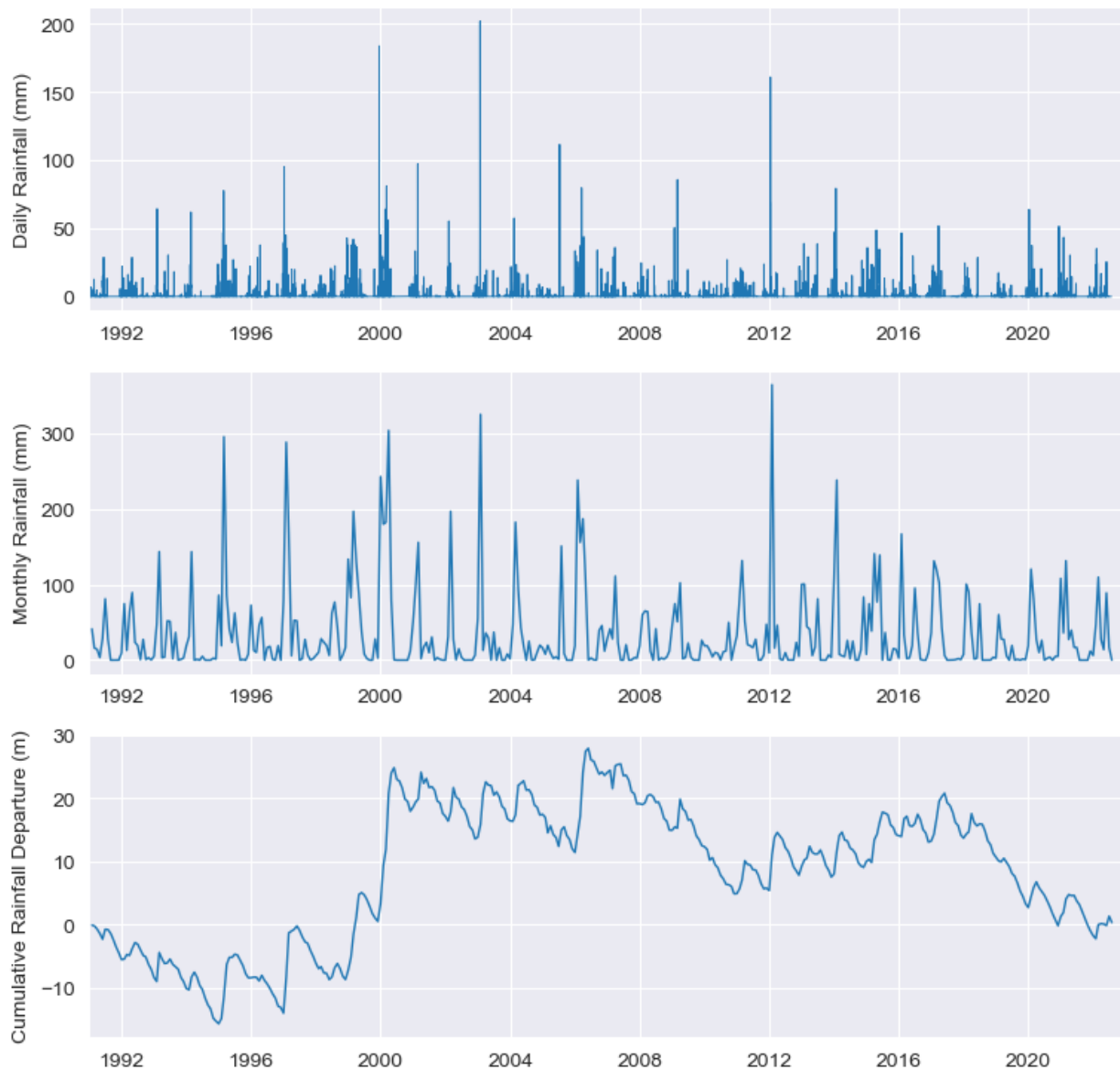
Figure 5-4: Historical rainfall data used in the model setup.

5.4.2 Evapotranspiration

The evapotranspiration (EVT) package was used to simulate evapotranspiration and evaporation (in situations where the groundwater level raise above topography). Evapotranspiration is defined as a function of three variables:

- Topographical elevation, above which full potential evaporation rates are applied; and

- Potential evaporation rate; and

- Extinction depth, which is the depth below which evapotranspiration no longer occurs.

Potential evaporation rates were estimated based on the average value from the SILO data set (1598 mm/year), while a nominal initial value of 5 m was assigned to the extinction depths. Both parameters were further adjusted during history matching.

5.4.3 Marillana Creek seepage

Water exchanges between Marillana Creek and underlying units have been implemented using general head boundaries using the GHB package. Fluxes between these boundaries and its containing cell are a function of the head difference between the boundary and cell, multiplied by a conductance factor which relates to the aquifer hydraulic conductivity, interface area and distance to the boundary.

Seepage from Marillana Creek constitutes the main recharge source within the model domain. From a conceptual point of view, and given the ephemeral characteristic of this creek, recharge episodes from Marillana Creek are expected to occur following significant rainfall events after which the creek remains wet long enough to promote seepage.

The boundary head values assigned in the model equated to the topographic elevation (as a proxy for the creek water elevation) and the conductance term. Conductance values were defined as a function of vertical hydraulic conductivity and cell size, plus an additional conductance factor was included to enforce rainfall-based thresholds for the conductance. Two thresholds were adopted for the monthly-averaged daily rainfall, as illustrated in Figure 5-5. The lower threshold would ensure that significant seepage events occur only for months where the threshold has been exceeded, while a maximum conductance would be maintained by the high threshold in the case of extreme rainfall events. The conductance factor varies from 0 (minimum threshold) to 1 (max threshold) using a sigmoid function.

For the steady-state stress period, the average rainfall value (413 mm/year) has been utilized for calculation of rainfall-based conductance factor, while historical average monthly rainfall values were used for the transient stress periods.
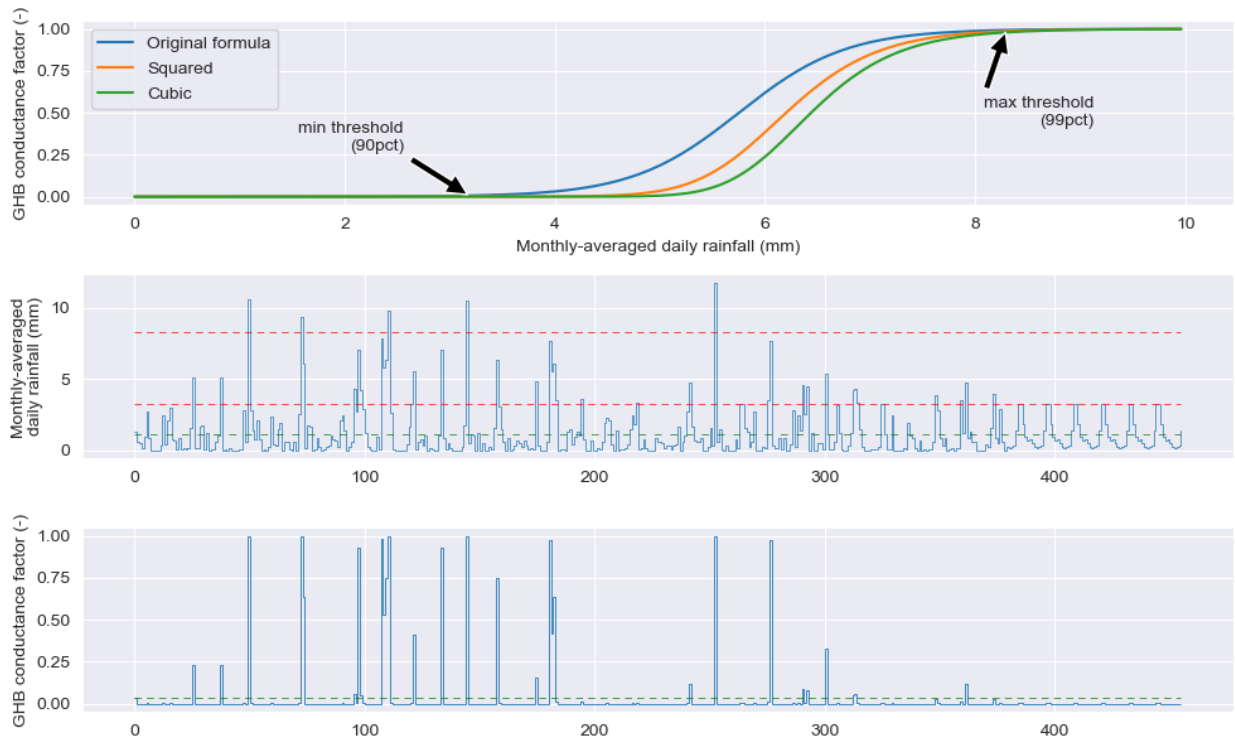
Figure 5-5: Example of threshold-based conductance adjustments for the Marillana Creek boundaries.

5.4.4 Surface water drainage

Drain boundaries using the DRN package were implemented to simulate groundwater discharge in the main creeks in the model domain other than Marillana Creek. These boundaries were assigned with an elevation equating to the topographic level (i.e., top elevation of model layer 1) minus a depth of up 3 metres which was adjusted during the history matching process. The distribution of these drain boundaries is illustrated in Figure 5-6.

Figure 5-6: Distribution of surface water drainage cells.

5.5 Boundary conditions – Historical and future mining

5.5.1 Rainfall recharge and Marillana Creek seepage

Boundary conditions that used rainfall as input (i.e., recharge and seepage from Marillana Creek) were adopted to account for the transient behavior of rainfall, replacing the average rainfall value used in the steady-state pre-mine with the monthly rainfall series from the SILO data set.

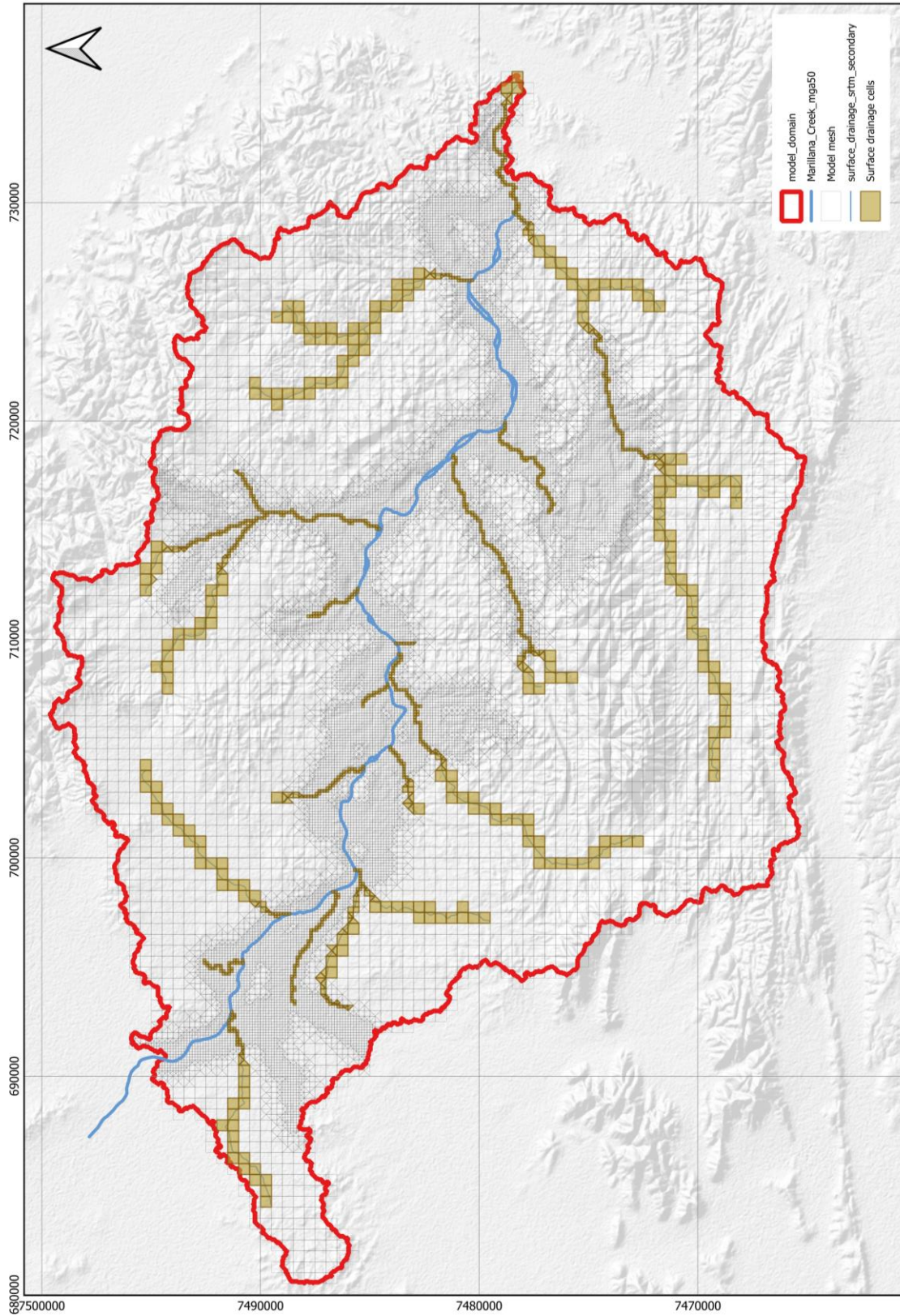For the predictive period (2023-2029), rainfall inputs were defined cycling monthly-average rainfall values for the year 2022.

5.5.2 Well abstraction (dewatering)

BHP WAIO dewatering activities throughout the history of the mine were undertaken with the use of dewatering wells and in-pit sumps over a large number of locations (Figure 5-8) with pumping rates that varied substantially over the simulated period (Figure 5-7).

Both dewatering well and in-pit sumps were implemented using the well package (WEL), with rates based on historical records, presented in Appendix B. The well package was used with the auto-flow-reduce option, which prevents simulated heads going below the cell bottom by reducing prescribed pumping rates. Simulated pumping rates were then compared to historical actual rates during the history matching-process to ensure that hydraulic properties were adjusted to allow the prescribed rates to occur.

For the predictive period, all groundwater abstraction from dewatering wells and in-pit sumps were set to zero (and replaced by pit drain boundaries for estimation of future pit inflows).

5.5.3 River diversion

Over the life of mine, two stretches of the Marillana Creek were diverted so that the pits E1, E2356 and E4 could be excavated. These diversions occurred in June 2018 and June 2019. The river diversion was implemented in the general head boundaries used for Marillana Creek as illustrated in Figure 5-9. General head boundaries from the diverted stretches were deactivated while new boundaries were assigned for the new stretches.
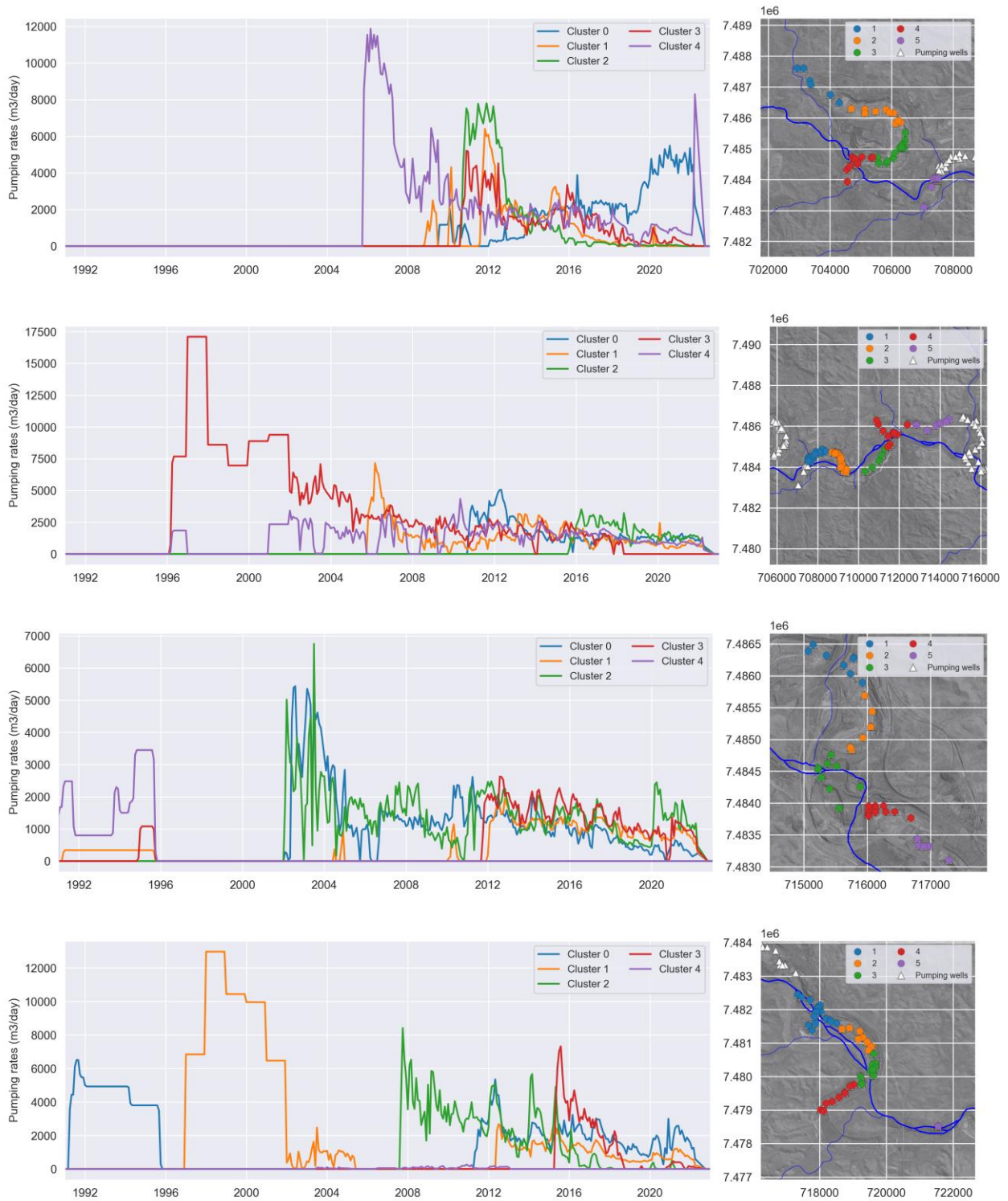
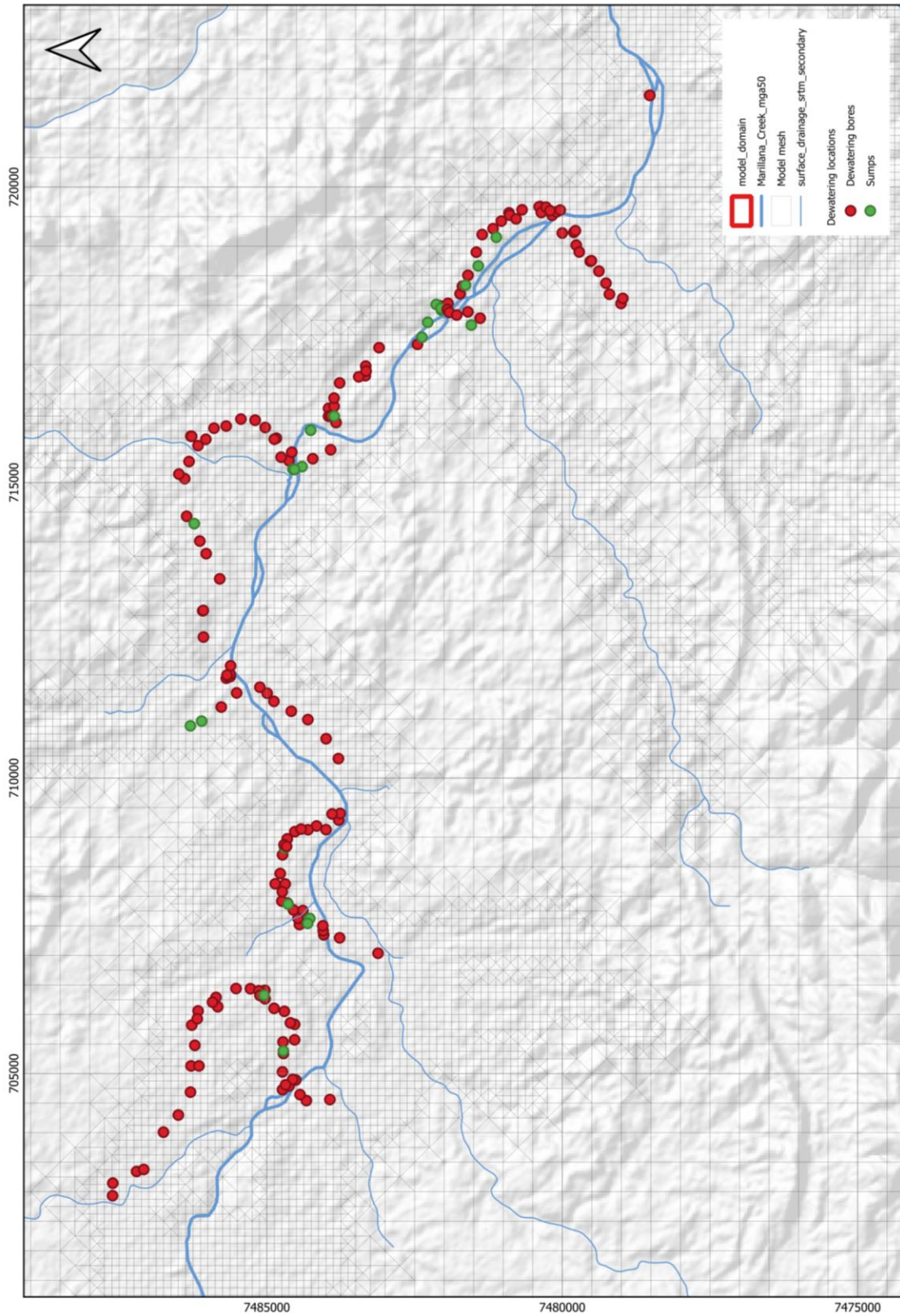Figure 5-7: Historical groundwater abstraction rates used in the model.

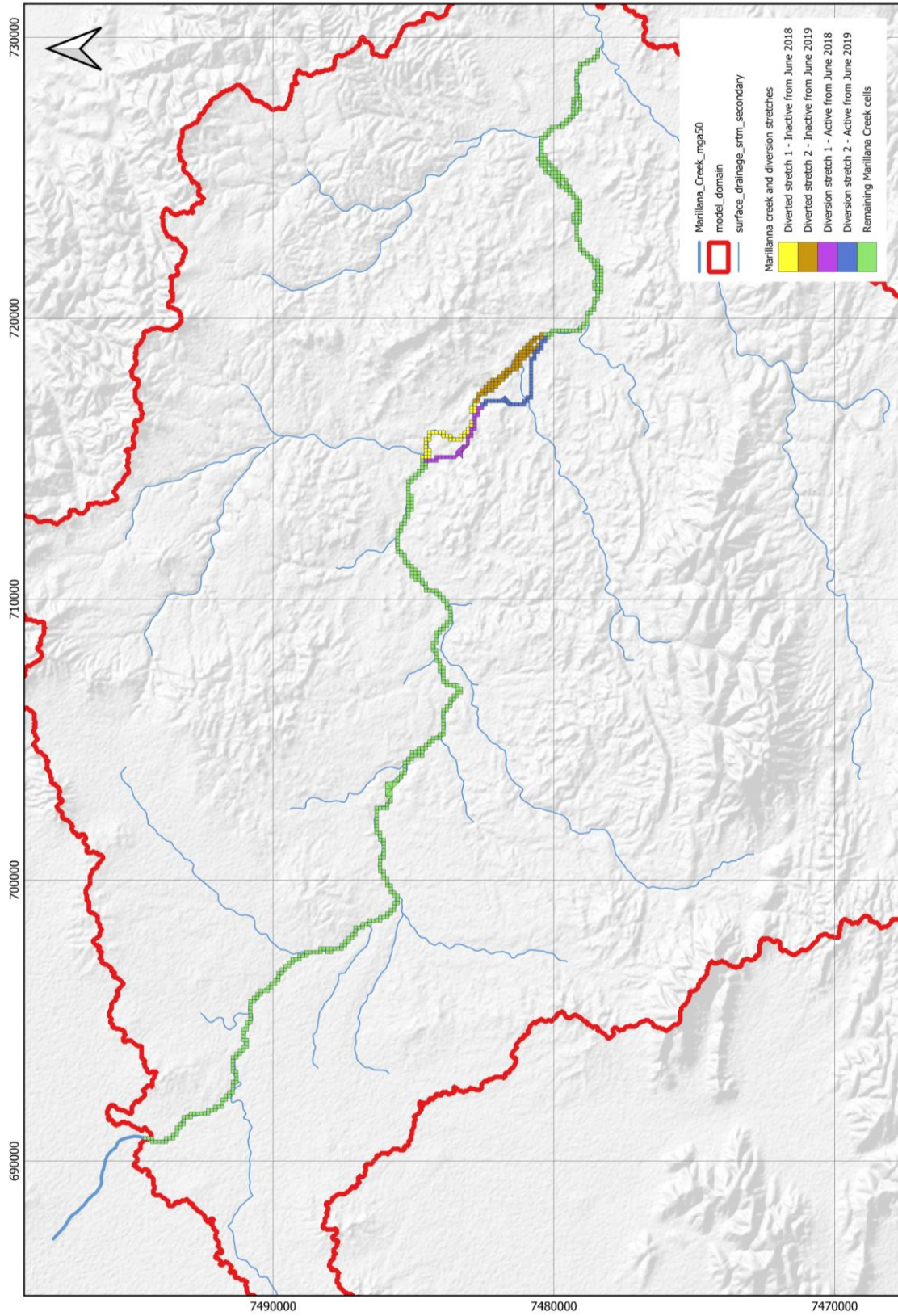Figure 5-8: Distribution of dewatering bores and sumps.

Figure 5-9: General head boundaries and diversion setup for Marillana Creek.

5.5.4 Creek discharge

Excess water originatingfrom the dewatering operations was discharged to Marillana Creek in three discharge locations (West, Central and East) since 1996, at rates displayed in Figure 5-10. Seepage from the discharge into the Alluvium Aquifer was expected to occur and is simulated using prescribed flow boundaries (WEL package).

The creek discharge boundaries were assigned in three stretches along the Marillana Creek. Each stretch was defined from the discharge point to maximum wetting front distance, based on anecdotal information from BHP WAIO (Figure 5-11). Historical discharge rates were split evenly between the cells of each discharge section, with the addition of a multiplier (adjusted during history matching) to represent the fraction of the discharged water that seeped into the Alluvium Aquifer.

For the predictive period, it was assumed that discharge rates on the West and Central points will be ceased, and that a continuous discharge of 10 ML/d will be take place at the eastern discharge point.
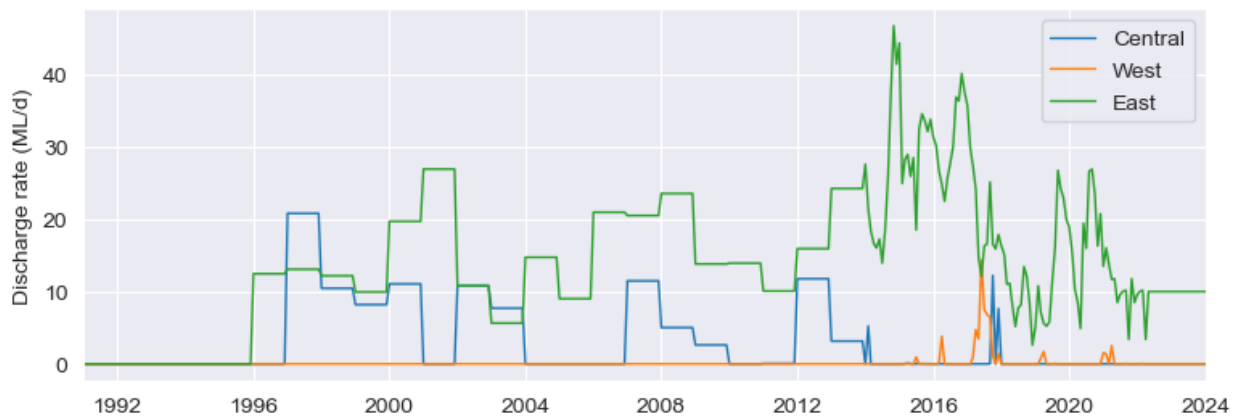

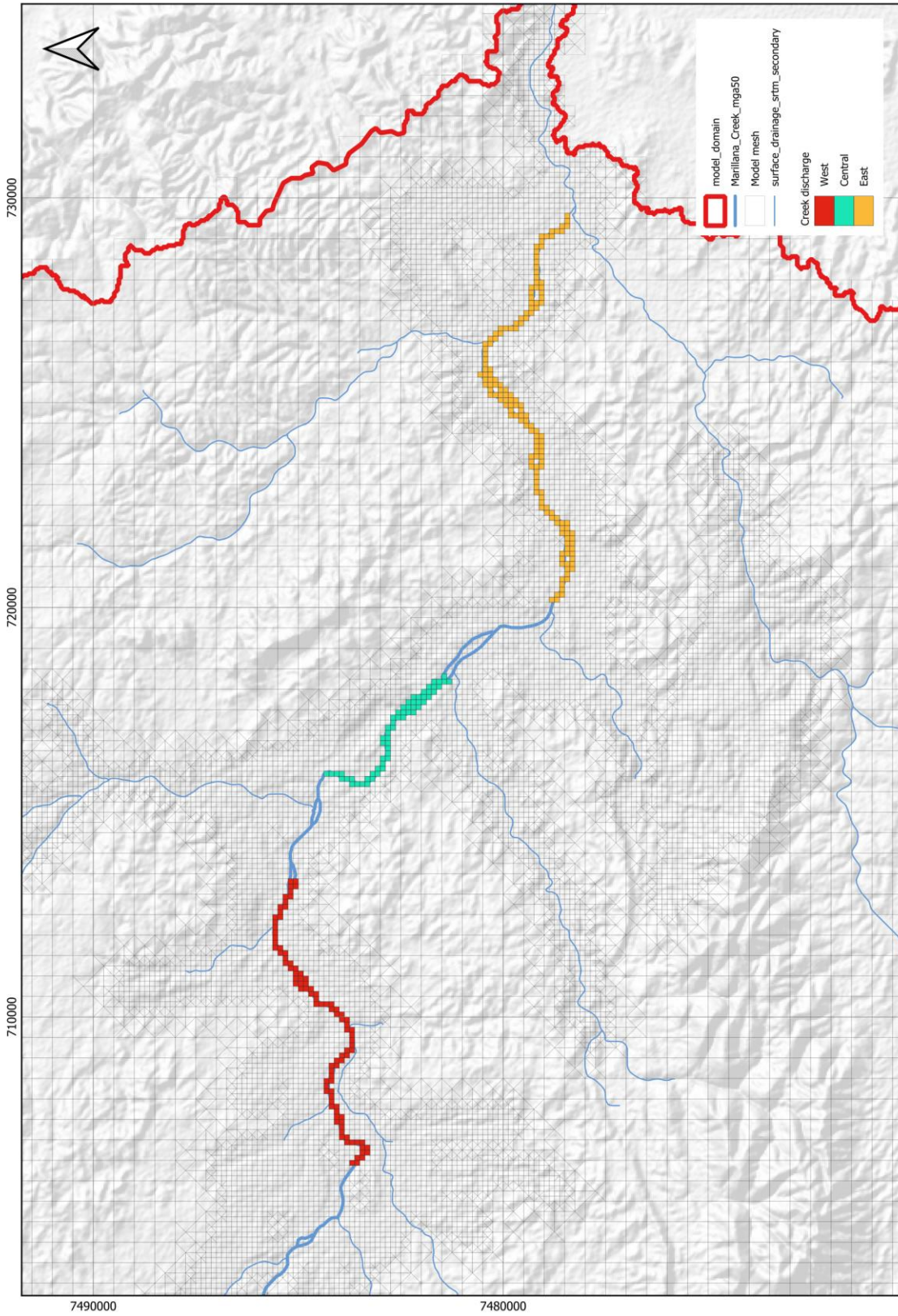Figure 5-10: Marillana Creek historical discharge rates.

Figure 5-11: Distribution of creek discharge cells.

5.5.5 Rio Tinto dewatering

Dewatering from two Rio Tinto pits (Mungadoo and Junction South West) was included in the model and simulated using the drain package (DRN).

Given that dewatering information on those pits were not available, estimates of pit elevations were created based on historical groundwater levels from nearby monitoring boreholes (in particular, HYE0113M). These values (displayed in Figure 5-12) were assigned as the boundary elevations on the CID zone, as displayed in Figure 5-13. The elevation of the pit boundaries was kept constant, once it reached the lowest level (485 mAHD), towards the end of simulation, assuming both pits will remain active throughout the life of mine.

Rio Tinto also have two other dewatering operations on Junction Central and South East pits, located in the western portion of the data. Dewatering from this pit was not included in the model given the absence of data.
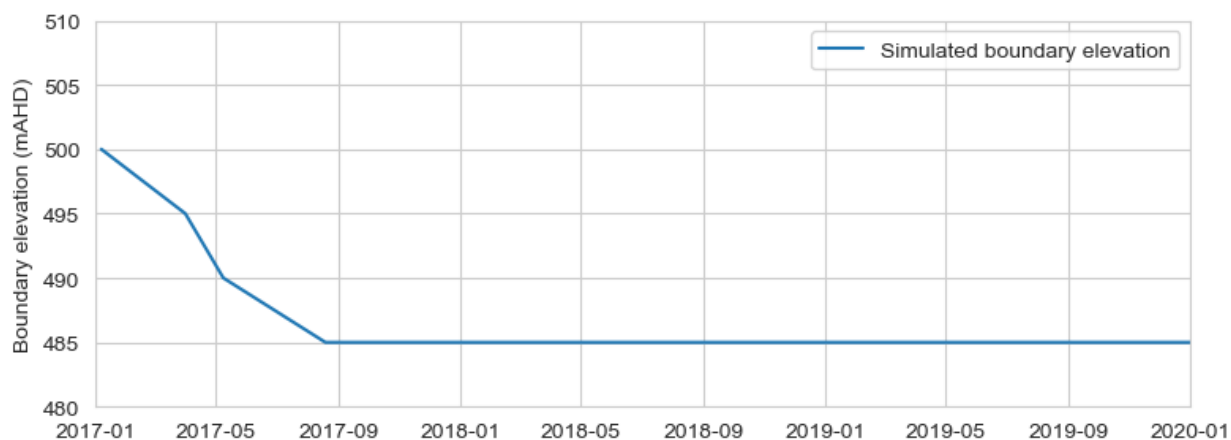
Figure 5-12: Simulated boundary elevations for the Rio Tinto Mungadoo and Junction South West pits.
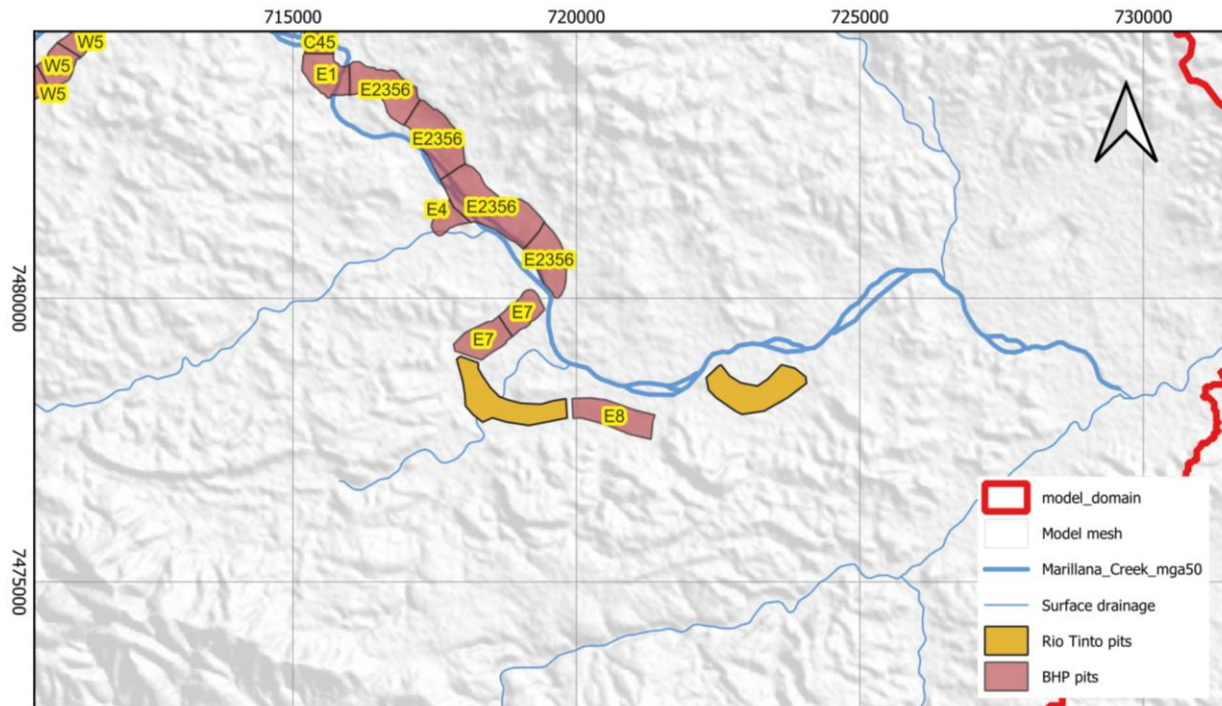
Figure 5-13: Location of the simulated Rio Tinto pits.

5.5.6 Future dewatering

Throughout the predictive period, all active BHP Yandi dewatering was simulated using drain boundary conditions (illustrated in Figure 5-14). Boundary elevations were assigned based on target groundwater levels provided by BHP WAIO, as shown in Figure 5-15.

Figure 5-14: Location of predictive BHP pits.

Figure 5-15: Simulated Yandi pit elevations for the predictive period.

6. Parameterization

6.1   Pilot point setup

The definition of model parameters was conducted using the highly-parameterized approach with pilot points, as described by Doherty and Hunt (2010). In this approach, values for the various paramete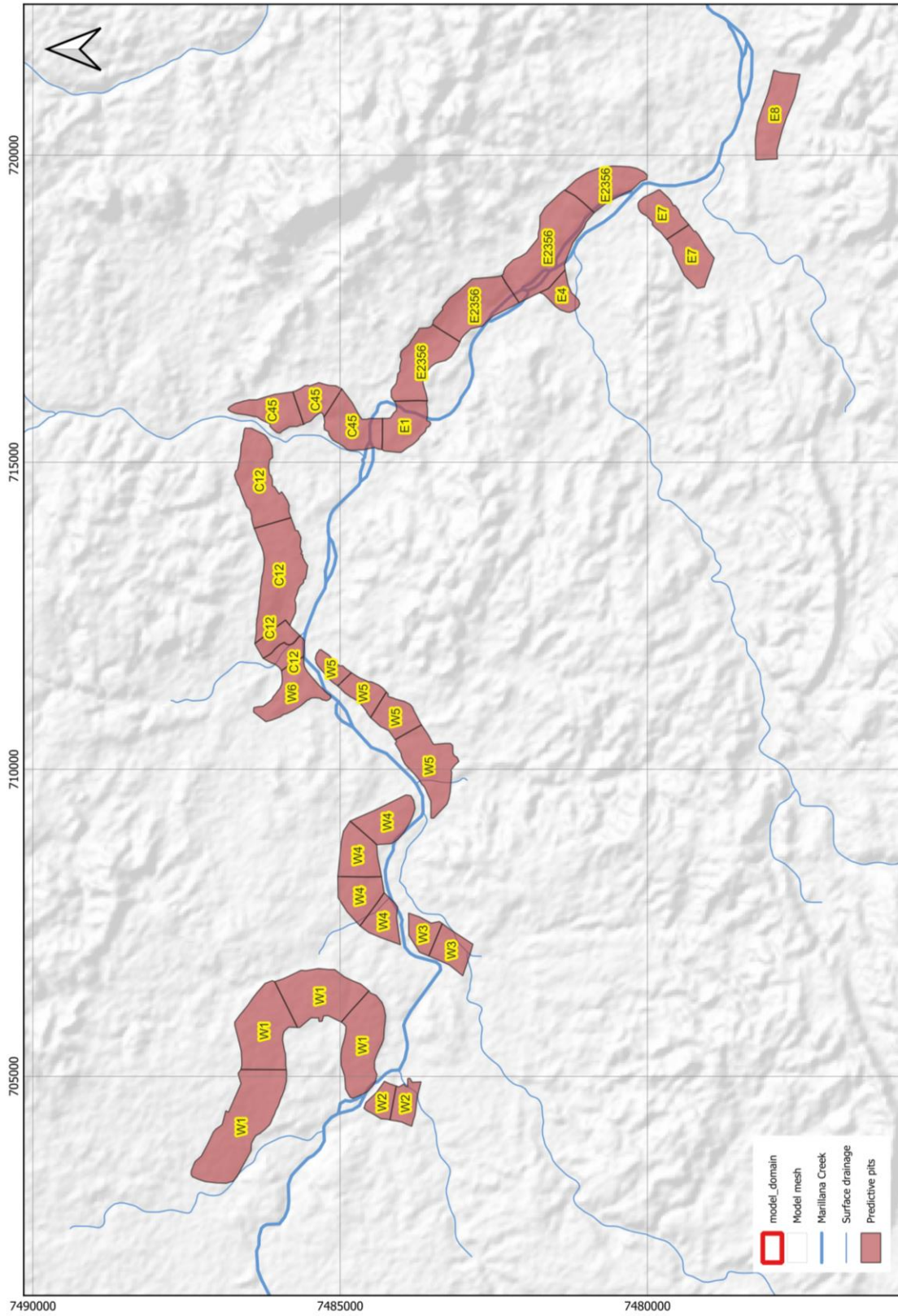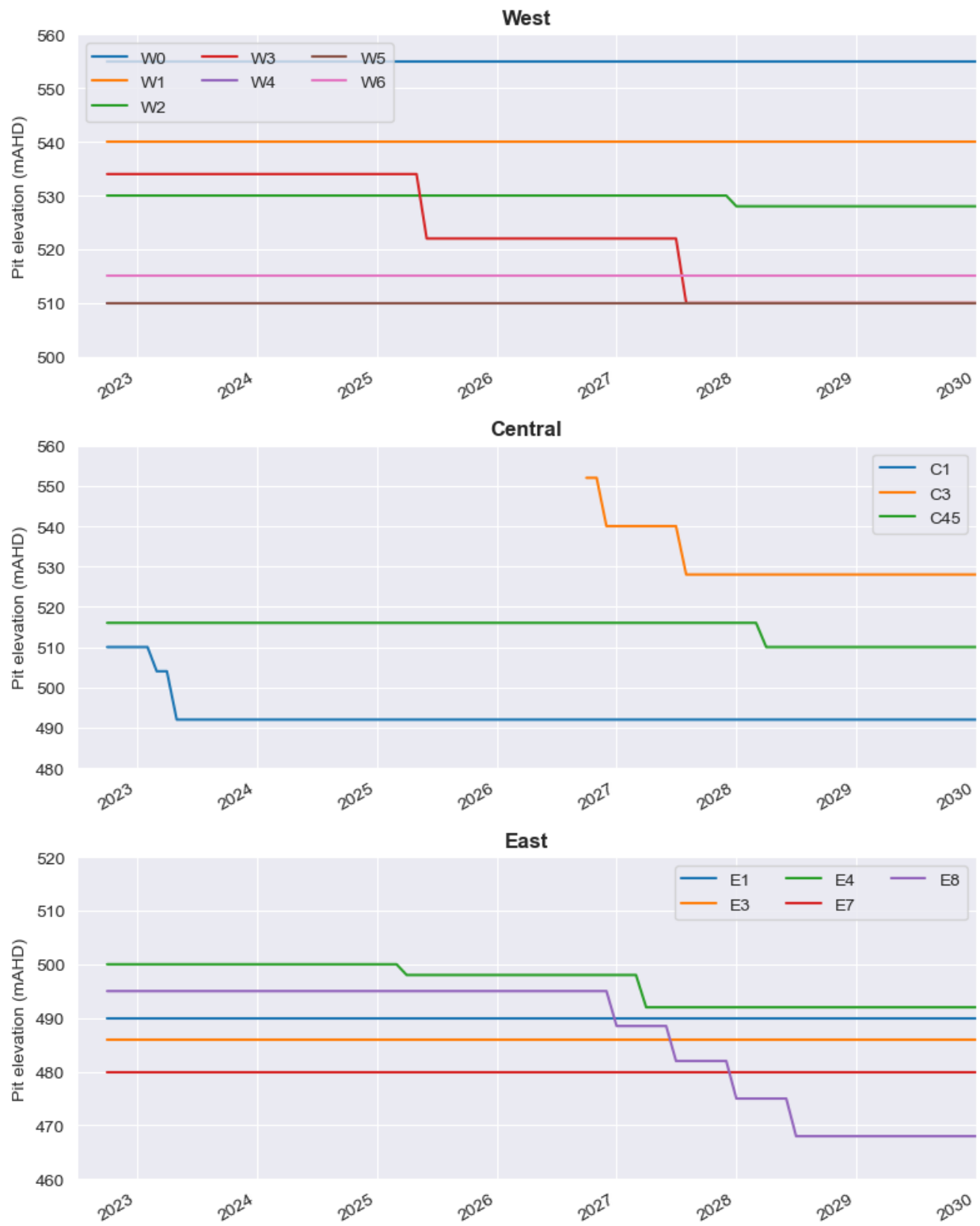rs (for both aquifers and boundary conditions) were assigned at multiple locations, known as pilot points. The values for each model cell were then determined by interpolation of the pilot point values. This method captured the variability within the different hydrogeological units and boundaries, and also laid the basis for the uncertainty analysis workflows.

Multiple pilot point groups were defined for the different hydrogeological units and boundary conditions, displayed in Figure 6-1. Pilot points for the different aquifer properties were defined in a regular grid pattern with local refinement, while pilot points for the boundary parameters were distributed along their extension. The pilot point spacing was defined roughly as the distance between 4 cells to ensure a smooth transition of pilot point values.
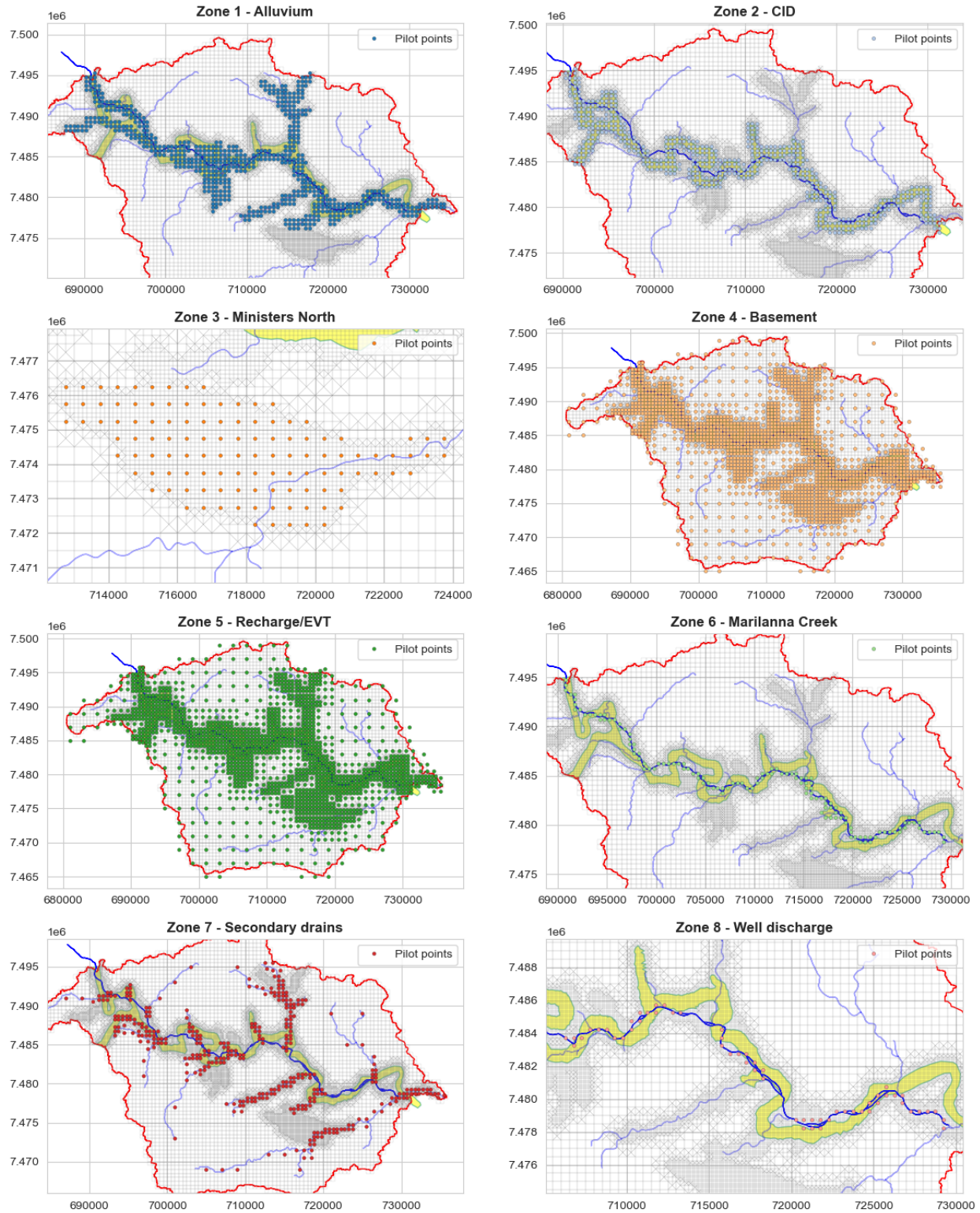
Figure 6-1: Distribution of the pilot points for the different zones.

6.2 Hydrogeological parameter ranges

Pre-calibration ranges for the different model inputs were developed based on conceptualization and earlier hydrogeological studies conducted in the area.

Table 2 summarizes the parameter ranges adopted in the model recalibration. Prior parameter realizations were used using the initial values as parameter means, while the upper and lower bounds roughly equate to the 95% confidence intervals. Spatial correlation between pilot points was also incorporated in the definition of prior realizations with the use of covariance matrices, under the assumption that pilot point values lose correlation (i.e., reach the sill of the defined variograms) beyond three times the pilot point spaces.

7. History Matching

7.1 Methodology

History matching refers to the process of adjusting model parameters, within ranges compatible with hydrogeological conceptualization, until the model is able to adequately reproduce historical data or past system behavior. The PESTPP-IES (White et al., 2018) iterative ensemble smoother (IES) was employed to calculate a suite of parameter fields, all of which minimize the misfit between simulated and measured observations. In broad terms, IES works by iteratively adjusting an ensemble of initial model parameter sets (the prior parameter ensemble) until they all adequately fit observation data. The prior parameter set is generated by sampling random parameter values from a user-specified statistical distribution which encapsulates expert knowledge (i.e., conceptualization) of parameter values and their co-variances. Thus, the parameter sets obtained through history matching (the posterior parameter ensemble) reflects the information content of both expert knowledge and measured observation data. By simulating a prediction with the posterior parameter ensemble, a sample of the forecast uncertainty is obtained.

The IES procedure was performed using an ensemble of 1,000 parameter realizations and over 55,000 observations. A relatively large number of parameter realizations (typically between 200-500) has been adopted to avoid the need of localization procedures (which may delay the IES iterations on model runs with more than 10,000 parameters) and minimize the potential for spurious correlations.

Parameter bounds were enforced both during the generation of the prior realizations and throughout the IES iterations, ensuring that the parameter values stayed within the conceptual model ranges.

Table 2 – Pre-calibration (prior) parameter values and likely ranges.

Parameter	Hydrogeological Unit / model feature	Initial parameter value	Lower Bound	Upper Bound
Horizontal Hydraulic Conductivity – Kh (m/d)	Alluvium Aquifer	1.07E1	1.00E-1	4.00E1
	CID Aquifer	2.38E1	1E0	7.5E1
	Basement Aquifer	3.08E-1	1.00E-3	1.00E0
	Ministers North Aquifer	1.56E0	1.00E-1	4.00E1
Vertical Hydraulic Conductivity – Kv (m/d)	Alluvium Aquifer	8.00E0	1.00E-1	4.00E1
	CID Aquifer	2.50E1	1.00E-1	7.50E1
	Basement Aquifer	1.00E-2	1.00E-4	1.00E0
	Ministers North Aquifer	1.00E1	1.00E0	4.00E1
Specific Yield – Sy (-)	Alluvium Aquifer	1.61E-1	1.00E-3	2.50E-2
	CID Aquifer	6.56E-2	1.00E-3	2.00E-1
	Basement Aquifer	5.80E-2	1.00E-3	2.00E-1
	Ministers North Aquifer	8.40E-2	1.00E-3	2.00E-1
Specific Storage – Ss (-)	Alluvium Aquifer	1.00E-4	1.00E-6	1.00E-3
	CID Aquifer	4.45E-6	1.00E-6	5.00E-4
	Basement Aquifer	1.75E-4	1.00E-6	5.00E-4
	Ministers North Aquifer	8.00E-4	1.00E-6	1.00E-4
Recharge (% of mean annual rainfall)	Layer 1	6.10E-3	1.00E-3	1.50E-1
Evapotranspiration – multiplier (-)	Layer 1	1.1E-8	8.00E-1	1.10E0
Evapotranspiration – Extinction Depth (m)	Layer 1	1.00E0	5.00E-1	1.00E1
Marillana Creek conductance	Marillana Creek	5.28E1	1.00E-1	1.00E2
Marillana Creek max. constraint (mm)	Marillana Creek	2.62E0	1.00E0	5.00E0
Marillana Creek min. constraint (mm)	Marillana Creek	6.70E0	5.1E0	1.00E0
Surface drainage elevation correction (m)	Layer 1	2.00E0	1.00E-3	3.00E0
Marillana Creek discharge multiplier	Marillana Creek	5.30E-3	1.00E-3	1.00E-2

7.2   Observation data

The history matching was undertaken against historical groundwater level measurements from hundreds of monitoring boreholes (Figure 7-1) distributed over the entire model domain and dating back to 1991. For reporting purposes, priority boreholes were chosen based on their location, data quality and time series length. All the groundwater levels utilized in the history matching are presented in the Appendix A.

Temporal head differences were included as an additional metric for history matching. This metric was particularly important for the Yandi model to encapsulate information regarding the drawdown induced by the mining operations, as well as groundwater level changes associated with transient recharge (both diffuse rainfall infiltration and seepage from Marillana Creek). Groundwater level time series from each monitoring borehole were evenly divided in five parts, and head differences between the start and end of each part were included as observations. Furthermore, the total head difference between the first and last measurement of each borehole was also included as an observation.

Lastly, given that the auto flow reduce option was enabled in the model, simulated pumping rates were compared against their corresponding prescribed values to ensure that historical rates were properly simulated. This metric was introduced to constrain hydraulic parameters to ranges that would enable historical pumping rates to be simulated (for example, high-yielding dewatering boreholes would require high conductivity values).

Figure 7-1: Location of monitoring boreholes used in the history matching.

7.3   Calibration results

7.3.1 Groundwater levels

Statistics were generated for each simulated groundwater level hydrograph based on simulated results from the 1,000 model realizations obtained during history matching. Simulated median groundwater levels from all the calibrated realizations are illustrated for the priority monitoring boreholes on Figure 7-2 to Figure 7-7. Full statistical plots showing hydrographs percentiles for all monitoring boreholes are presented in Appendix A.

Simulated groundwater levels for the historical period show in general a very good agreement with the historical measurements for the vast majority of boreholes. In the few monitoring locations where there is a discrepancy between simulated and observed groundwater levels, the mismatch can be attributed to the following reasons:

- Potential errors in historical dewatering and sump rates (in particular prior to 2010),
- Simplifications associated with the development of Rio Tinto pits and lack of information regarding dewatering on Rio Tinto's Junction Central and South East pits,
- Mismatch between screen elevations of the monitoring boreholes and model layers,
- High density of monitoring boreholes (in relation to model cell size and pilot point spacing),
- Model defects associated with the geometry of the different hydrogeological units.

The high density of monitoring boreholes may reflect heterogeneity and hydrogeological features in scales that are not fully incapsulated by the model, especially when the distance between monitoring boreholes is shorter than the pilot point spacing (cell size). In situations where multiple boreholes are positioned within the same model cell or are closest to the same pilot point, sub-optimal matching between simulated and observed heads may occur as the same parameter is being adjusted to replicate the behavior of multiple hydrographs.
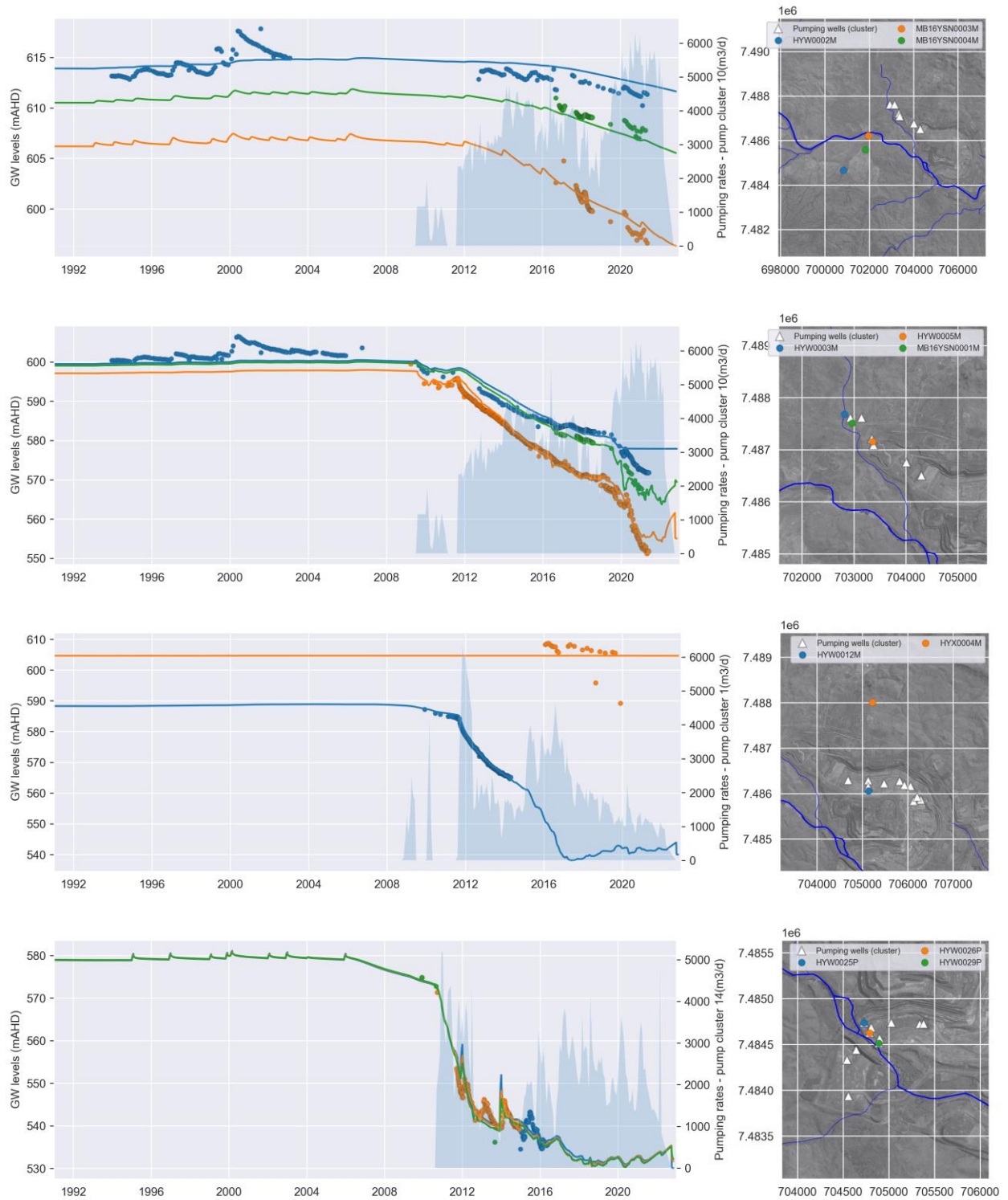
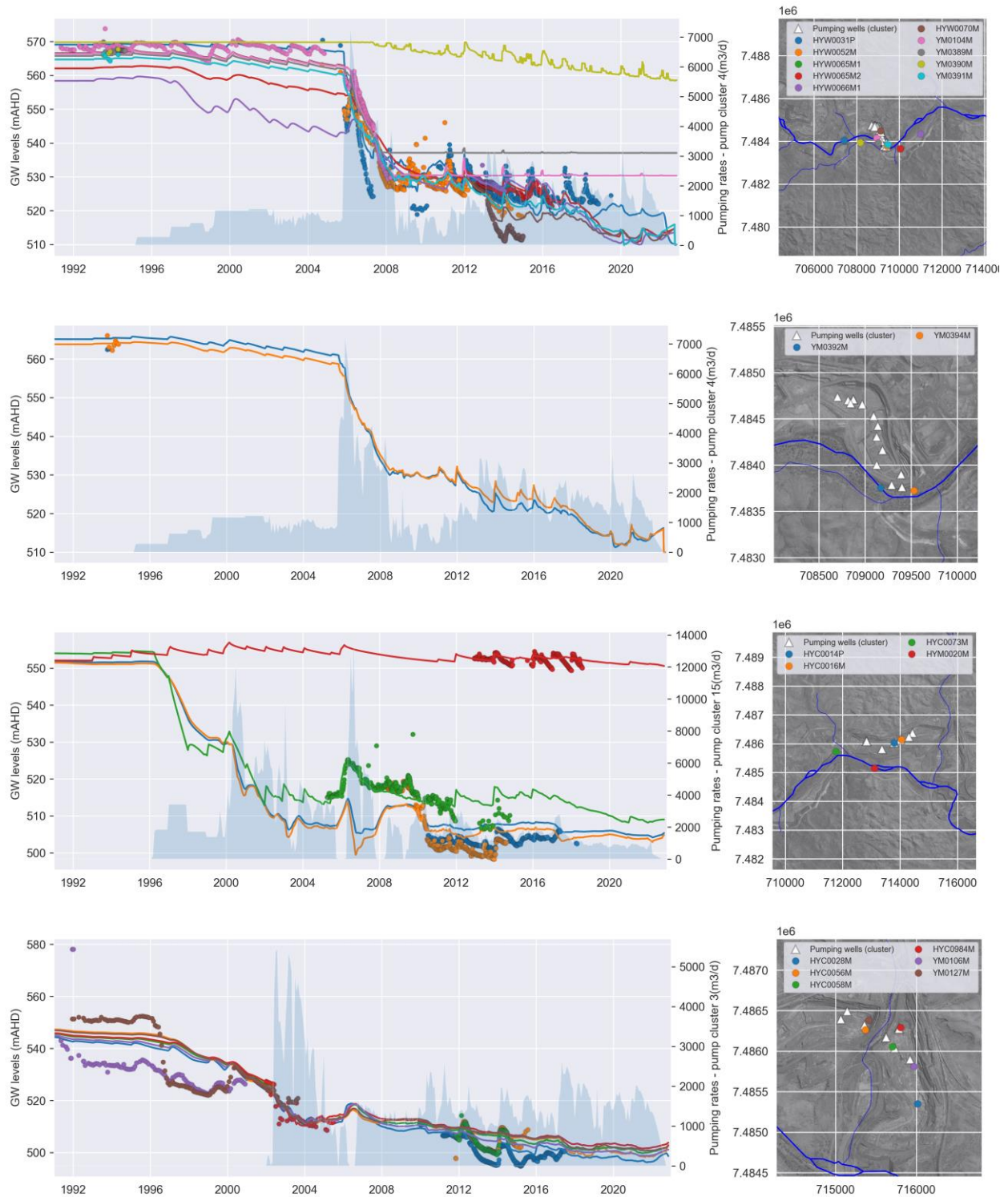Figure 7-2: Simulated (median) and observed groundwater levels at selected locations.

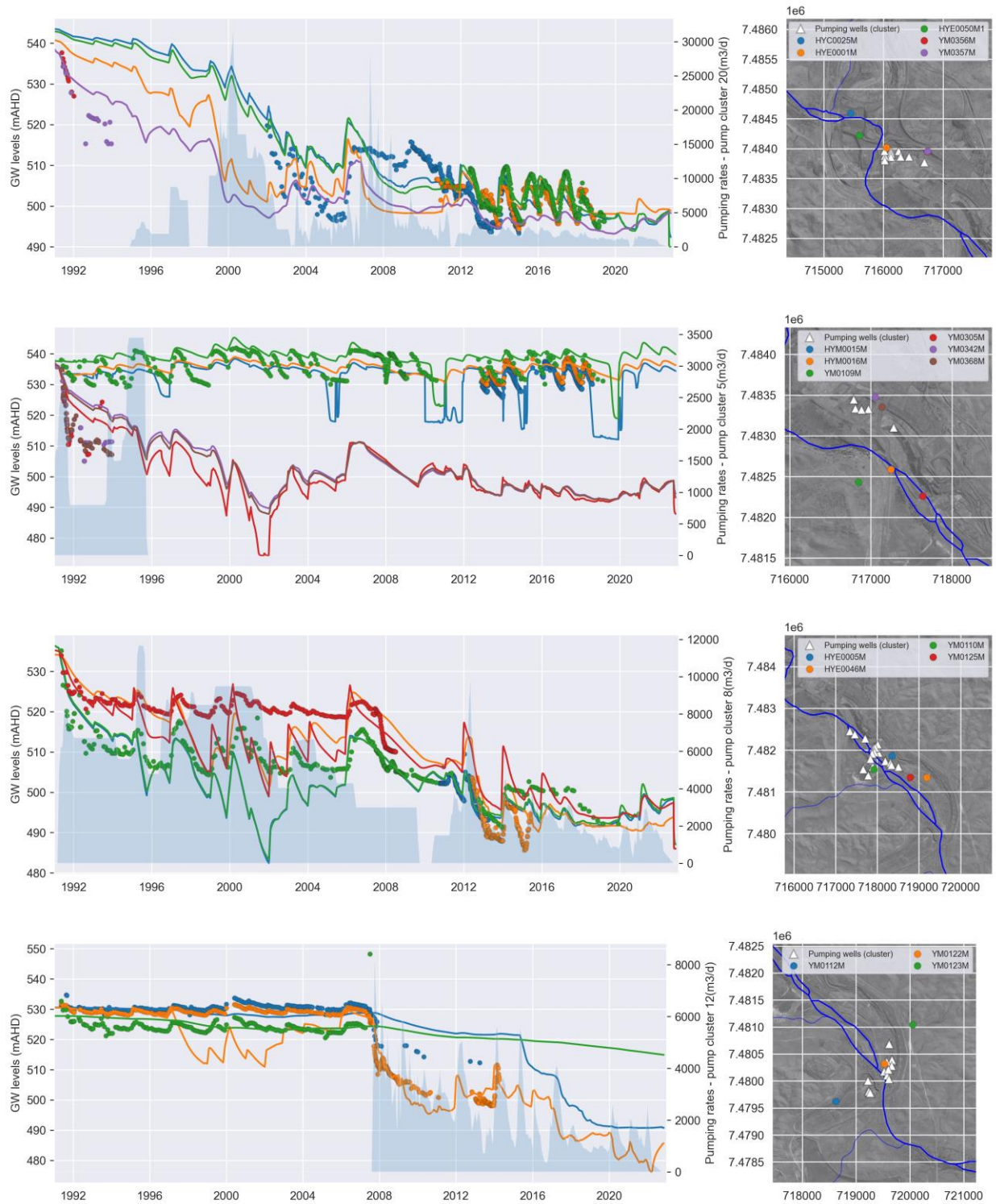Figure 7-3: Simulated (median) and observed groundwater levels at selected locations (continuation).

Figure 7-4: Simulated (median) and observed groundwater levels at selected locations (continuation).
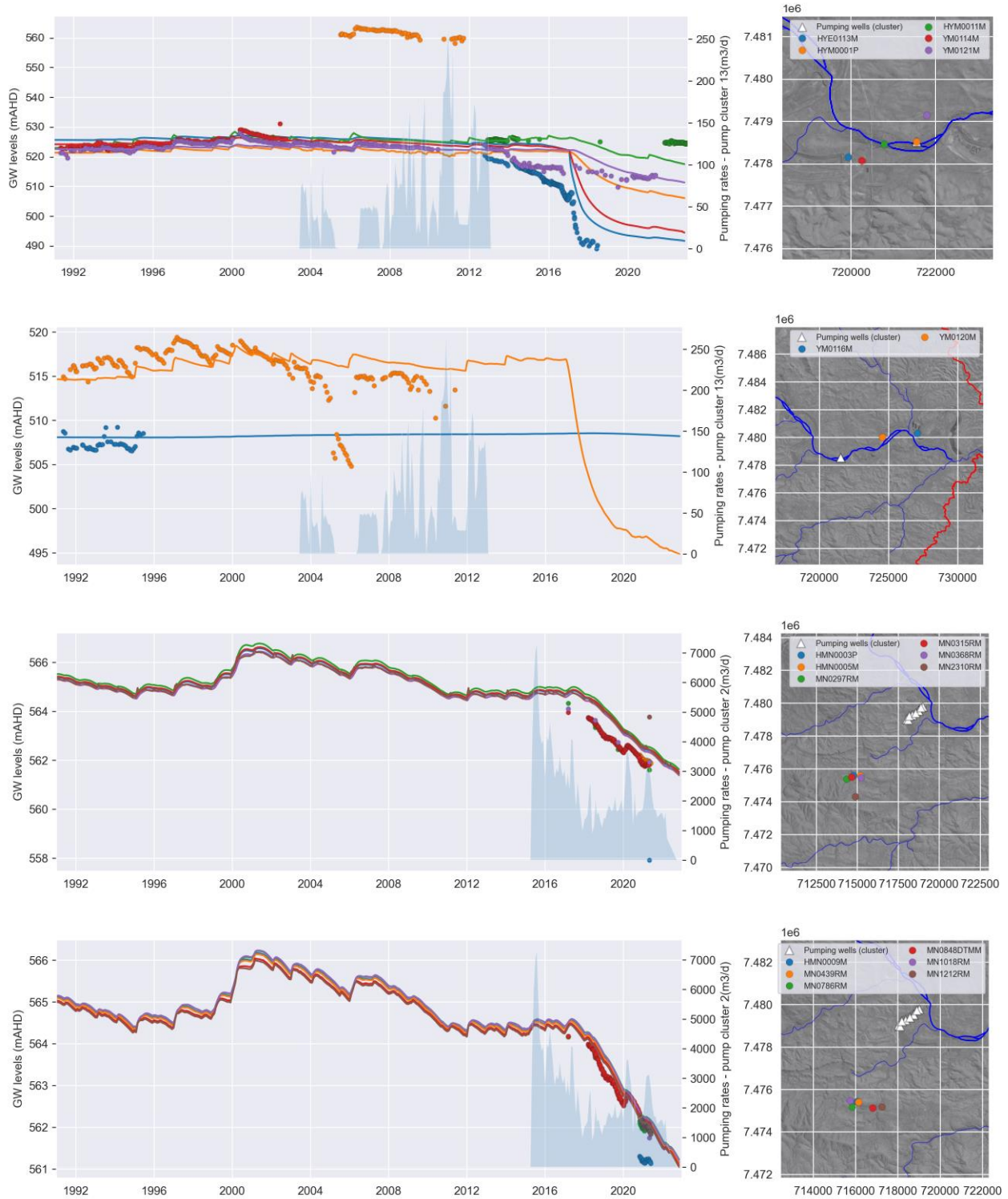
Figure 7-5: Simulated (median) and observed groundwater levels at selected locations (continuation).
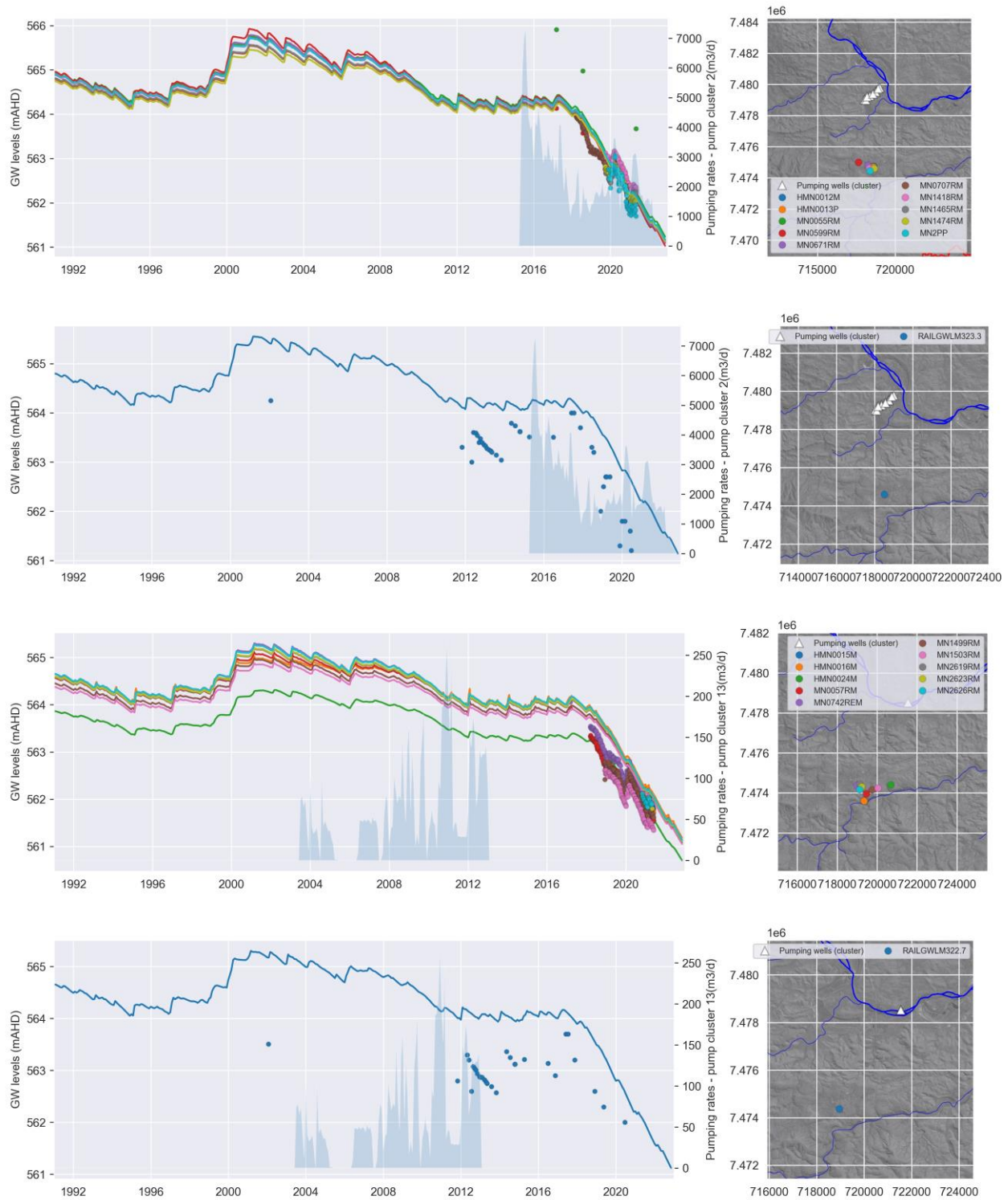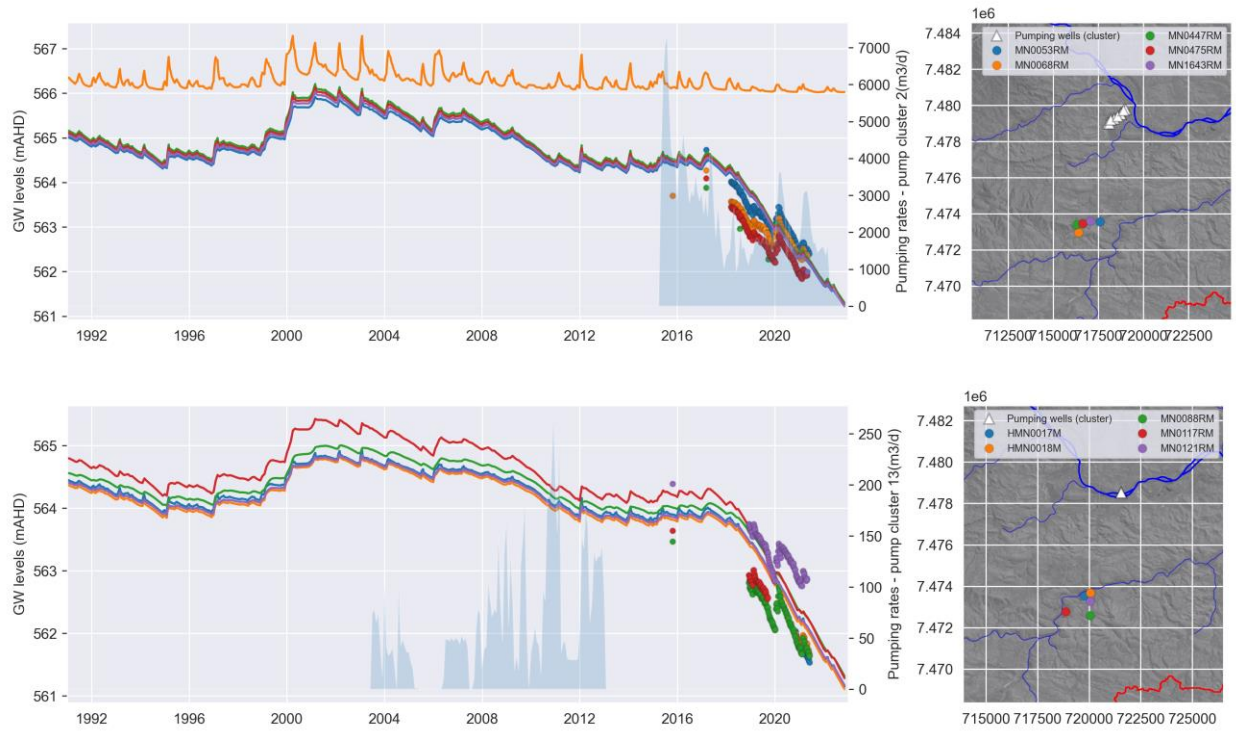
Figure 7-6: Simulated (median) and observed groundwater levels at selected locations (continuation).

Figure 7-7: Simulated (median) and observed groundwater levels at selected locations (continuation).

7.3.2 Hydrogeological parameters

Histograms for the calibrated pilot point values of the different groups are displayed in Figure 7-8 and Figure 7-9, while spatial distribution of mean parameter values are displayed in Figure 7-10 to Figure 7-14. The broad range of parameter values denotes the high degree of non-uniqueness and parameter uncertainty, despite its reduction through the history matching process. Hydrogeological parameters for the CID Aquifer tend in general to present a lower spread than the other units, probably related to the fact that the majority of monitoring boreholes in the area are within this unit or in its immediate vicinity. It also noted that several parameter distributions show a relative regular distribution with higher percentage values at the parameter bounds, sometimes resembling a bi-modal distribution. This is associated with fact that IES is enforcing parameters to comply with the parameter bounds defined by conceptualization.

The spatial distribution of the mean parameter values shows reasonable patterns and in line with conceptualization. Smaller scale variations are observed within the footprint of Alluvium and CID aquifers, associated with the fact that the pilot point density is higher in these locations.
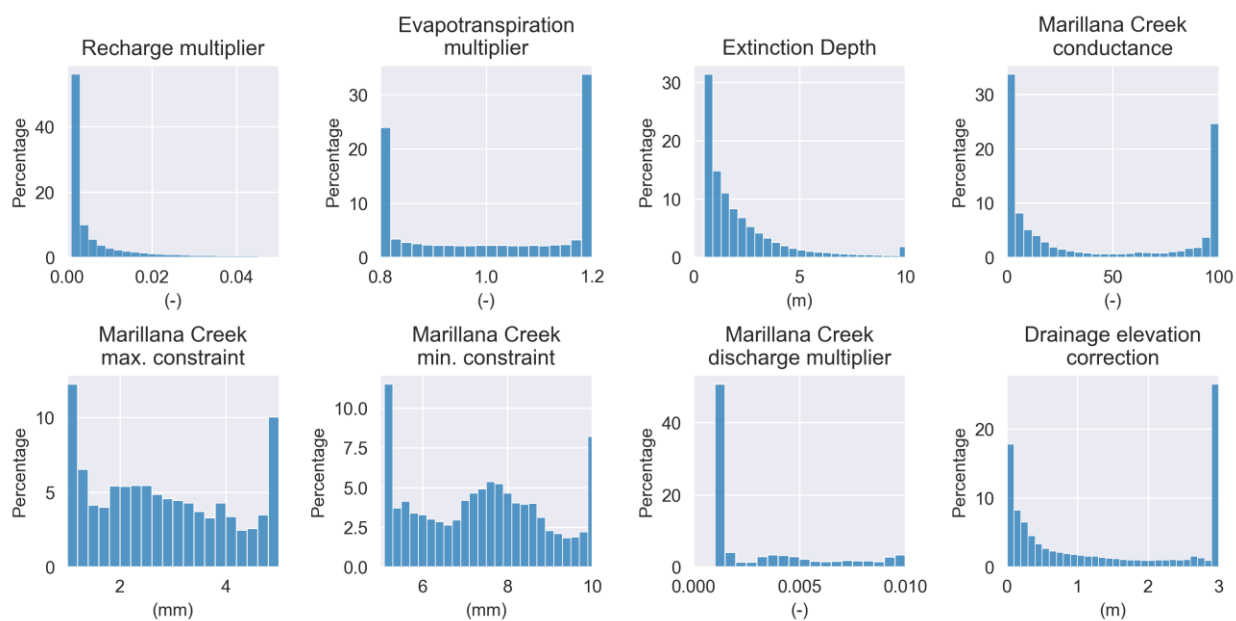

Figure 7-8: Calibrated parameter values (pilot points) for the different units and parameter types.
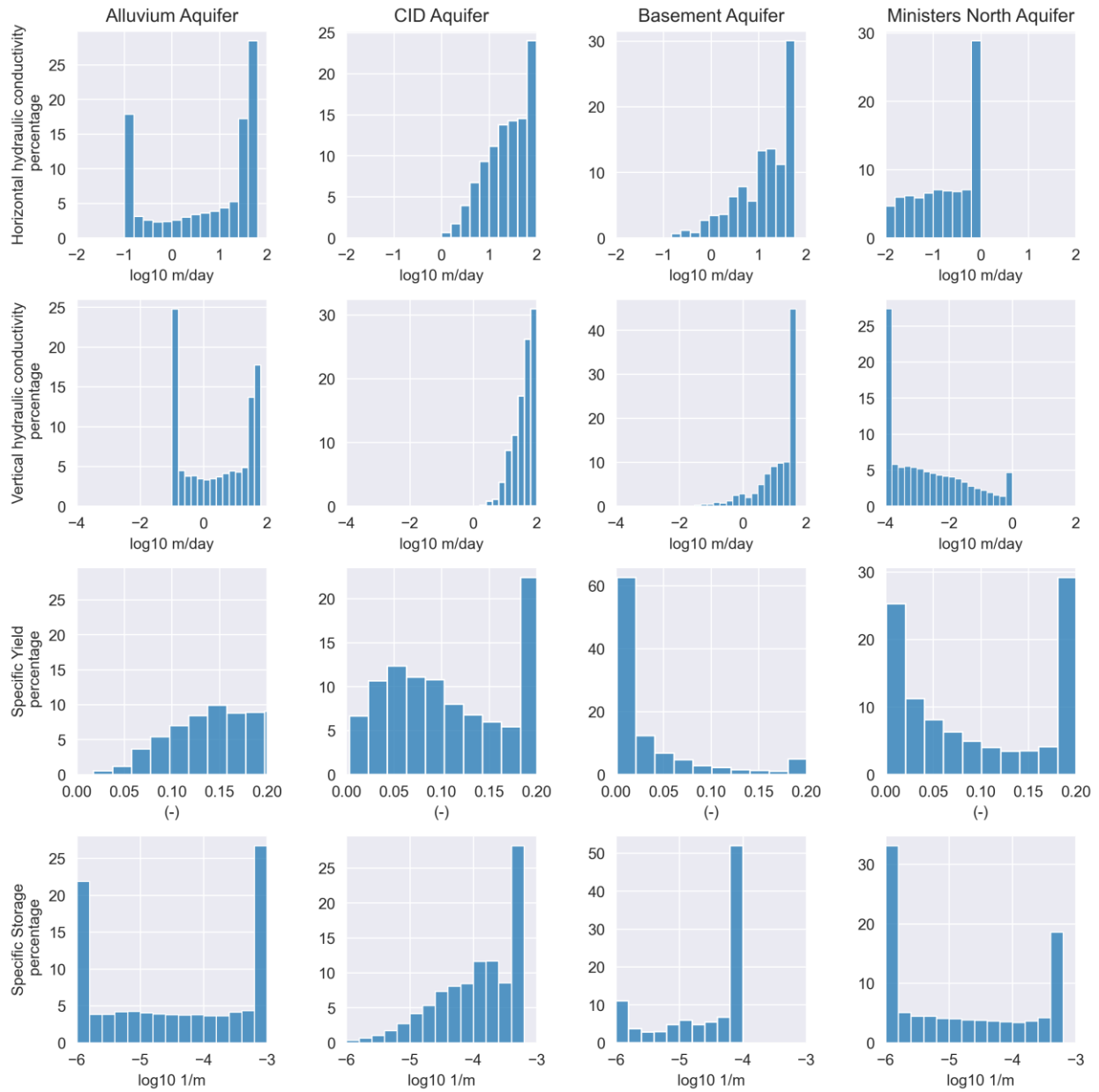
Figure 7-9: Calibrated parameter values (pilot points) for the different units and parameter types (continuation).
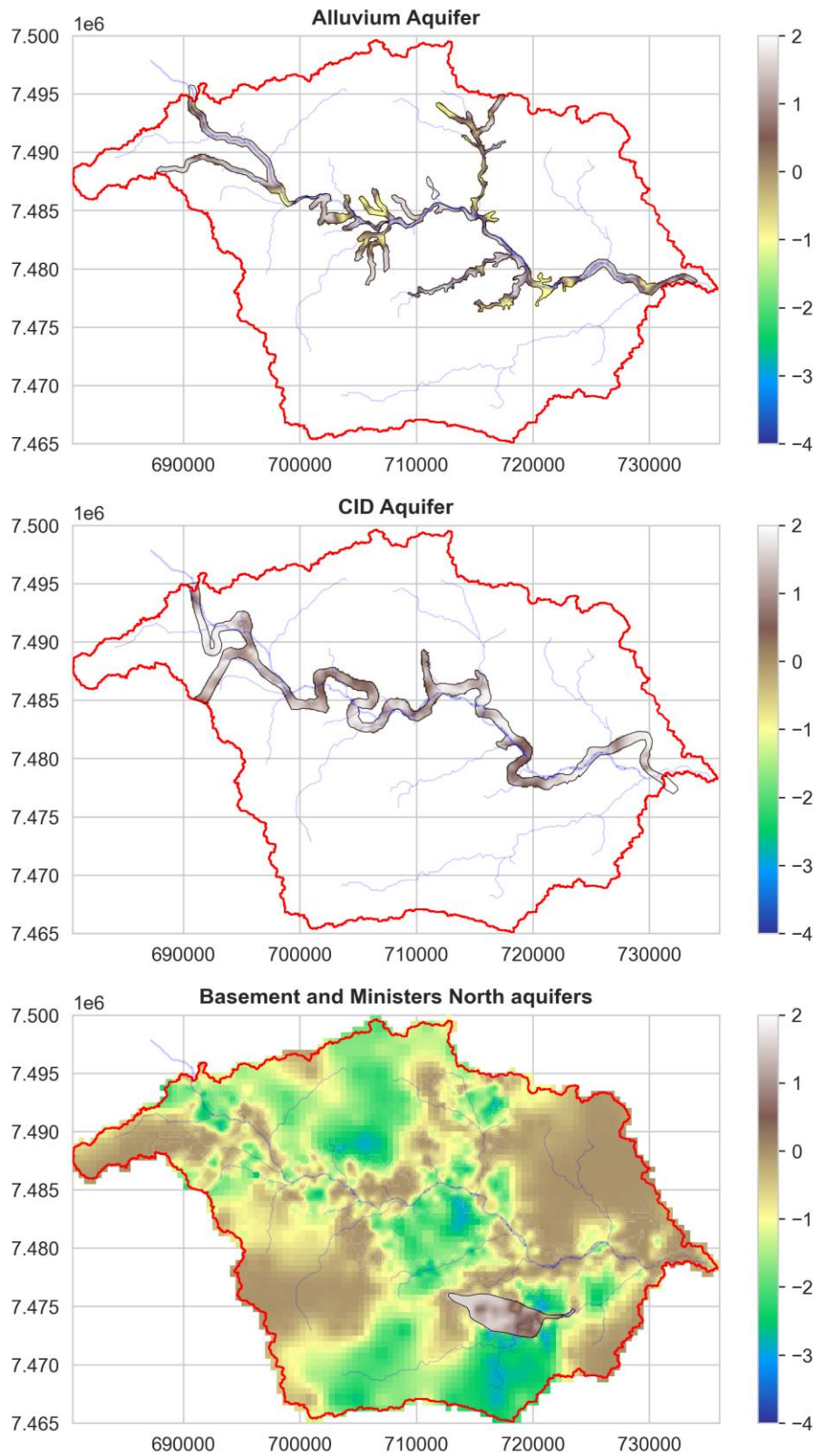
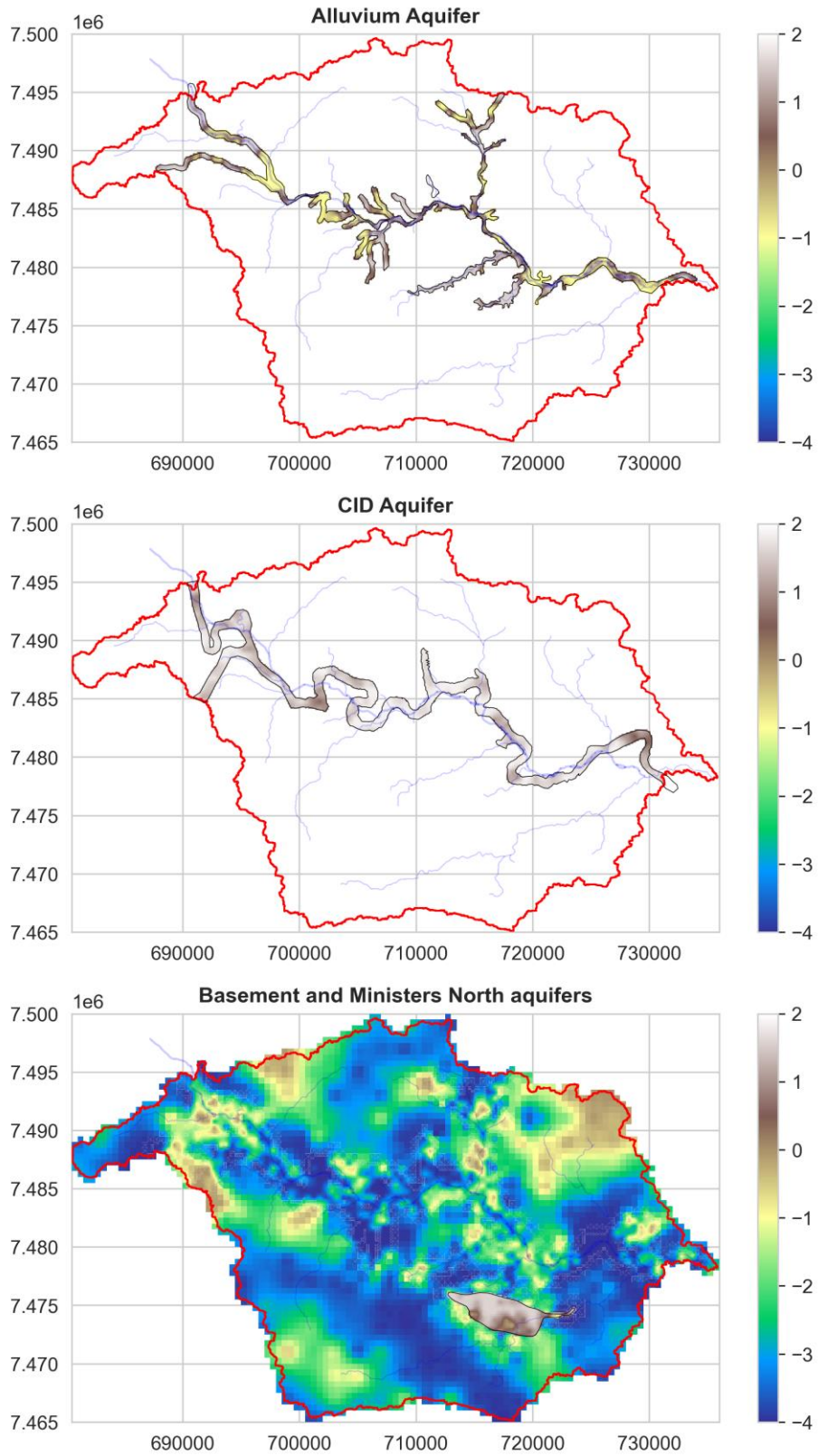Figure 7-10: Median horizontal hydraulic conductivity values (log10, m/day).

Figure 7-11: Median vertical hydraulic conductivity values (log10, m/day).
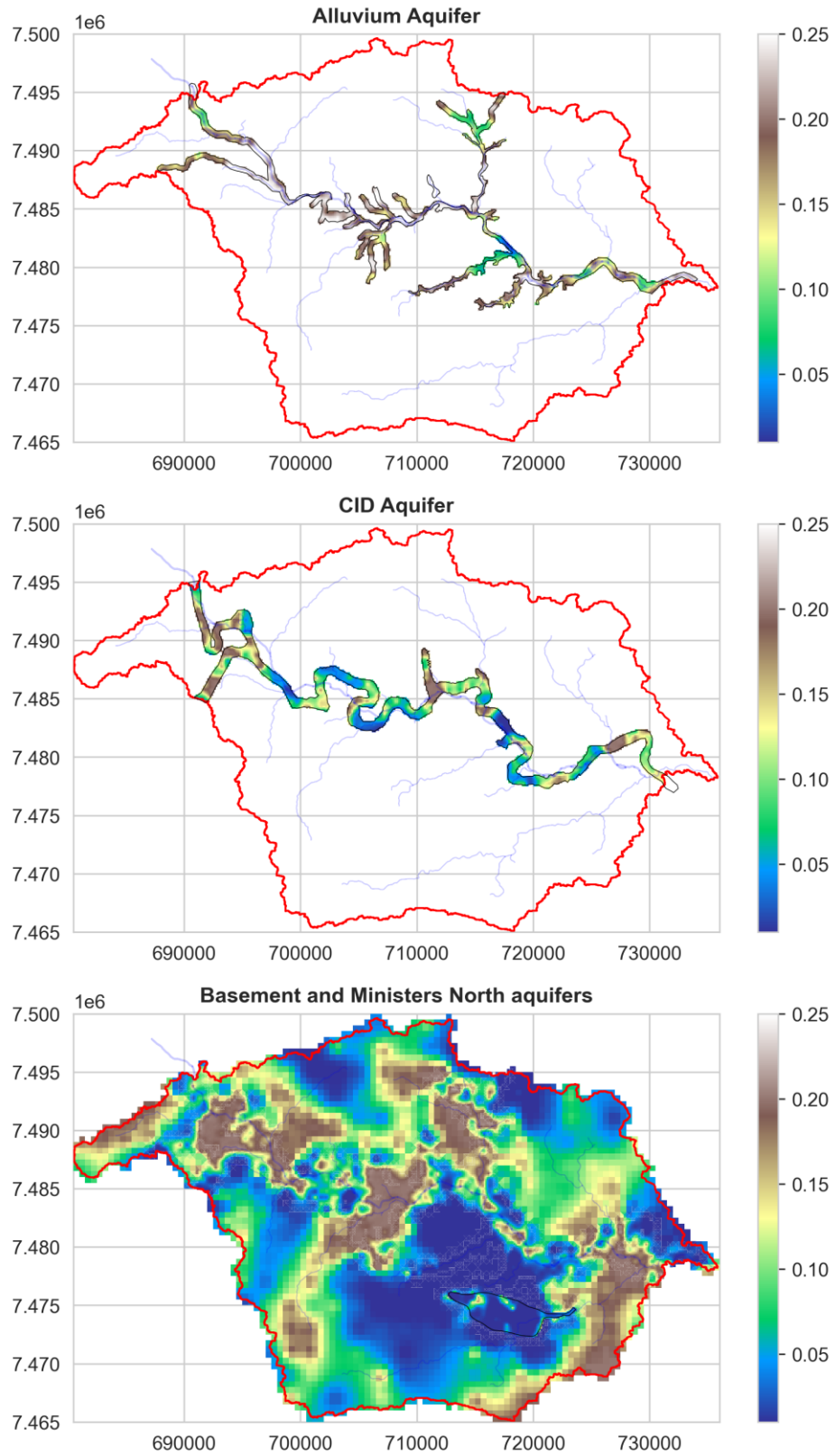
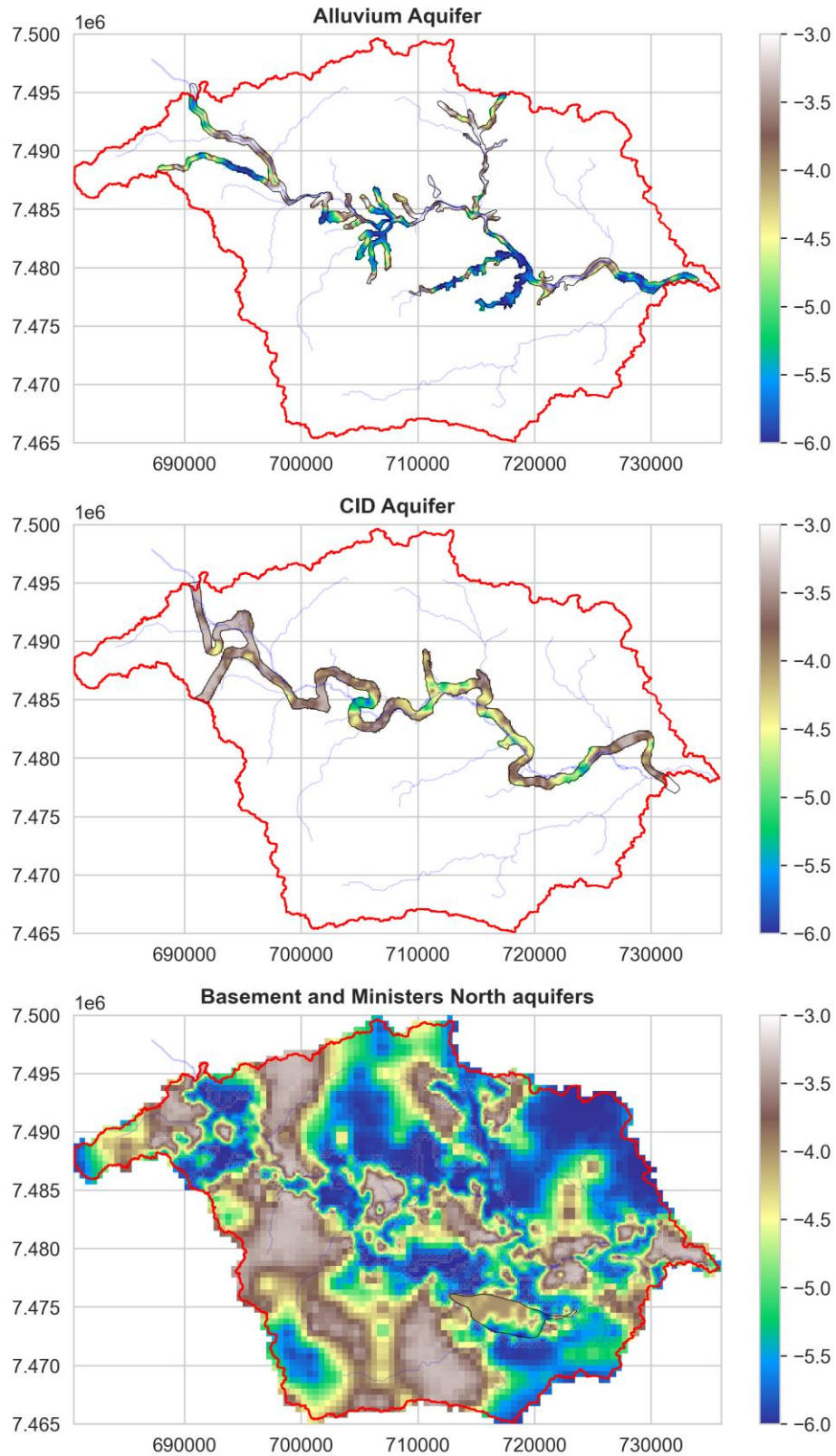Figure 7-12: Median specific yield values (-).
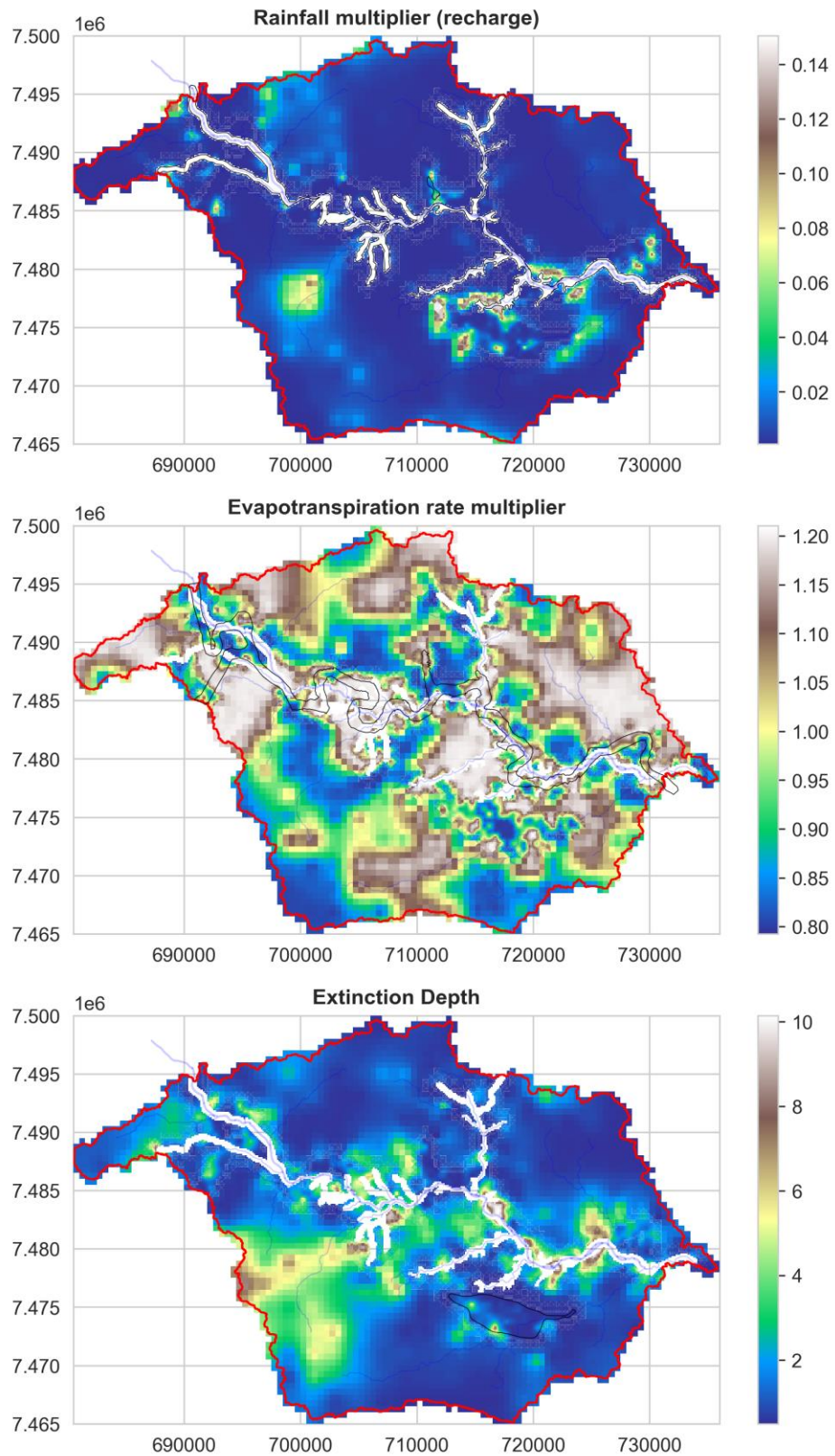
Figure 7-13: Median specific storage values (1/m).

Figure 7-14: Median values for rainfall multiplier (-), evapotranspiration rate multiplier (-) and extinction depth (m).

7.3.3 Mass balance

Hydrographs plots displaying flow rates for the different component parameters are presented in Figure 7-15 to Figure 7-18. Simulated flow rates for dewatering wells and sumps are reported for each well/sump individually and reconciled with prescribed values in Appendix B.

Overall, the mass balance plots show the predominance of unconfined storage for both in- and outflows, which agrees with the conceptual model (where lower recharge rates were expected). Diffuse recharge shows considerable volumes over the model domain but are relatively small compared to Marillana Creek when areas of influence are considered. Inflows from Marillana Creek occur in quasi-discrete episodes, which are triggered by the minimum thresholds defined for the General Head Boundaries. Lastly, simulated seepage flows originated from discharge into Marillana Creek indicated that, from the total water volumes discharged in the creek, approximately 50% infiltrates into underlying aquifers.

In terms of outflows, evapotranspiration (after unconfined storage outflows) is the main outflow source, occurring predominantly in topographical depressions surrounding present day surface drainage. Evapotranspiration in the vicinity of Marillana Creek is also considerable, given the seepage from the creek into surrounding aquifers, as well as discharge into the creek. Small flows from the aquifers into Marillana Creek are also observed following large rainfall events. Lastly, simulated dewatering at Rio Tinto pits shows substantial rates, with a peak of approximately 60 ML/d in 2017, decreasing to 10 ML/d towards the end of the calibration period.

Mass balance errors (displayed in Figure 7-19) show small values under 2% for most realizations and time steps. Slightly higher values of up to 5% are observed in periods of elevated rainfall and are likely related to significant episodic inflows from rainfall recharge and the Marillana Creek General Head Boundaries.

Unconfined storage inflow

Confined storage inflow
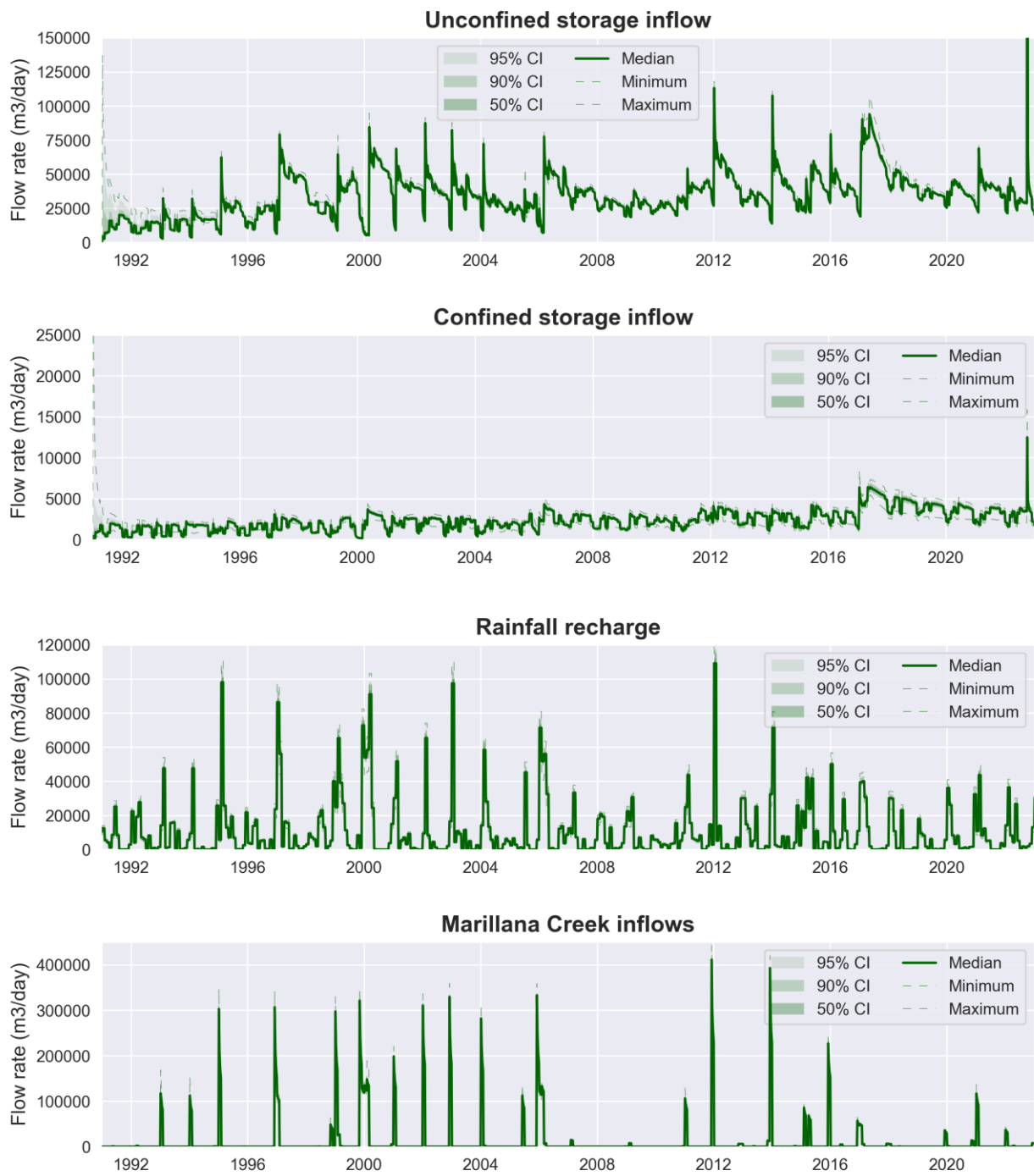
Rainfall recharge

Marillana Creek inflows

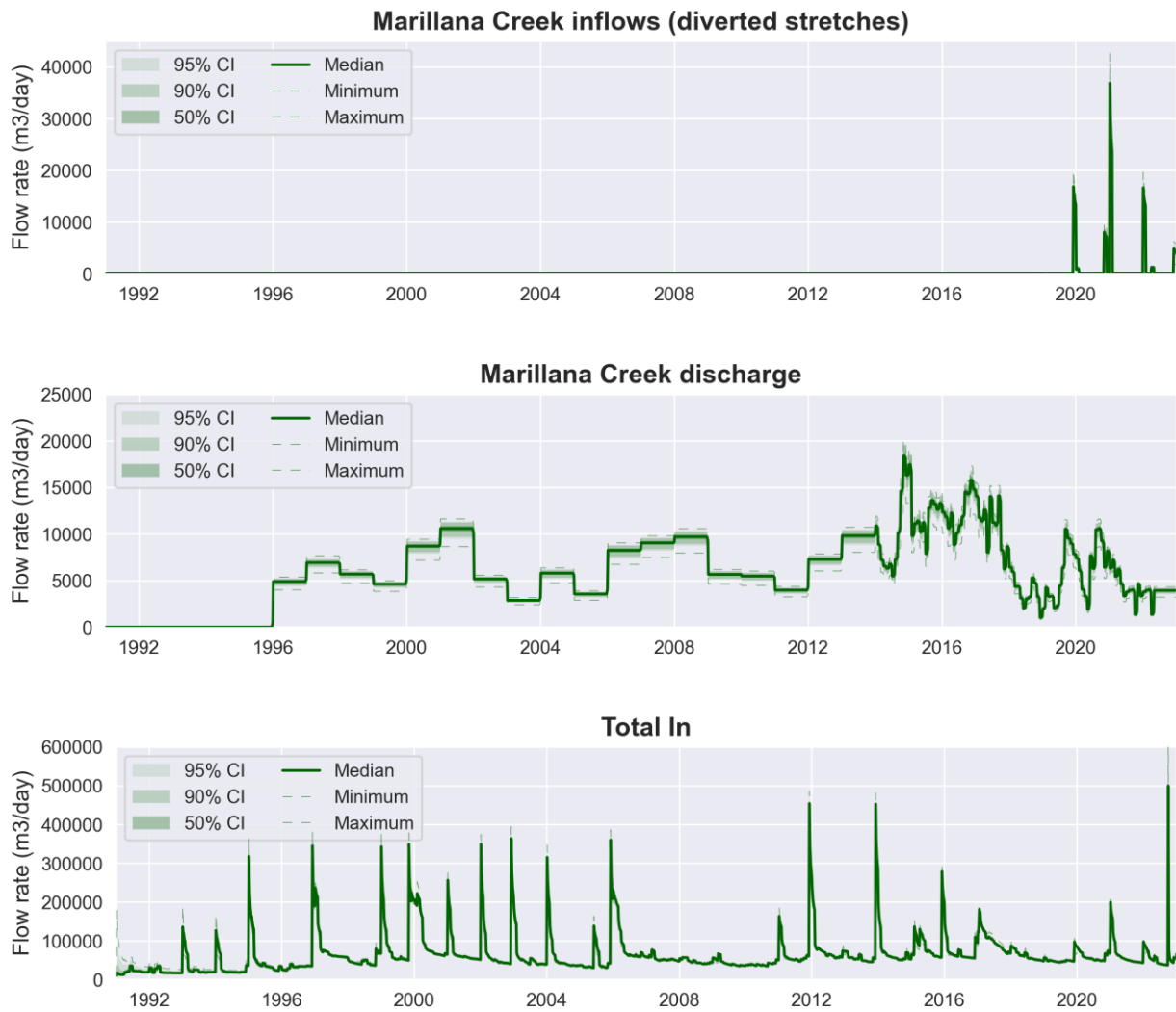Figure 7-15: Simulated groundwater inflows over the calibration period.

Figure 7-16: Simulated groundwater inflows over the calibration period (continuation).
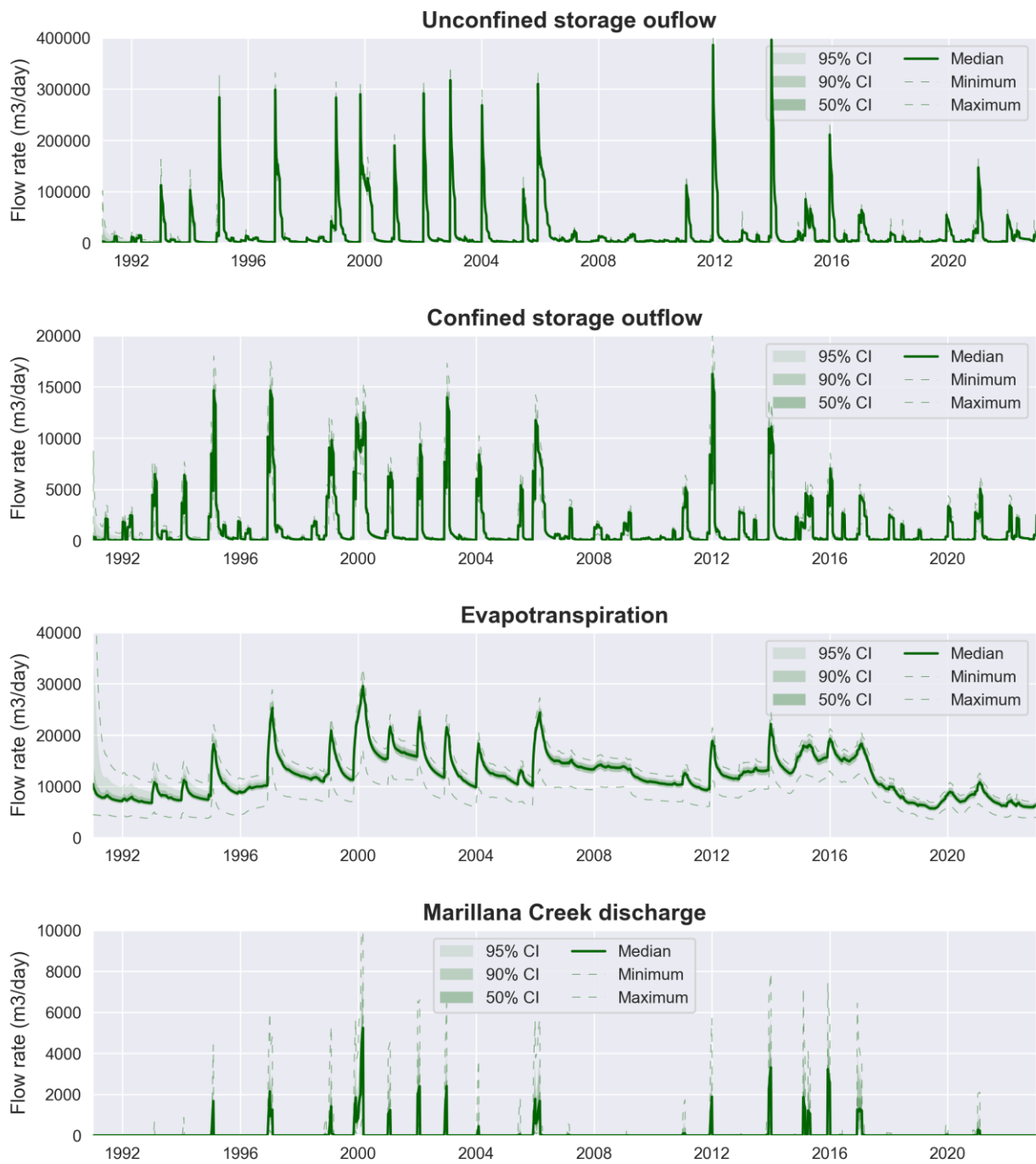
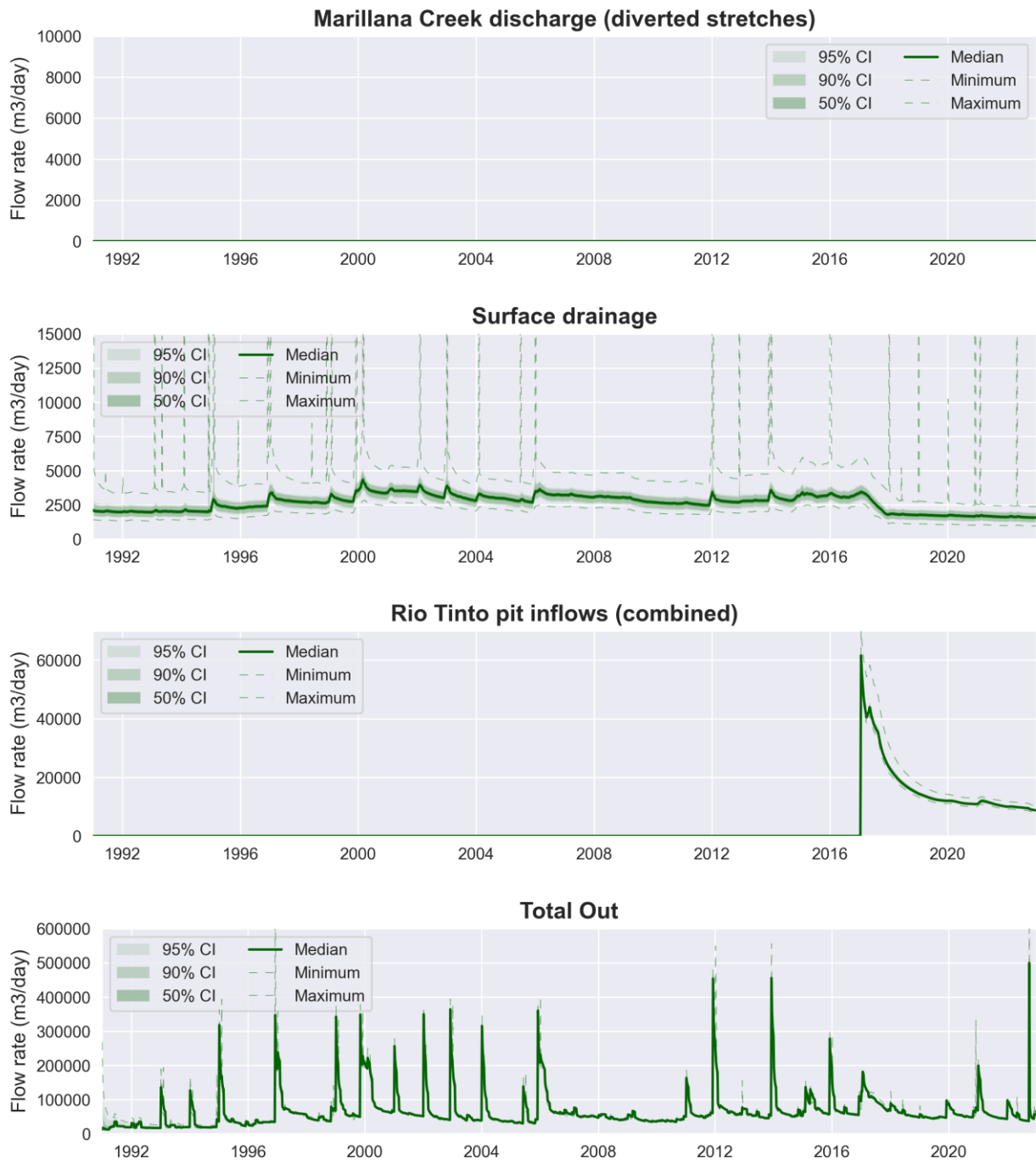Figure 7-17: Simulated groundwater outflows over the calibration period.

Figure 7-18: Simulated groundwater outflows over the calibration period (continuation).
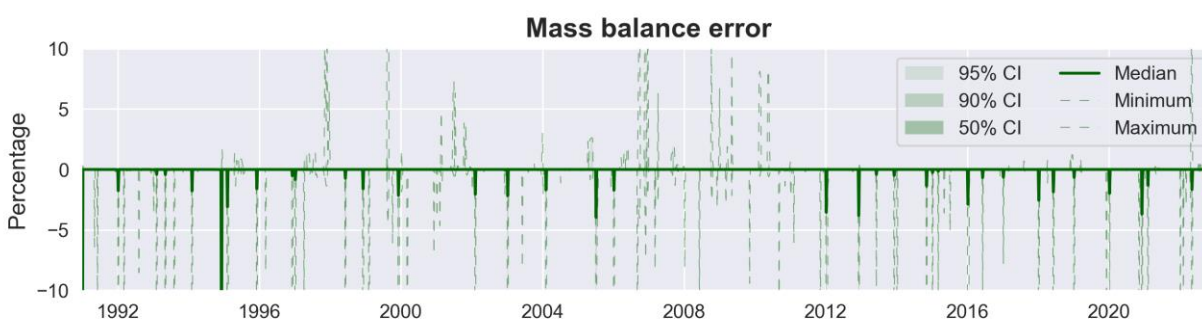
Figure 7-19: Simulated mass balance errors over the calibration period.

8. Predictive modelling

8.1 Predictive setup

The main purpose of the predictive modelling is to provide predictive estimates of drawdown associated with the mining operations (in particular, E8 pit) over the life of mine. Groundwater levels over the predictive period will be subject to several different stressors, such as changes in rainfall, seepage from the Marillana Creek and dewatering operations in the various pits.

In order to differentiate drawdown contributions from the different stressors, three different scenarios were simulated as follows:

- A no-mining scenario for both historical and predictive periods, to capture groundwater level changes associated with transient rainfall signal;
- A mining scenario, which was then compared against from the no-mining scenario to quantify drawdown contributions from the entire mining operation (historical and future); and
- A mining scenario without the E8 pit, which was used to calculate drawdown contributions associated with E8 pit.

Total mining drawdown contributions were calculated subtracting the heads from the mining scenario from the no-mining scenario, while the drawdown contributions from E8 pit were calculated by subtracting the heads from the mining scenarios from the no-E8 pit scenario.

Predictive model runs for each scenario were performed for 500 realizations from the calibrated parameter ensemble. These runs were undertaken in tandem with the historical period, avoiding the need to prescribe initial heads (present-day) for the predictive runs. Boundary conditions defined to represent the mining operations for the predictive period are discussed in section 6.

8.2   Drawdown

8.2.1 Spatial distribution – Mining Scenario

As described in the previous section drawdown values associated with the mining operations were calculated without the effect from change in rainfall rates, by subtracting the simulated hydraulic heads from the mining scenario from the no-mining scenario. Drawdown contours for median (as well as 5th and 95th percentiles) were generated for each model layer at two times, namely January 2023 (end of history matching period) and December 2030 (end of predictive period), presented in Figure 8-1 to Figure 8-12.

In terms of magnitude, the highest drawdown is found within the CID aquifer (which is expected since the dewatering takes place in this unit) with values of up to 60 m. By the end of 2029, one-meter drawdown contours extend as far as 5 km away from the CID aquifer, while drawdowns between 2 and 5 m are found within the majority of the Ministers North Aquifer.

The comparison of drawdowns from 2023 and 2029 show that, while no substantial increase in magnitude is noted, the extent of the drawdown increases in the CID and Alluvium aquifers towards both east and western ends of the Marillana Creek. Nevertheless, predictive estimates for the west portion of the model may have some bias and/or higher uncertainty than calculated as dewatering operations from Rio Tinto at Junction Central and South East were not incorporated in the model.

Contours for the 5th and 95th percentiles show relatively small differences to the median contours, given that uncertainty within the drawdown areas (where most of the historical observations are observed) is relatively small in relation to the simulated drawdown magnitude.

The comparison of predictive model results with additional data collected after the history matching (borehole HYM0011M) suggests that predictive drawdowns within the Alluvium Aquifer are being overestimated in the vicinity of E8. In this borehole, the observed groundwater level there has fallen approximately 1 m between 2013 and 2023, while the model predicts approximately 6 m. It is possible that the vertical connection between Alluvium and CID aquifers are overestimated in the model, given that a single layer was assigned for each aquifer and no representation was given to lower permeability portions of the CID. Other potential factors in the overestimation of Alluvium drawdown include:

- Limited monitoring in the alluvium
- Uncertain geometry of the alluvium, particular at local scales, and
- Uncertainty around the infiltration of Yandi discharge, both in time and duration.

Considering these facts, drawdown predictions within the Alluvium Aquifer should be considered with caution.
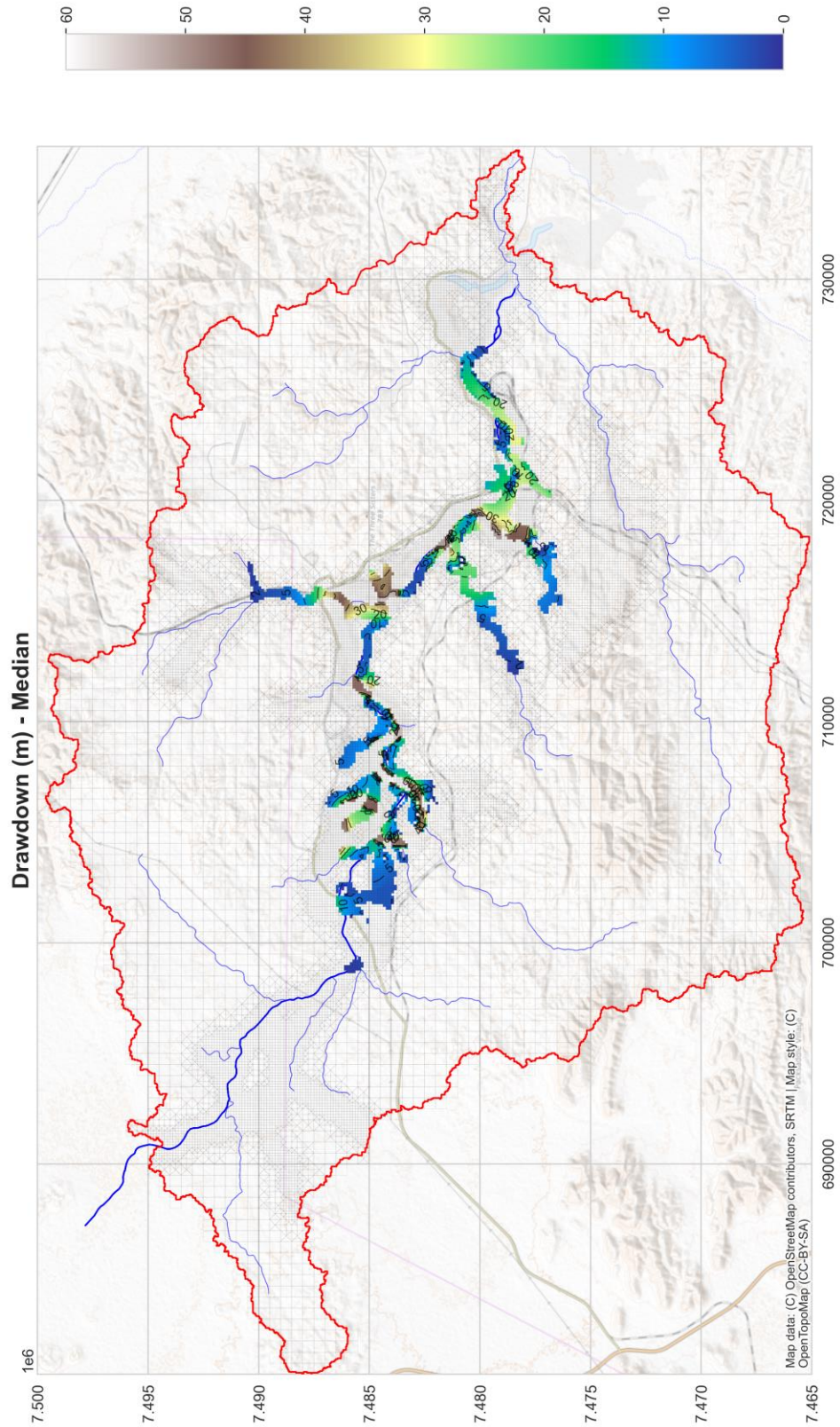
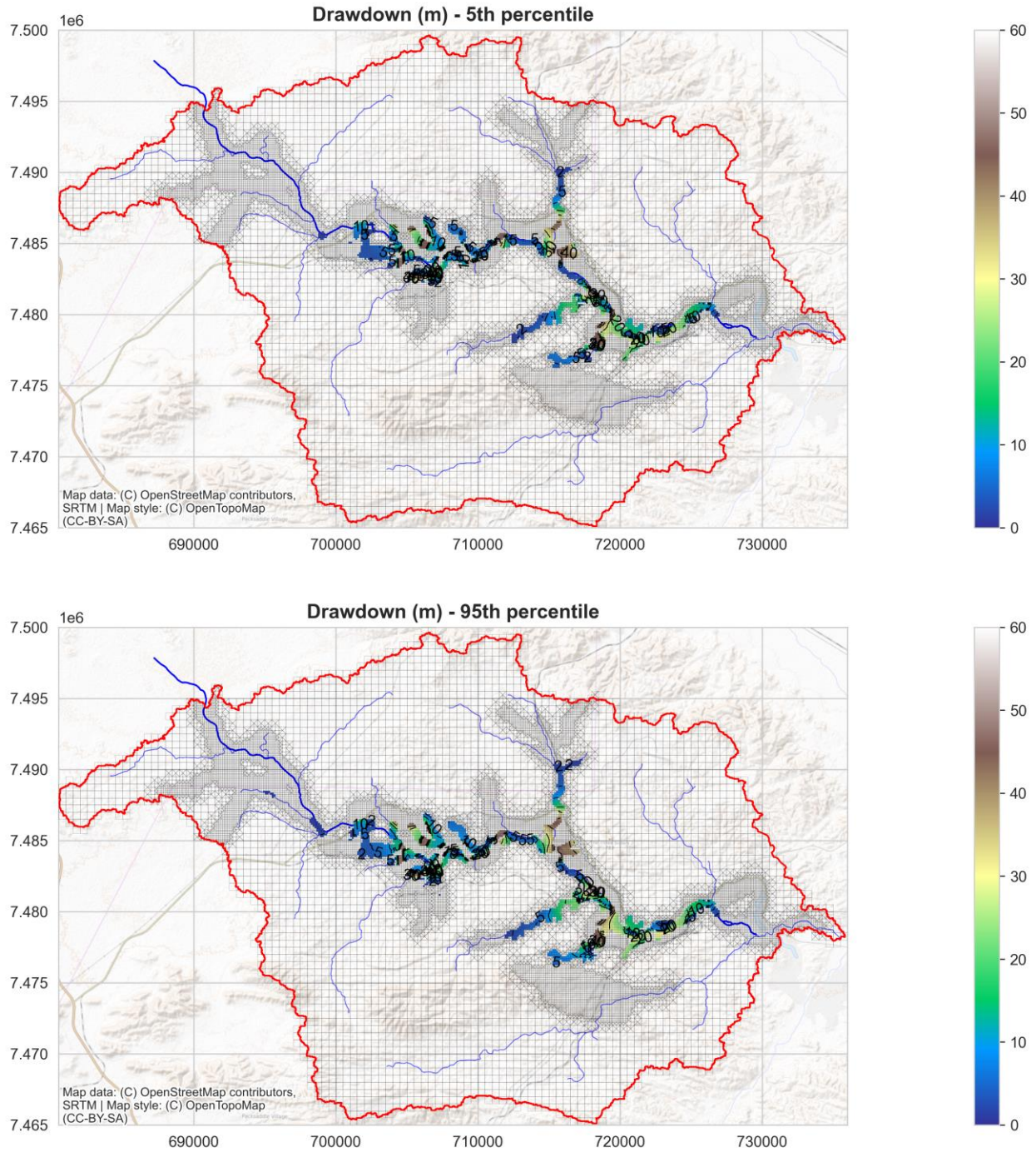Figure 8-1: Simulated drawdown contours (median) for the Alluvium Aquifer – January 2023.

Figure 8-2: Simulated drawdown contours (5th and 95th percentiles) for the Alluvium Aquifer – January 2023.
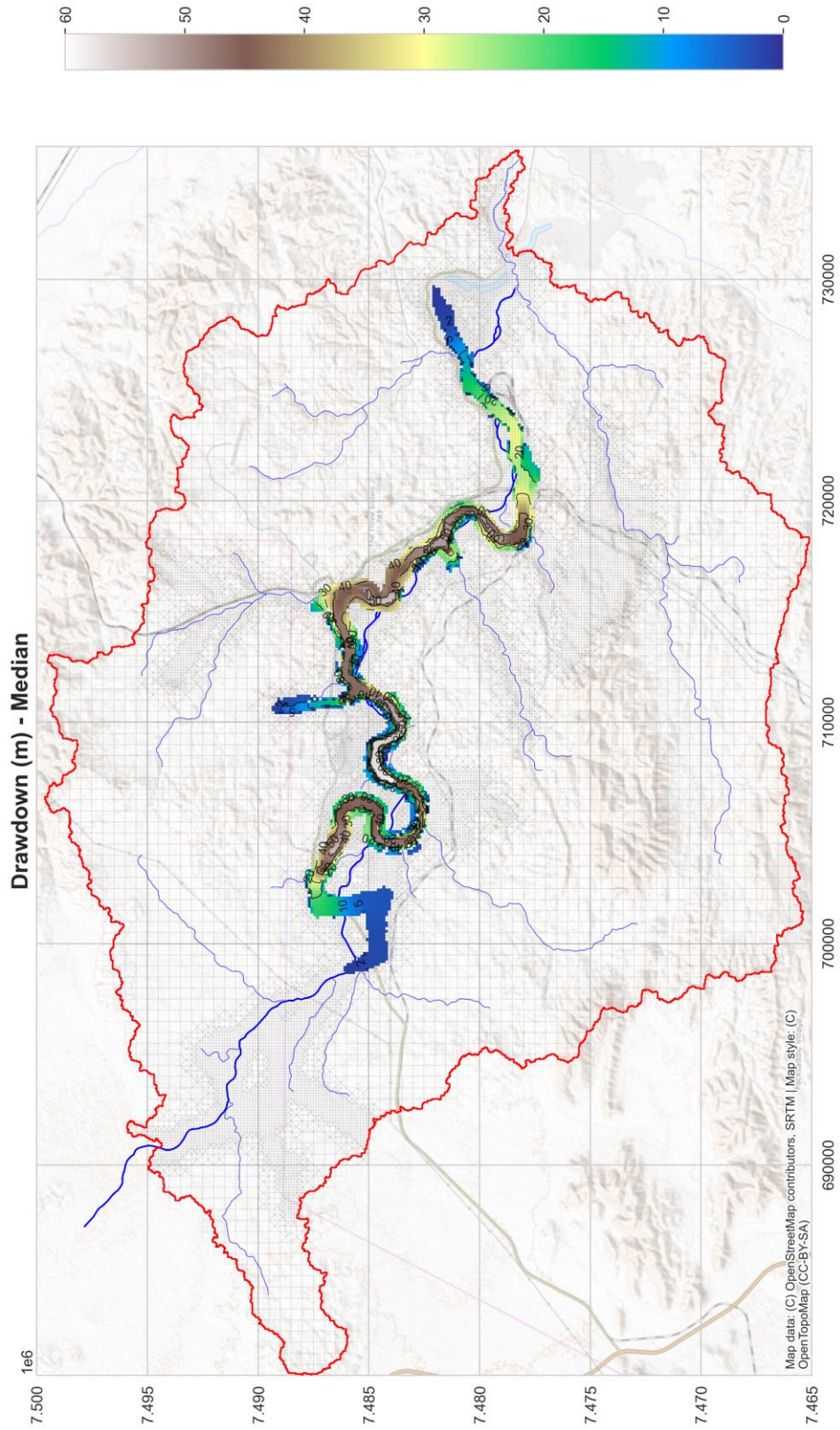
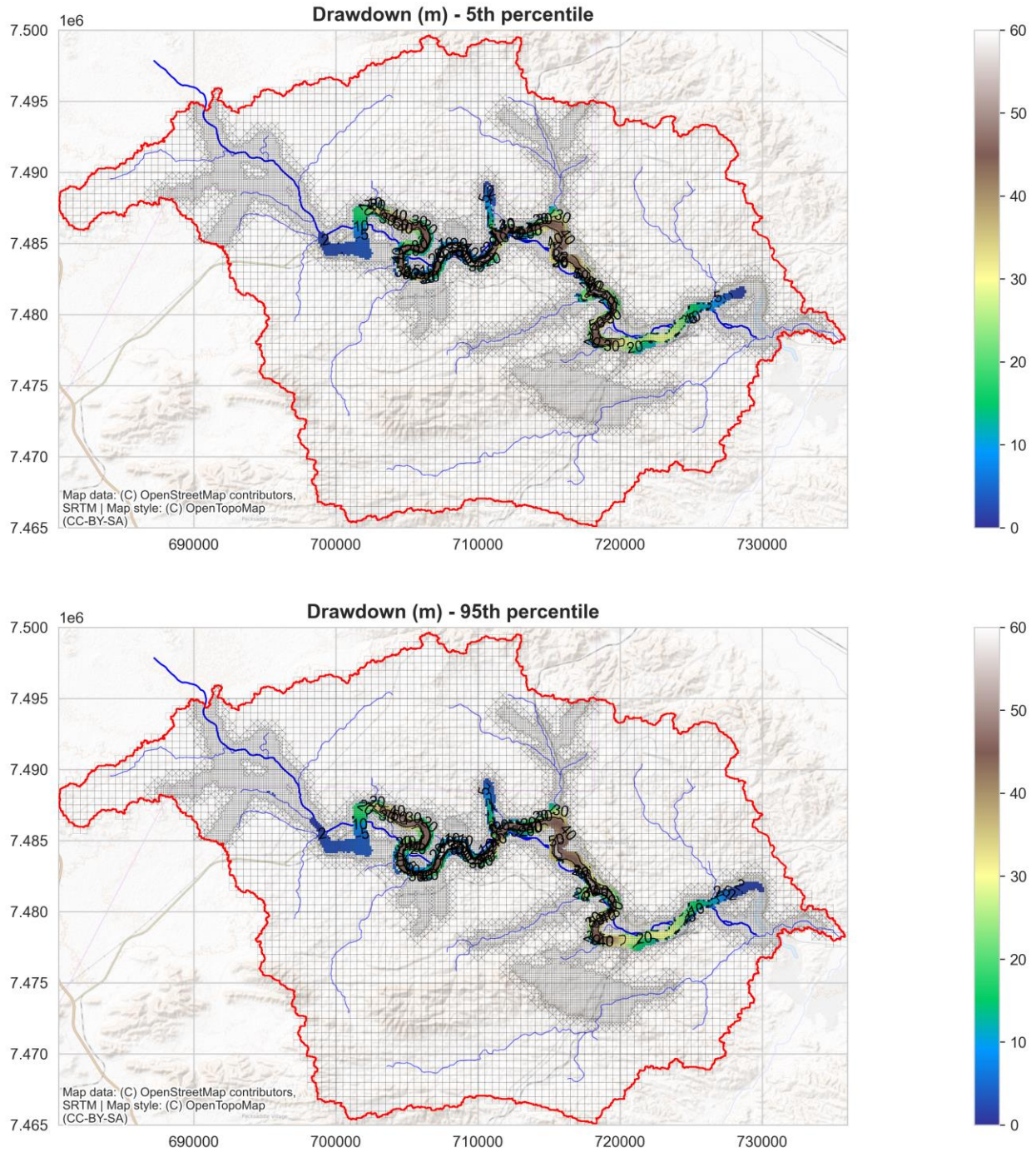Figure 8-3: Simulated drawdown contours (median) for the CID Aquifer – January 2023.

Figure 8-4: Simulated drawdown contours (5th and 95th percentiles) for the CID Aquifer – January 2023.
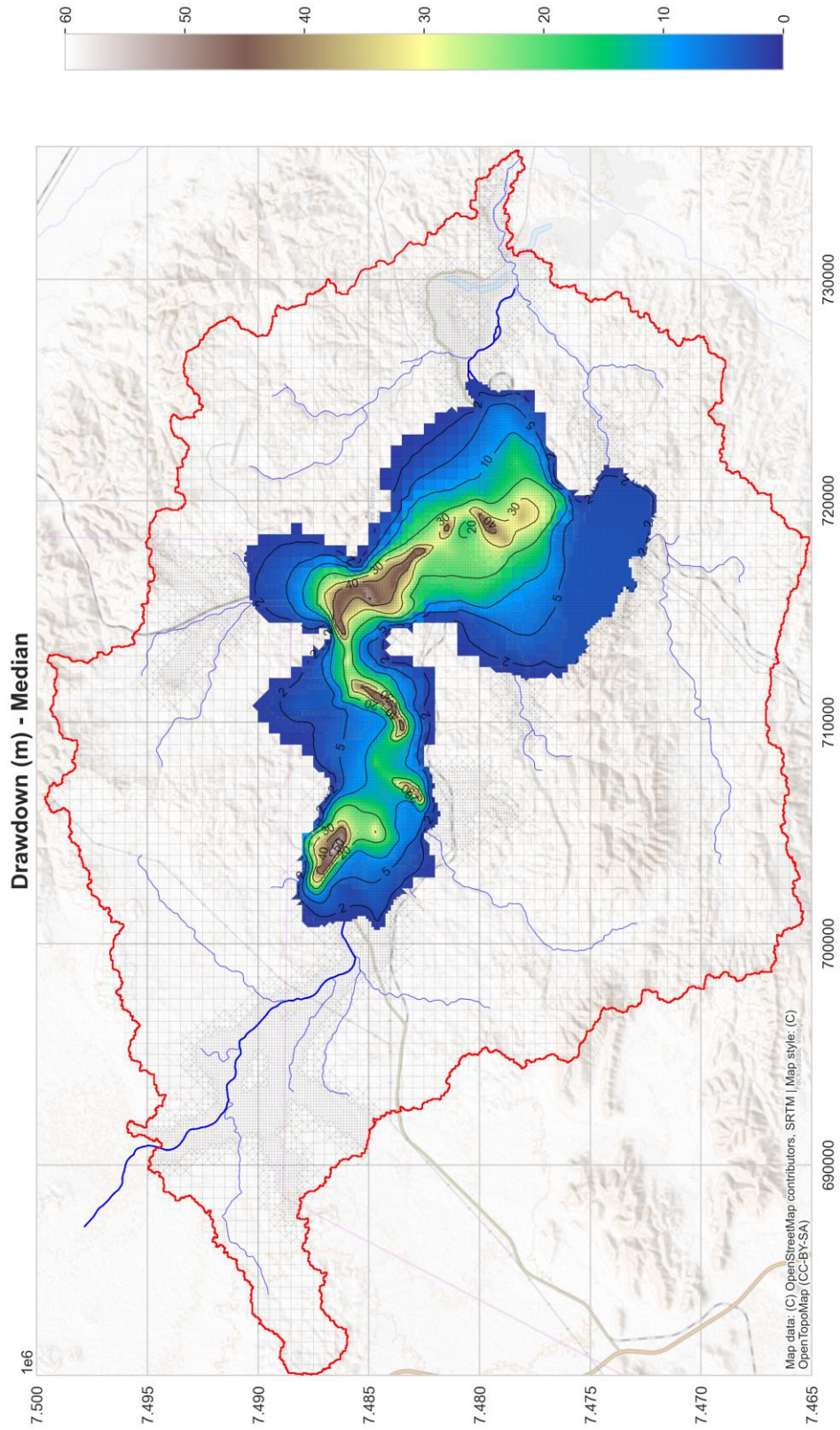
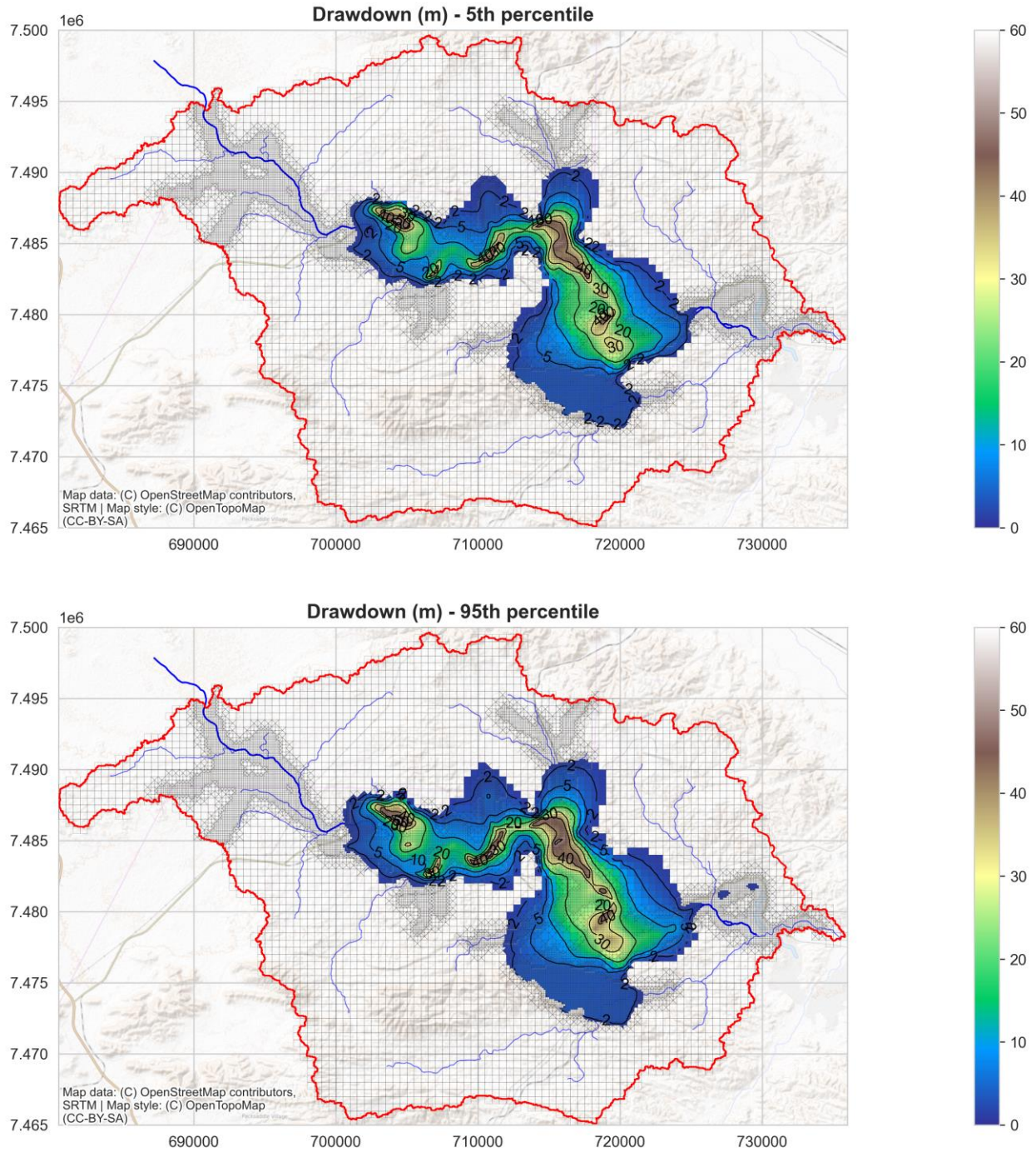Figure 8-5: Simulated drawdown contours (median) for the Basement and Ministers North aquifers – January 2023.

Figure 8-6: Simulated drawdown contours (5th and 95th percentiles) for the Basement and Ministers North aquifers – January 2023.
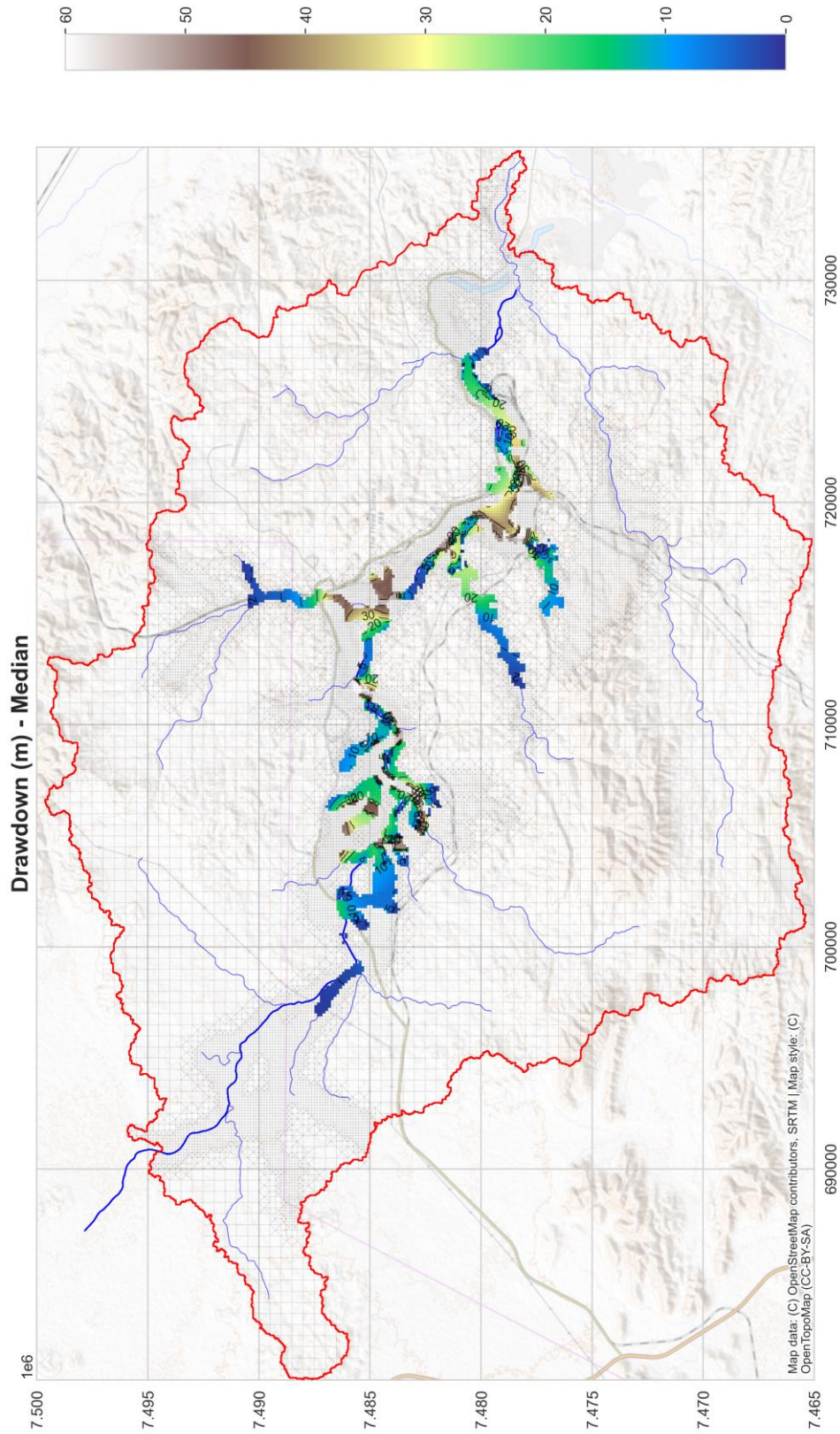
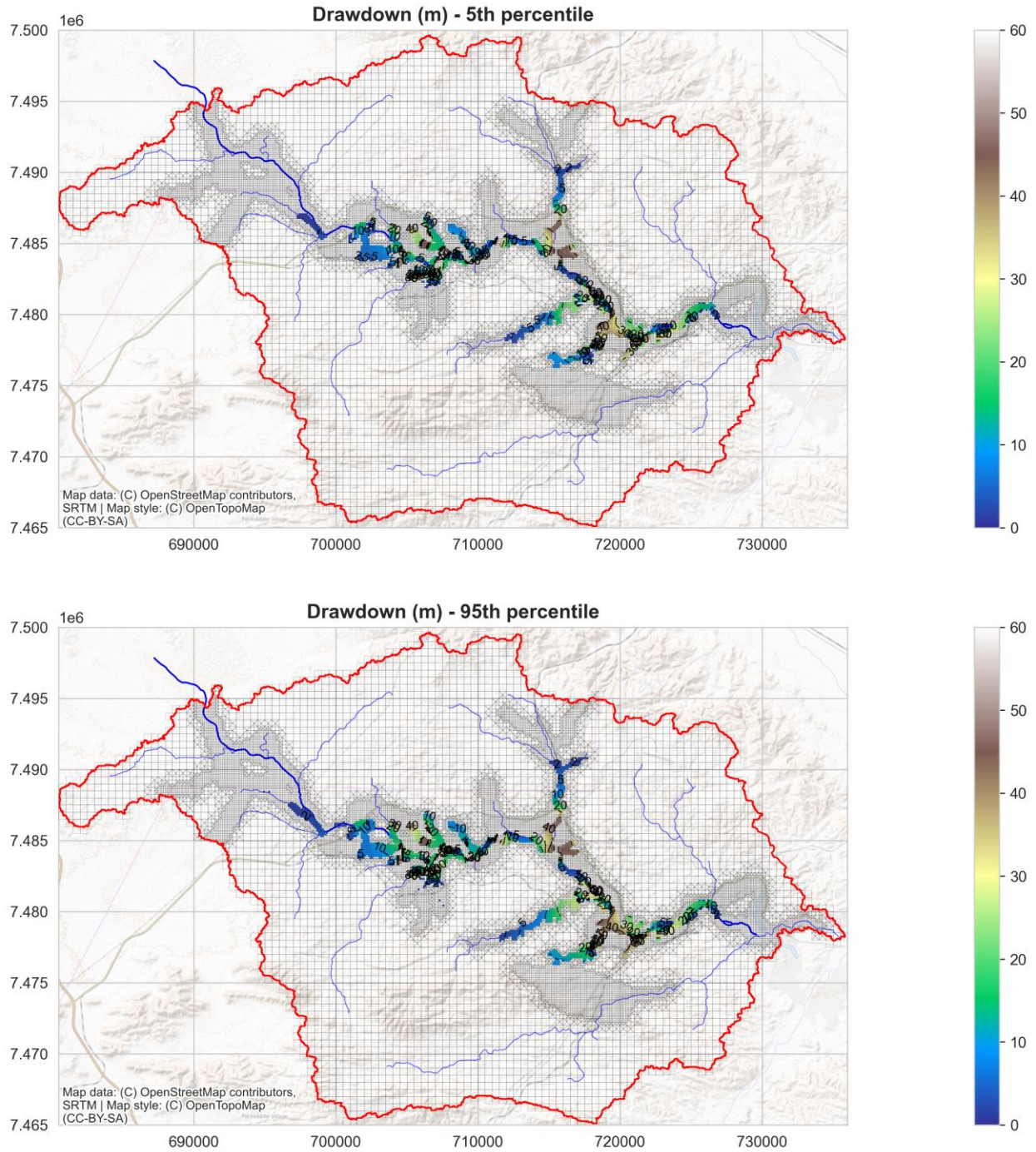Figure 8-7: Simulated drawdown contours (median) for the Alluvium Aquifer – End of 2029.

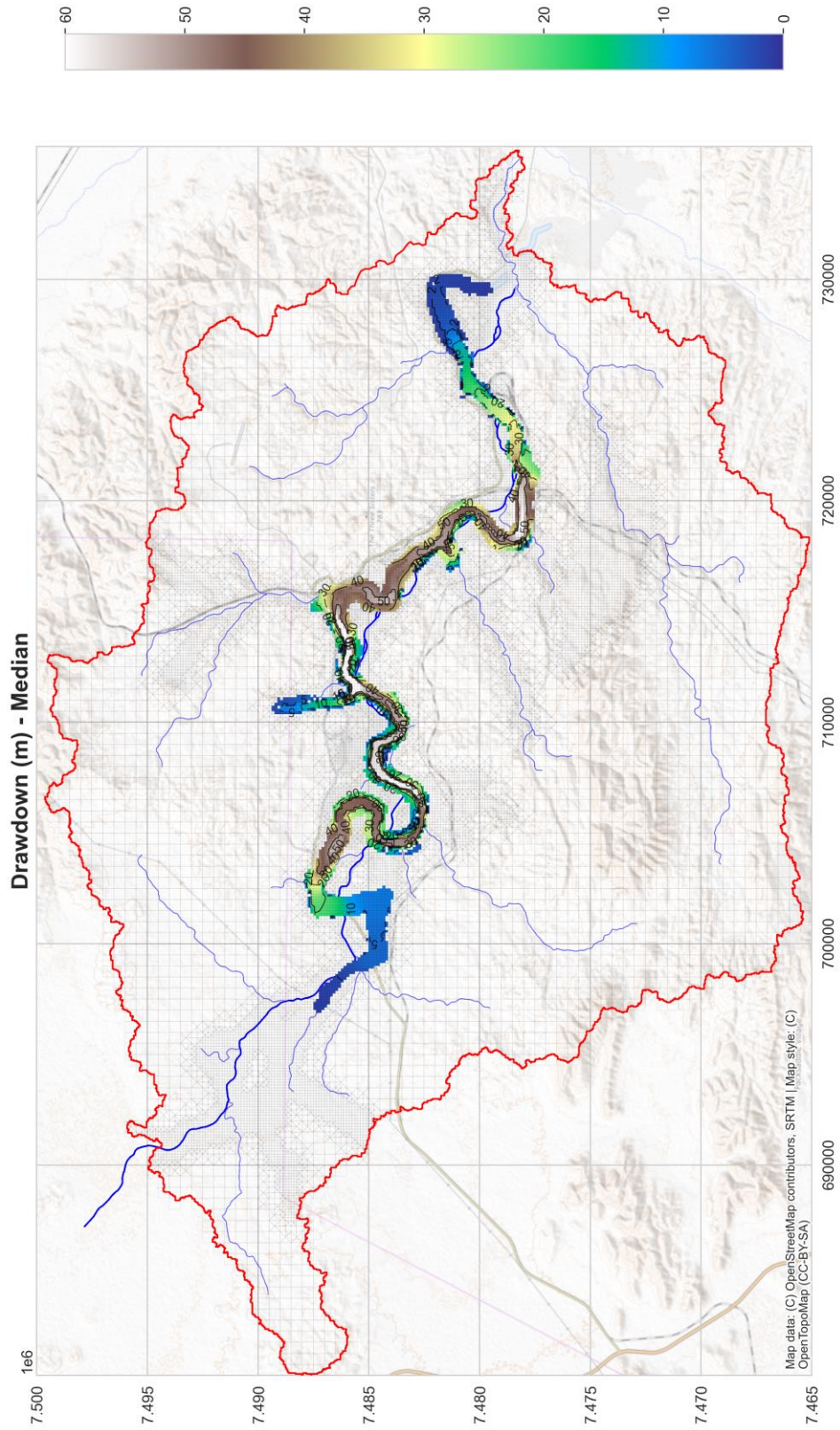Figure 8-8: Simulated drawdown contours (5th and 95th percentiles) for the Alluvium Aquifer – End of 2029.

Figure 8-9: Simulated drawdown contours (median) for the CID Aquifer – End of 2029.
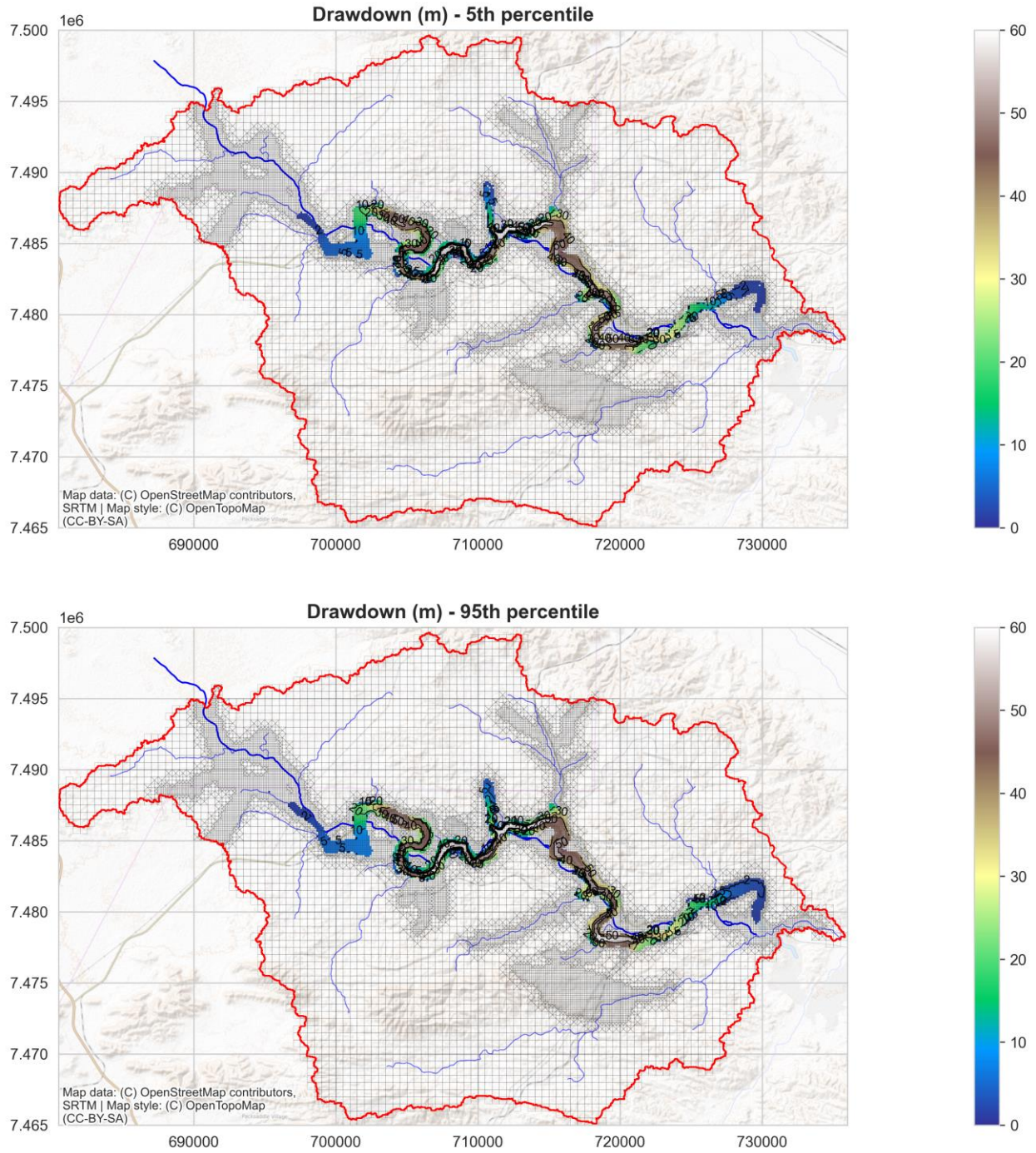
Figure 8-10: Simulated drawdown contours (5th and 95th percentiles) for the CID Aquifer – End of 2029.
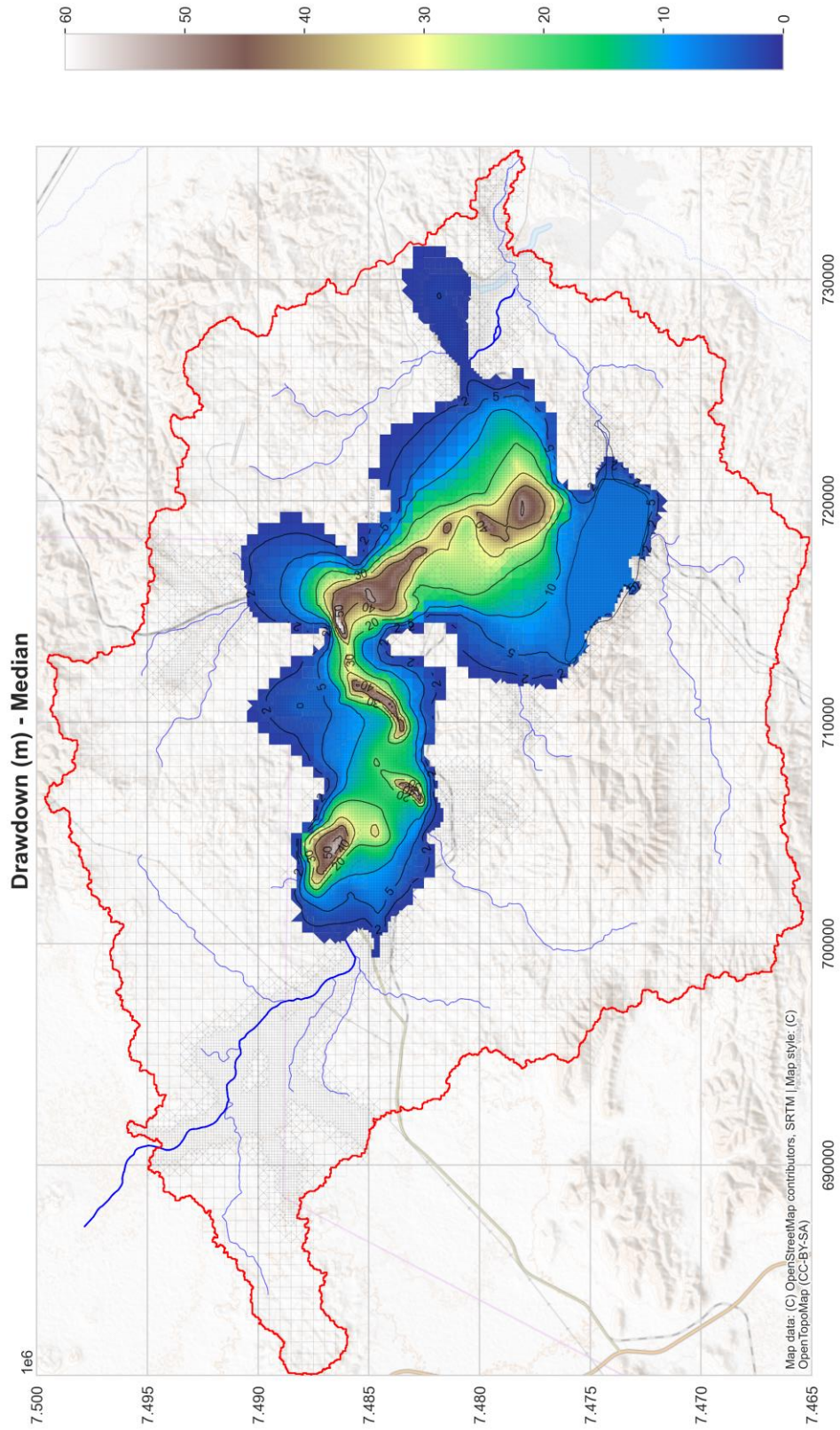
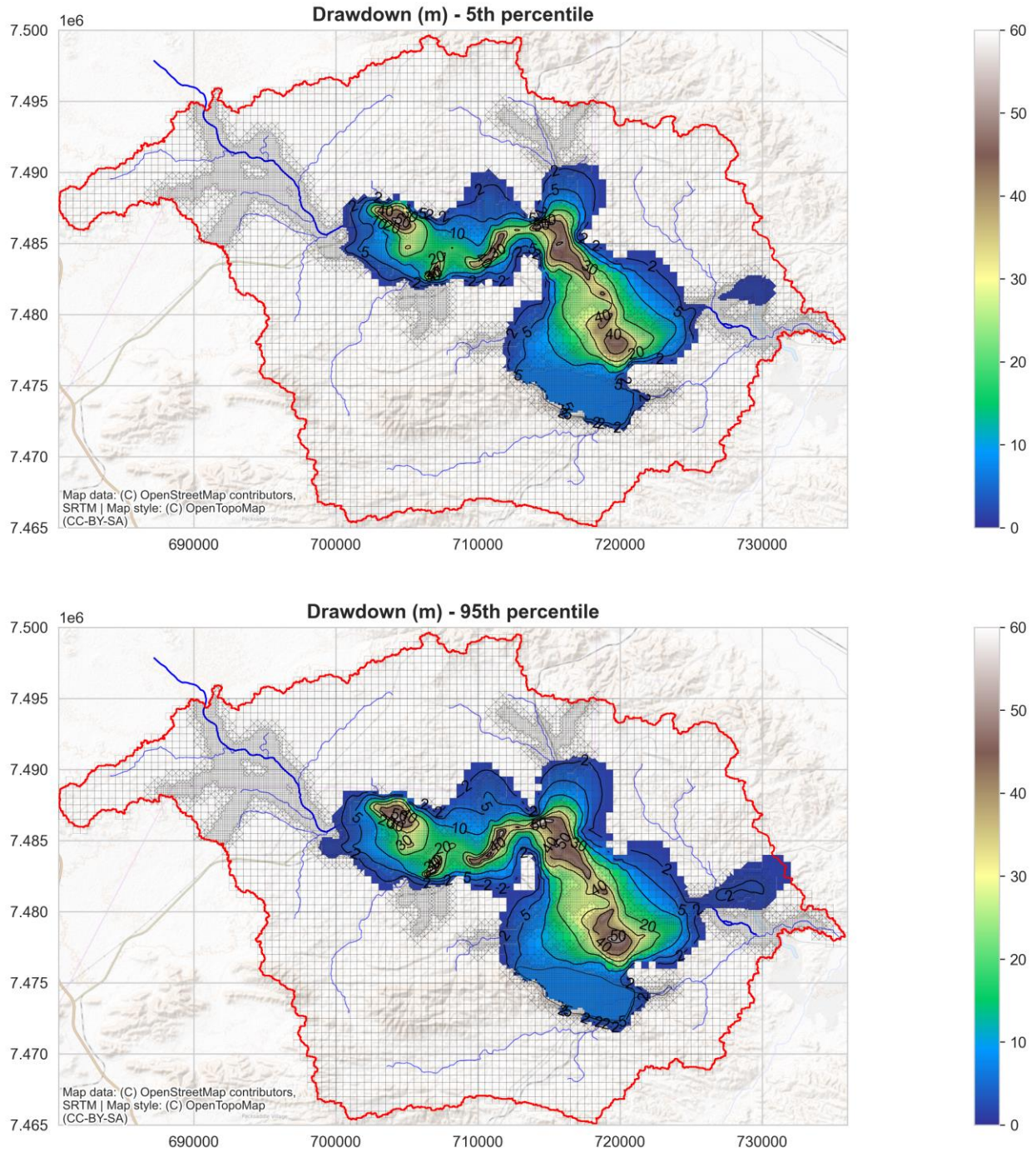Figure 8-11: Simulated drawdown contours (median) for the Basement and Ministers North aquifers – End of 2029.

Figure 8-12: Simulated drawdown contours (5th and 95th percentiles) for the Basement and Ministers North aquifers – End of 2029.

8.2.2 Spatial distribution – E8 only

As previously described, drawdown contributions from the proposed E8 pit were calculated by subtracting the simulated heads from the mining-scenario (inclusive of E8), from the no-E8 scenario. Drawdown contours for median, 5th and 95th percentiles were generated for each model layers at the end of simulation (December 2030) and illustrated in Figure 8-13 to Figure 8-18.

Although the proposed E8 pit will have a relatively small footprint, due to its location the base of the pit, and therefore the target dewatering level, will have the lowest final elevation (468 mAHD) of all Yandi pits. As a result, effects from the dewatering are relatively widespread.

Within the CID aquifer, drawdown of up to 20 m is predicted within the vicinity of E8, with at least 1 m of drawdown extending to the western extent of the Mungadoo pit and to the central part of the Junction South West pit.

The simulated magnitude of drawdown within the Basement is lower than in the CID (maximum of 14 m within E8 footprint), the lateral extent is greater. The footprint area for drawdowns larger than 1 m (Figure 8-17) does not extend to the Ministers North Aquifer however.

The drawdown contours for 5th and 95th percentiles present small differences in footprint compared to the median contours, as also observed in the mining scenario. Drawdown magnitude show differences of 2-5 m near E8 pit, with smaller differences in more distant areas.

8.3   Dewatering rates

Individual boundary fluxes for each of the predictive pits have been recorded and are presented in Figure 8-19 to Figure 8-22, and total dewatering rates for Yandi are presented in Figure 8-23. In general, simulated dewatering rates are relatively small (less than 5 ML/day) as the level of most pits remain stable from 2023 to 2030. Exceptions are:

- E8 pit, with a dewatering target of 495 mAHD (2023) lowered to 468 mAHD towards the end of simulation, resulting in peak flows of up to 12.5 ML/day stabilizing at up to 10 ML/day;
- C1, reaching the final elevation of 492 in 2023, with peak inflows of up to 30 ML/day, rapidly stabilizing to 4 ML/day; and
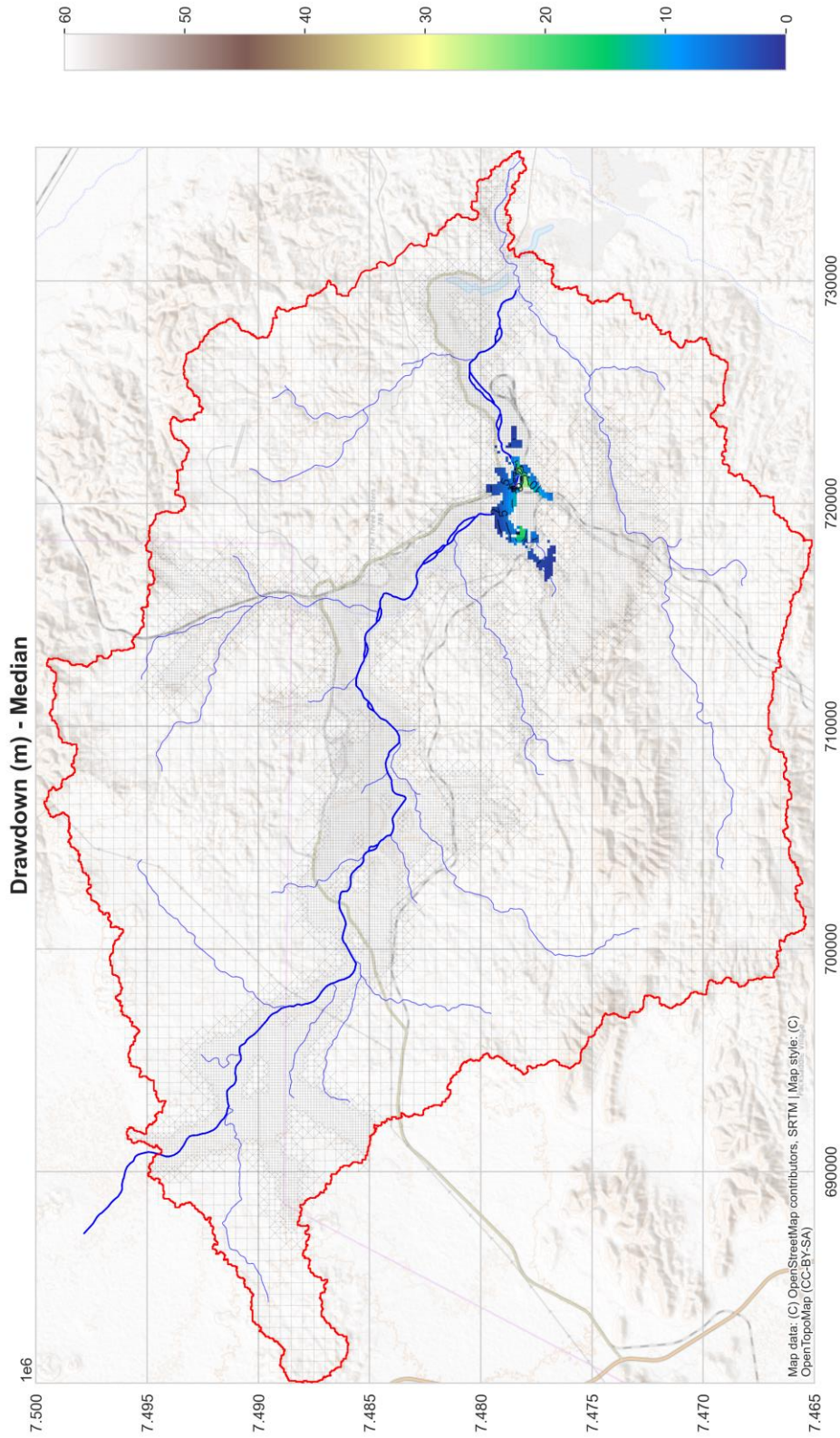- W3 pit, reaching the final elevation of 510 mAHD in 2027, resulting in peak inflows of up to 3.5 ML/day.

Figure 8-13: Simulated drawdown contours (median, E8 only) for Alluvium Aquifer – End of 2029.
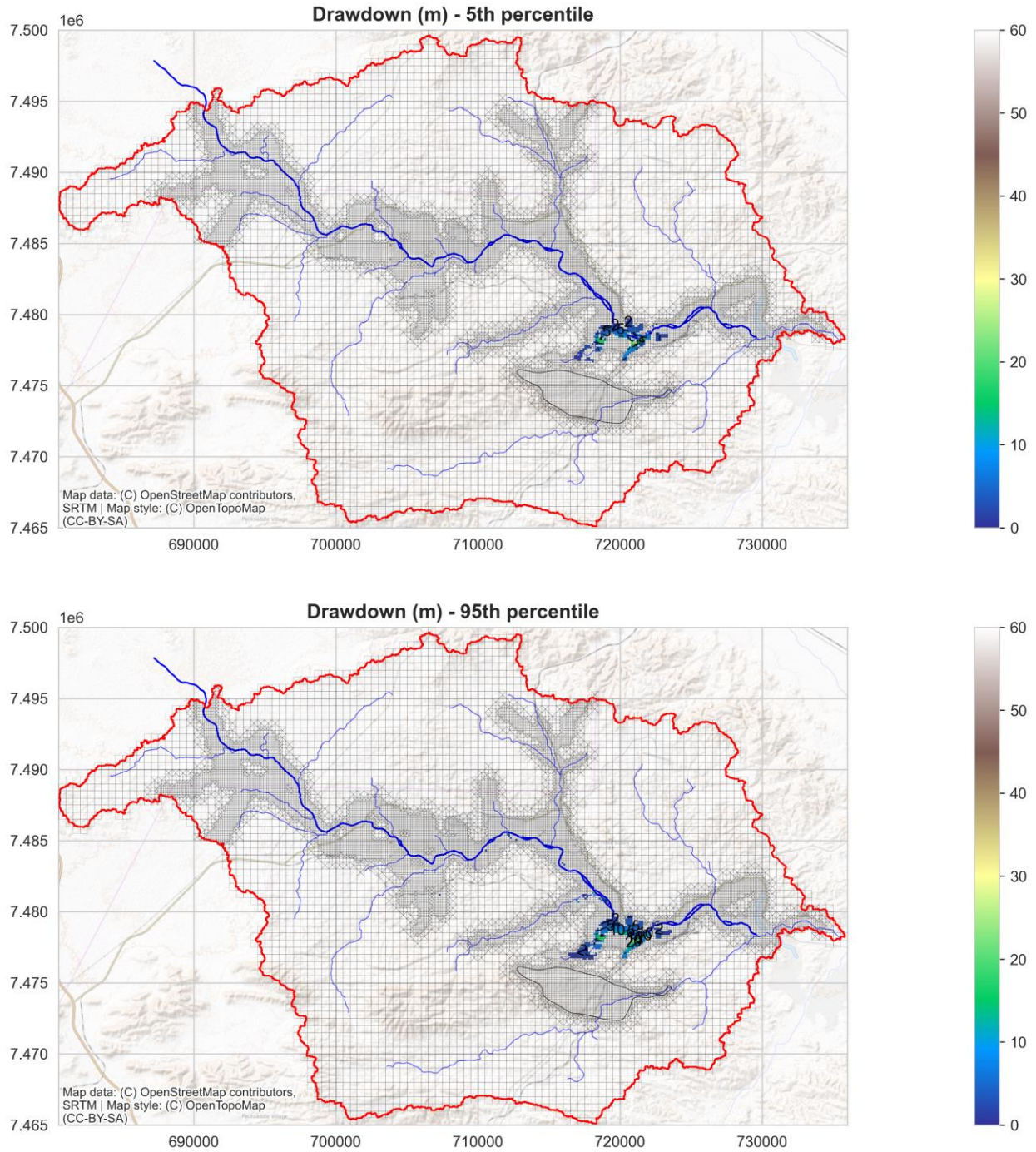
Figure 8-14: Simulated drawdown contours (5th and 95th percentiles, E8 only) for the Alluvium Aquifer – End of Mining.
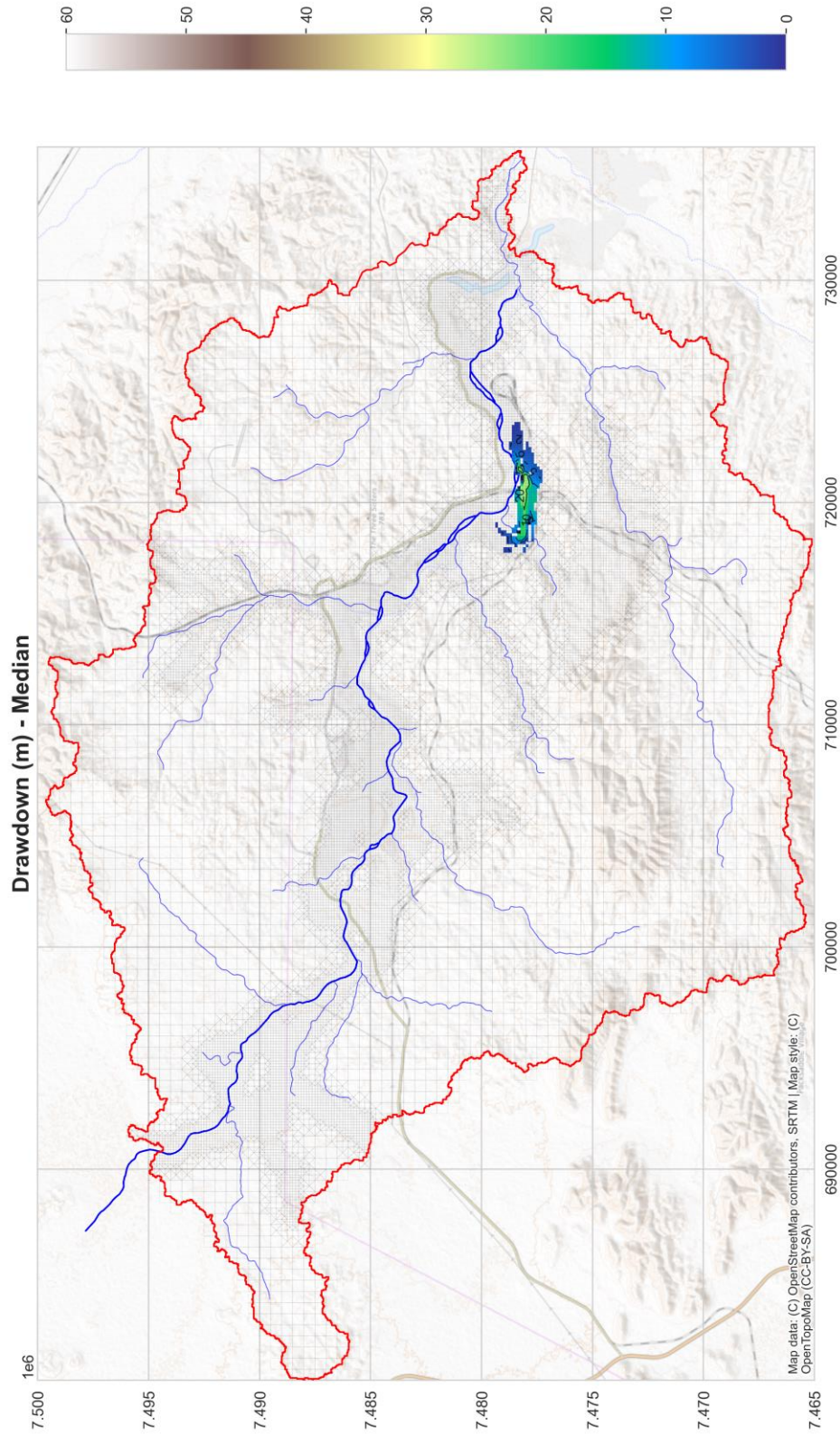
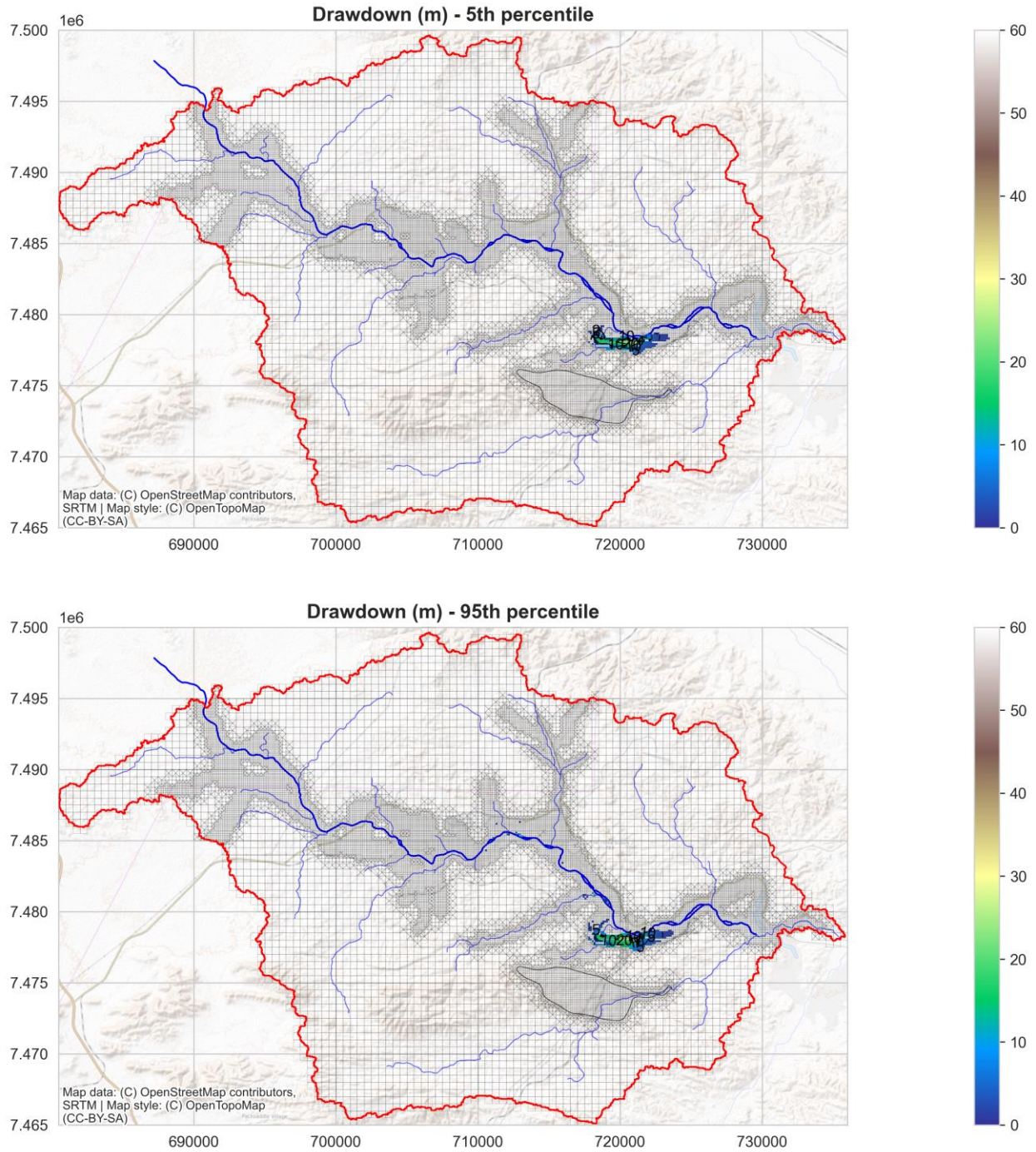Figure 8-15: Simulated drawdown contours (median, E8 only) for CID Aquifer – End of 2029.

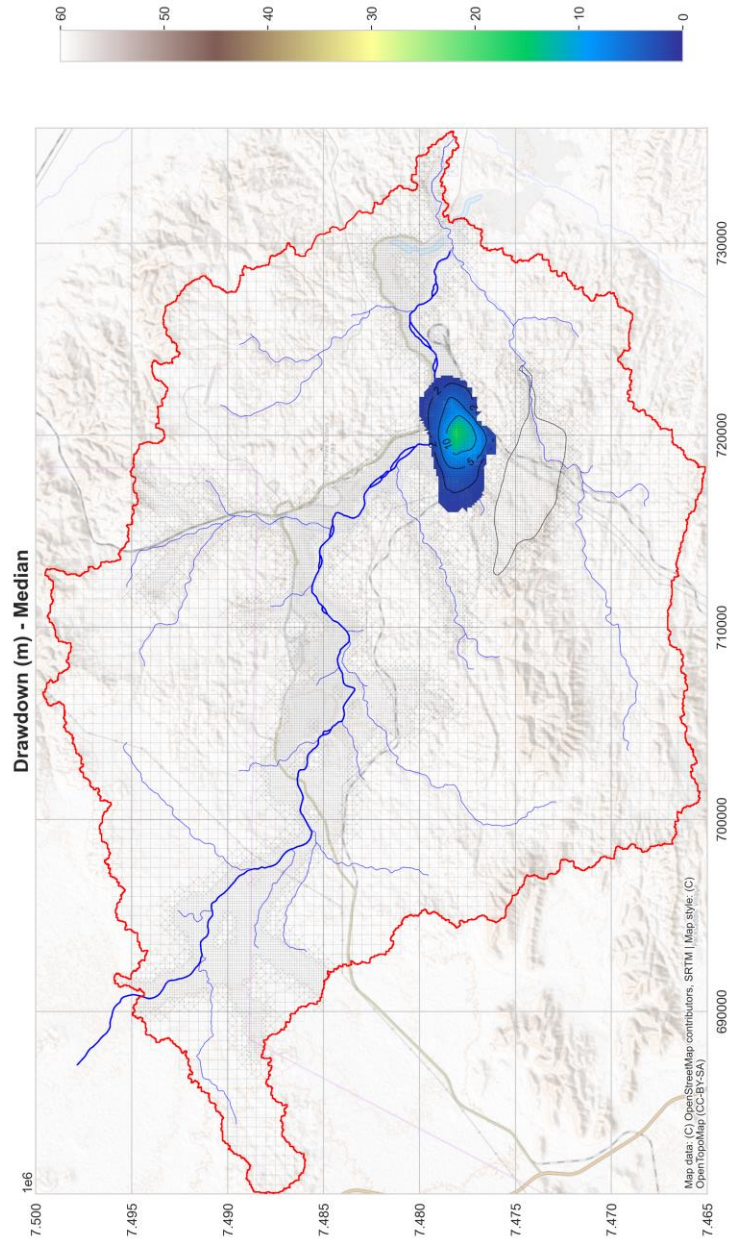Figure 8-16: Simulated drawdown contours (5th and 95th percentiles, E8 only) for CID Aquifer – End of 2029.

Figure 8-17: Simulated drawdown contours (median, E8 only) for Basement and Ministers North aquifers – End of 2029.
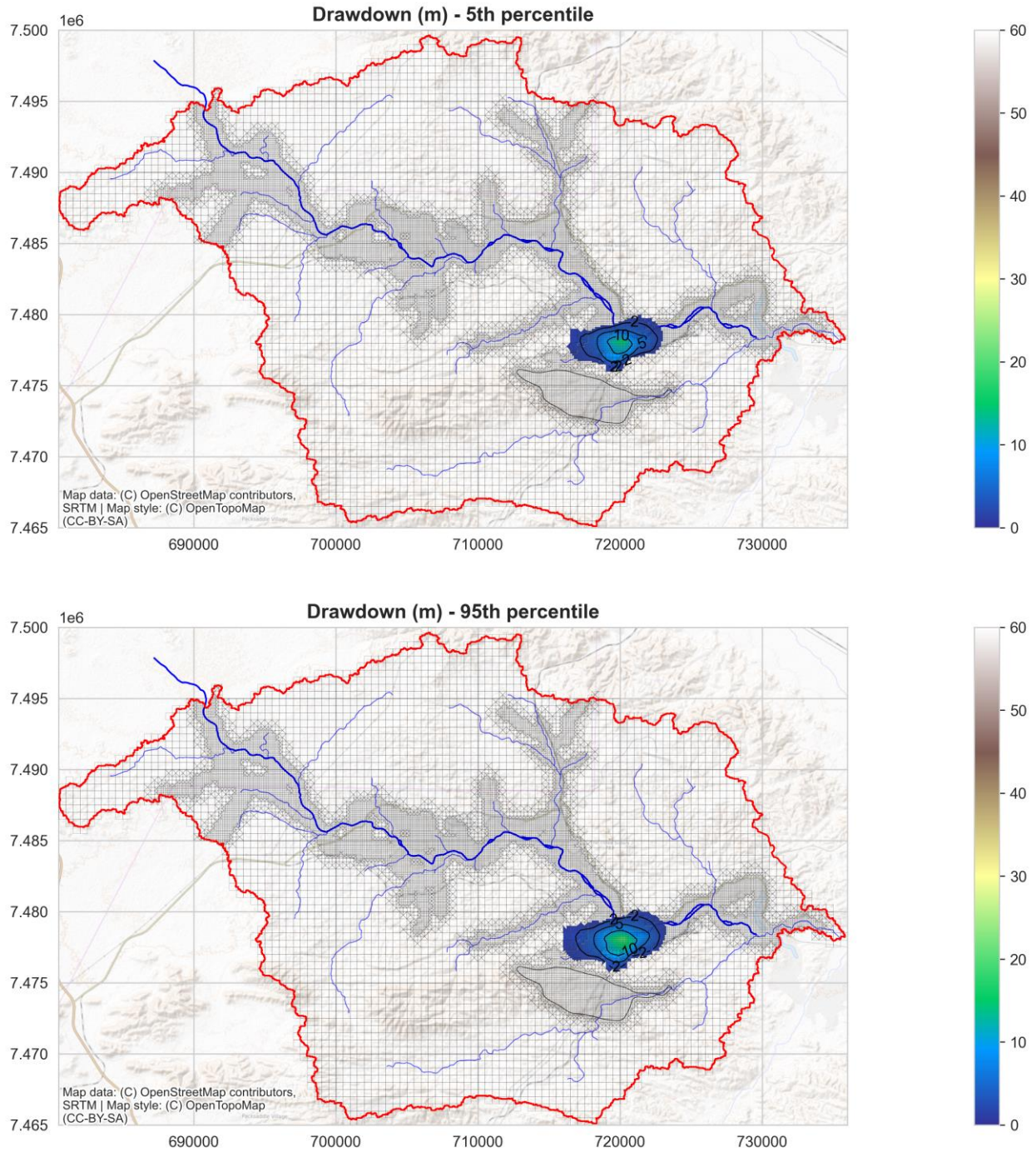
Figure 8-18: Simulated drawdown contours (5th and 95th percentiles, E8 only) for Basement and Ministers North aquifers – End of 2029.
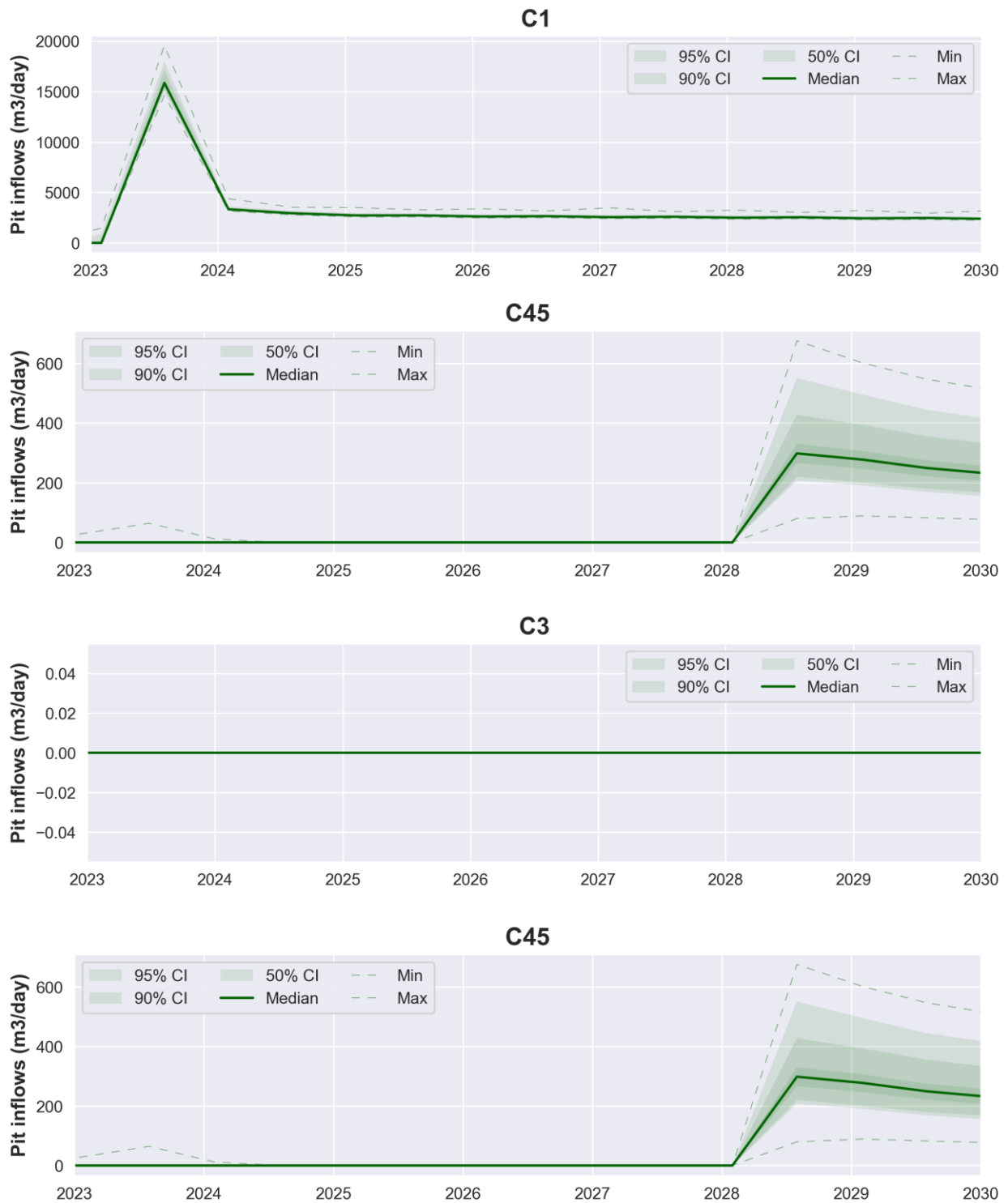
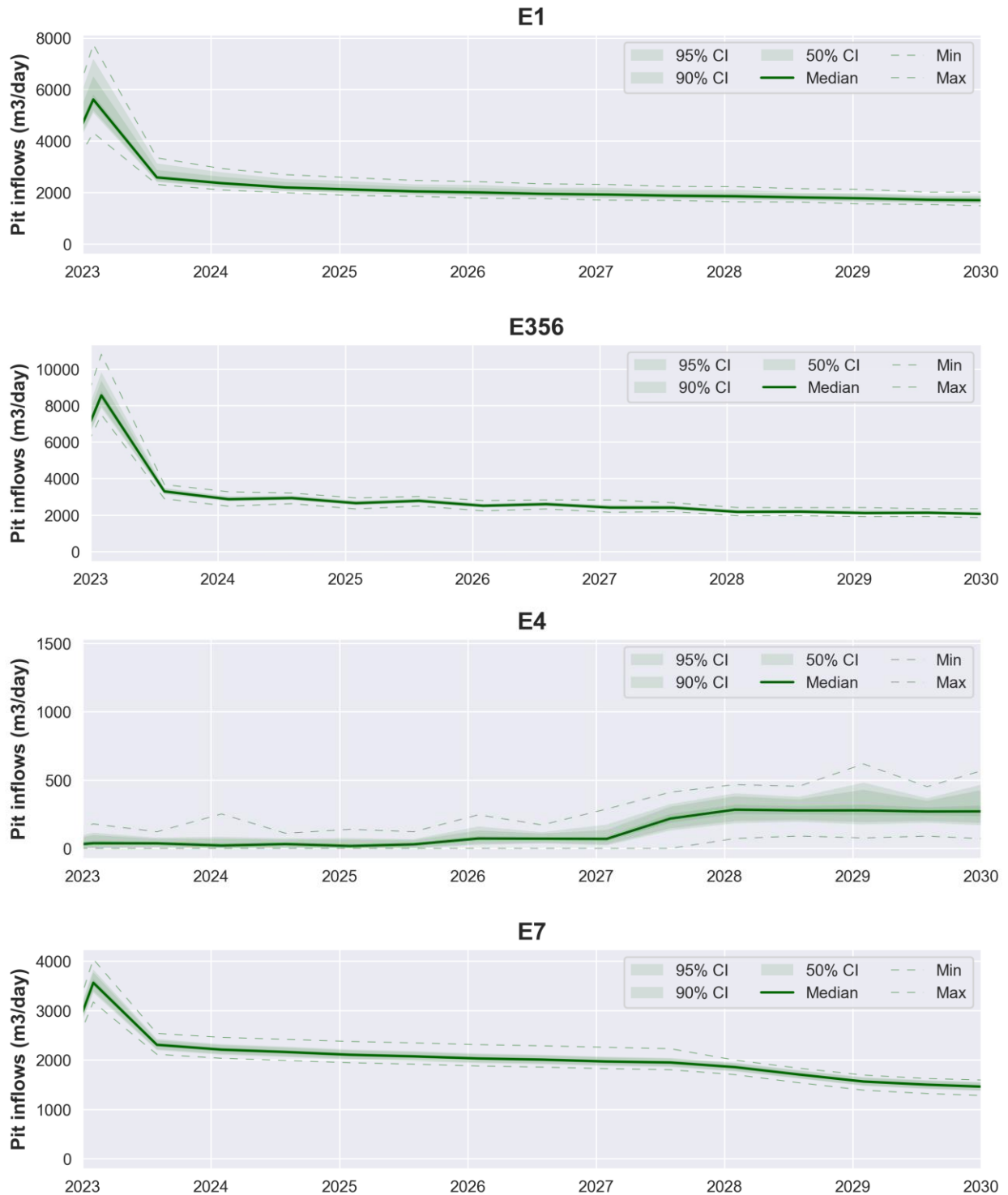Figure 8-19: Simulated dewatering rates (6-month moving average).

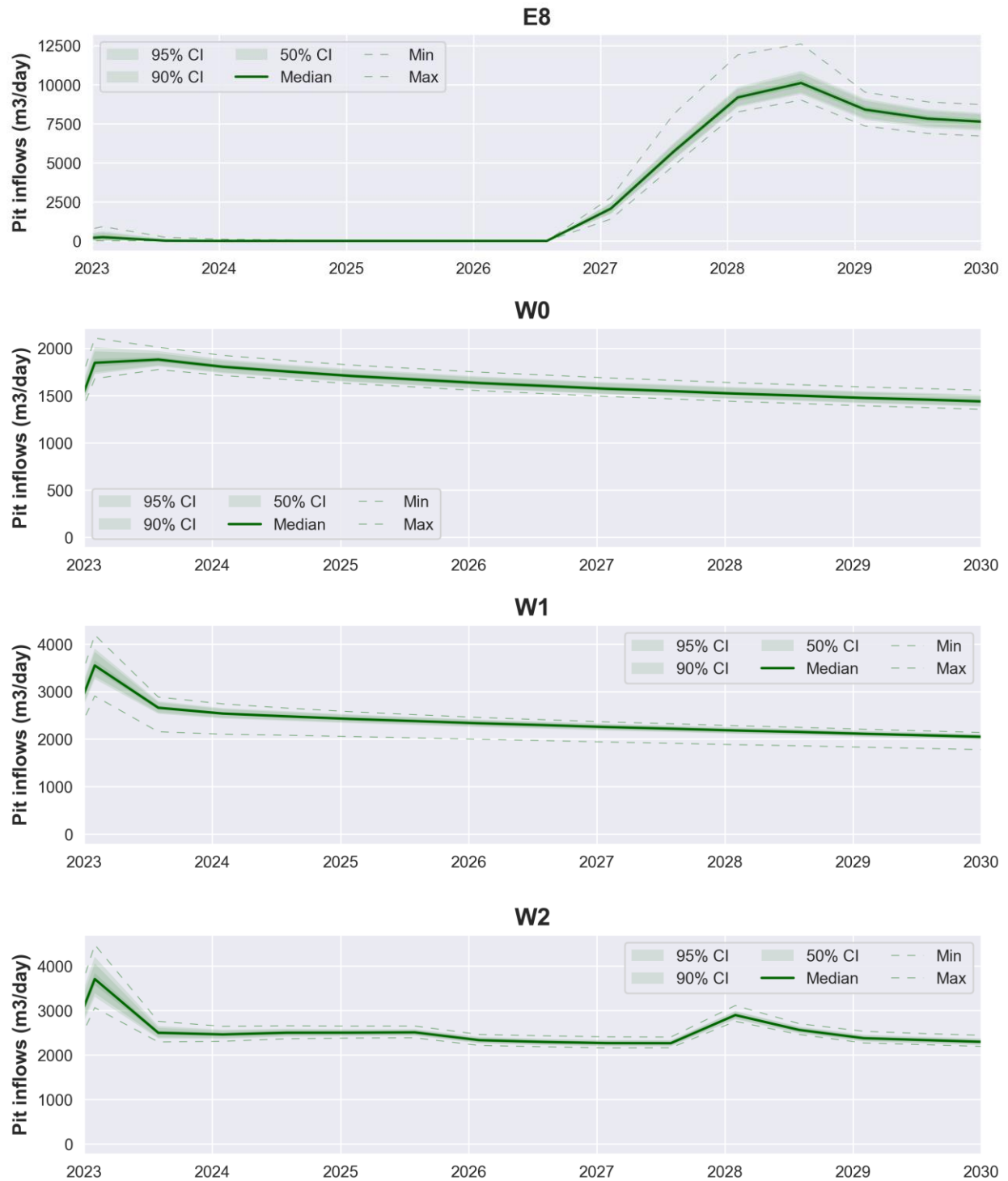Figure 8-20: Simulated dewatering rates (6-month moving average, continuation).

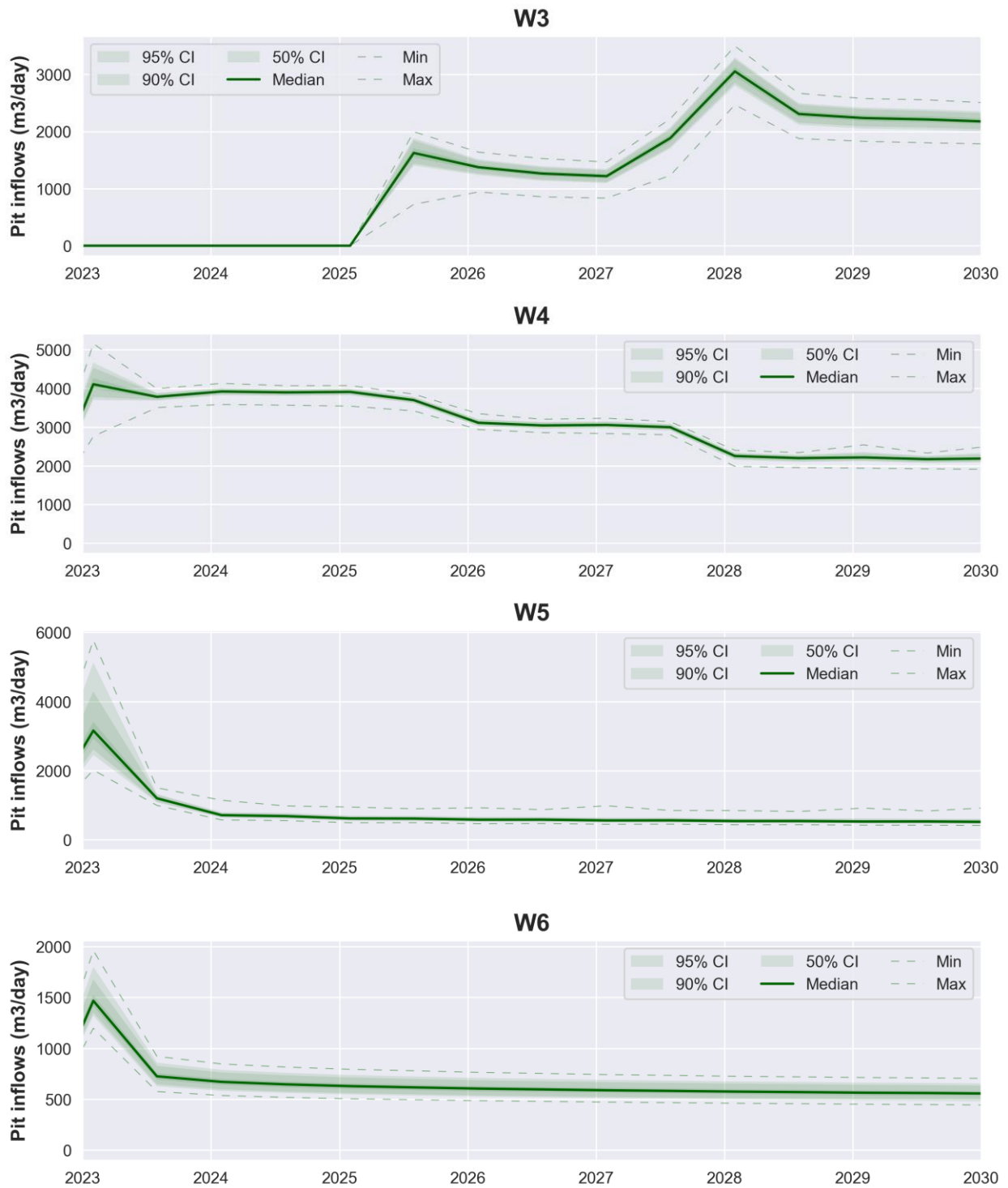Figure 8-21: Simulated dewatering rates (6-month moving average, continuation).

Figure 8-22: Simulated dewatering rates (6-month moving average, continuation).
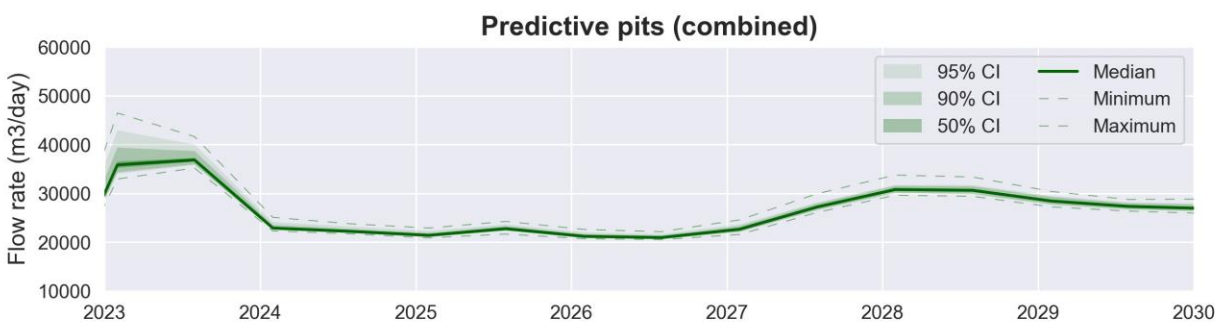
Figure 8-23: Total dewatering rates (6-month moving average, continuation).

9. Conclusions and recommendations

A numerical groundwater model has been developed for the Yandi mine. The numerical model had to include a large number of hydraulic stressors that occurred within the model domain since the commencement of mining operations in 1991. These stressors were both naturally occurring (namely changes in rainfall rates and subsequent diffuse recharge and seepage from Marillana Creek) and associated with the mine operations (including dewatering through wells and sumps, excess water discharge and diversion of Marillana Creek).

The model definition of parameter zones was simplified to four major hydrogeological units to optimize model run-times while encapsulating the main hydrogeological processes of the site. Heterogeneity within each of these units (as well as boundary conditions) was implemented using the pilot point methodology, which was also the foundation for the uncertainty analysis.

History matching was undertaken comparing simulated groundwater levels through historical measurements undertaken in hundreds of monitoring boreholes over a period of 30 years. Simulated heads show a very good agreement with historical measurements, with a few exceptions mostly associated with potential errors in historical pumping rates and boundary conditions used to represent the Rio Tinto Pits. To that end, it is recommended that more detailed information about the Rio Tinto pits is obtained for both historic and predictive periods, especially since those pits are located in the vicinity of E8 pit. Further information would improve history matching in the area (and consequently initial conditions prior to E8 development), as well as a better understanding of contributions from the Rio Tinto pits as the proposed E8 pit dewatering unfolds.

The main modelling objective was to provide predictive estimates of drawdown associated with the mining operations towards the end of mine (end of 2029), in particular the proposed E8 pit. Multiple scenario runs were undertaken to identify drawdown contributions associated with climate (i.e., rainfall rates), mining operations and the E8 pit. Model results suggest that the drawdown contributions from this pit will be restricted to its immediate vicinity. Simulated dewatering rates for E8 pit show maximum values of 12.5 ML/day, stabilizing to 10 ML/day from end of 2028.

The comparison of predictive model results with additional data collected after the history matching (borehole HYM0011M) suggests that predictive drawdowns within the Alluvium Aquifer are being overestimated in the vicinity of E8. It is possible that the vertical connection between Alluvium and CID aquifers are overestimated in the model, given that a single layer was assigned for each aquifer and no representation was given to lower permeability portions of the CID. Other potential factors in the overestimation of Alluvium drawdown include:

- Limited monitoring in the alluvium

- Uncertain geometry of the alluvium, particular at local scales, and

- Uncertainty around the infiltration of Yandi discharge, both in time and duration.

In light of these facts, drawdown predictions within the Alluvium Aquifer should be considered with caution.

10. References

Bakker, Mark, Post, Vincent, Hughes, J. D., Langevin, C. D., White, J. T., Leaf, A. T., Paulinski, S. R., Bellino, J. C., Morway, E. D., Toews, M. W., Larsen, J. D., Fienen, M. N., Starn, J. J., and Brakenhoff, Davíd, 2022. FloPy v3.3.7 — release candidate: U.S. Geological Survey Software Release, 15 December 2022, https://doi.org/10.5066/F7BK19FH.

Hughes, J.D., Langevin, C.D., and Banta, E.R., 2017, Documentation for the MODFLOW 6 framework: U.S. Geological Survey Techniques and Methods, book 6, chap. A57, 40 p., https://doi.org/10.3133/tm6A57.

White, J.T. 2018. A model-independent iterative ensemble smoother for efficient history-matching and uncertainty quantification in very high dimensions. Environmental Modelling & Software, 109, 191-201.

White, J.T., Hunt, R.J., Fienen, M.N., Doherty, J.E., 2020. Approaches to highly parameterized inversion: PEST++ version 5, a software suite for parameter estimation, uncertainty analysis, management optimization and sensitivity analysis. Technical Report. US Geological Survey.

White, J. T., Fienen, M. N., and Doherty, J. E., 2016. A python framework for environmental model uncertainty analysis. Environ. Model. Softw. 85, 217–228. doi: 10.1016/j.envsoft.2016.08.017